Technical Report Documentation Page

1. Report No.	2. Government Accession No.	3. Recipient's Catalog No.
FHWA/TX-91+1205-1		

4. Title and Subtitle	5. Report Date
AN EMPIRICAL-MECHANISTIC DESIGN METHOD USING BONDED CONCRETE OVERLAYS FOR THE REHABILITATION OF PAVEMENTS	January 1991
	6. Performing Organization Code
7. Author(s) Willem A. van Metzinger, B. Frank McCullough, and David W. Fowler	8. Performing Organization Report No. Research Report 1205-1
9. Performing Organization Name and Address Center for Transportation Research The University of Texas at Austin Austin, Texas 78712-1075	10. Work Unit No. (TRAIS)
	11. Contract or Grant No. Rsch. Study 3/11-8-89/0-1205
12. Sponsoring Agency Name and Address Texas Department of Transportation (formerly State Department of Highways and Public Transportation) P. O. Box 5051 Austin, Texas 78763-5051	13. Type of Report and Period Covered Interim
	14. Sponsoring Agency Code

15. Supplementary Notes
Study conducted in cooperation with the U. S. Department of Transportation, Federal Highway Administration
Research Study Title: "Finite-Element Analysis of Bonded Concrete Overlays"

16. Abstract

In this report, a design model for bonded concrete overlays was developed. The development included observations of the performance of existing bonded concrete overlays with varying depths, reinforcement types, and various bonding treatments. These observations were studied in detail and then analyzed statistically. The model development involved establishing the failure mechanisms which cause delamination and cracking in the bonded overlays. A finite-element program was then used to model the cracking and delamination of bonded overlays subjected to a variety of wheel loads and environmental stresses. The failure mechanisms, together with the stress information, were compared to performance observations and used to develop the design procedure.

17. Key Words	18. Distribution Statement
design model, bonded concrete overlays, observations, performance, reinforcement, mechanisms, stress, development, failure, finite-element program	No restrictions. This document is available to the public through the National Technical Information Service, Springfield, Virginia 22161.

19. Security Classif. (of this report)	20. Security Classif. (of this page)	21. No. of Pages	22. Price
Unclassified	Unclassified	98	

AN EMPIRICAL-MECHANISTIC DESIGN METHOD USING BONDED CONCRETE OVERLAYS FOR THE REHABILITATION OF PAVEMENTS

by

Willem A. van Metzinger
B. Frank McCullough
David W. Fowler

Research Report Number 1205-1

Research Project 3/11-8-89/0-1205

Finite-Element Analysis of Bonded Concrete Overlays

conducted for

Texas State Department of Highways and Public Transportation

in cooperation with the

**U. S. Department of Transportation
Federal Highway Administration**

by the

CENTER FOR TRANSPORTATION RESEARCH

Bureau of Engineering Research

THE UNIVERSITY OF TEXAS AT AUSTIN

January 1991

NOT INTENDED FOR CONSTRUCTION,
PERMIT, OR BIDDING PURPOSES

B. Frank McCullough, P.E. (Texas No. 19914)
David W. Fowler, P.E. (Texas No. 27859)
Research Supervisors

PREFACE

This report covers the development of an empirical-mechanistic design procedure for bonded concrete overlays on continuously reinforced concrete pavements. Existing design procedures are discussed and critiqued. A finite-element method program is used to analyze wheel and environmental stresses in an overlaid system which is used to develop a design model. Field data from projects in Houston are evaluated and used to develop the mechanism of failures for bonded concrete overlays. Using the finite-element model and field data, considerable insight is obtained into the behavior of bonded concrete overlays. A long-term performance model previously developed for continuously reinforced concrete pavements is selected for use with bonded concrete overlays due to the long-term performance data for overlays. Furthermore, the failure mechanism of BCO is similar to that of CRCP. The same long-term performance model can, therefore, be used.

LIST OF REPORTS

Research Report 1205-1, "An Empirical-Mechanistic Design Method Using Bonded Concrete Overlays for the Rehabilitation of Pavements," by Willem A. van Metzinger, B. Frank McCullough, and David W. Fowler, presents the background and techniques used in developing a design model for bonded concrete overlays. January 1991.

ABSTRACT

In this report, a design model for bonded concrete overlays was developed. The development included observations of the performance of existing bonded concrete overlays with varying depths, reinforcement types, and various bonding treatments. These observations were studied in detail and then analyzed statistically. The model development involved establishing the failure mechanisms which cause delamination and cracking in the bonded overlays. A finite-element program was then used to model the cracking and delamination of bonded overlays subjected to a variety of wheel loads and environmental stresses. The failure mechanisms, together with the stress information, were compared to performance observations and used to develop the design procedure.

SUMMARY

A better understanding of bonded concrete overlay was developed in this project by comparing the initial performance of a newly constructed facility with the mechanistic behavior developed through theoretical concepts. The performance of overlays placed in Houston, Texas, was modeled to analyze their behavior as wheel and environmental stresses were applied. In a similar manner, observations and mechanistic models were used to develop information concerned with the point at which a bonded concrete overlay should not be placed. A finite-element technique was used to study cracks and stresses at the interface of the overlay and the existing pavement. A sensitivity analysis indicates that modulus values and thermal coefficients of the existing and overlay pavement, as well as crack spacing, overlay thickness, and existing pavement thickness, significantly influence the environmental stresses occurring at the interface. Reinforcing type, thickness, and aggregate type are important in the development of transverse cracks. Finally, after studying fatigue cracking, a design procedure for bonded concrete overlay has been prepared.

IMPLEMENTATION STATEMENT

Observations and studies explained in this report have concluded that bonded concrete overlay (BCO) will act the same as newly constructed pavement. However, the condition or remaining life of the existing pavement does influence the stress development in the pavement and therefore the performance. Repairs to the existing pavement may be required before overlay.

At the time of this report, the oldest BCO on continuously reinforced concrete pavement in Texas has been in place about seven years. This BCO is performing well with no signs of distress.

BCO on continuously reinforced concrete pavement seems to be a viable rehabilitation procedure. BCO should be constructed at a cost lower than that of unbonded overlay. Therefore, BCO is recommended for use on other applicable projects.

TABLE OF CONTENTS

CHAPTER 1. INTRODUCTION

1.1 BACKGROUND

In the United States many sections of the Interstate highway system are nearing the end of their design life. In large metropolitan areas this becomes very obvious when major highways and freeways are investigated for structural and/or functional failure. The structural and functional capability of these highways can be improved by either ongoing maintenance, rehabilitation, or new construction. Rehabilitation has become an important factor in the Interstate system, because it improves riding quality as well as structural capacity at a lower cost than new construction and is also more permanent and effective than routine day-to-day maintenance. The Interstate system consists of various types of pavement structures. Some are flexible pavements, where asphalt concrete is normally the support layer, while others are rigid pavements, where the support layer is portland cement concrete. This study was mainly concerned with portland cement concrete pavement rehabilitation, specifically bonded concrete overlays (BCO) on existing continuously reinforced portland cement concrete pavements.

Various concrete overlay design procedures are available for engineers to use. Most of these design procedures are based on the U. S. Army Corps of Engineers design procedure. This procedure was mainly developed for overlays of airport structures, which differ considerably in size and type of loading from highway overlays. Two main factors need to be considered when overlays are designed for highway applications. The first is the design system used to obtain an overlay thickness. The second factor involves establishing how long the overlaid system will last. Current procedures give some indication based on limited empirical results.

In order to evaluate the long-term performance of the pavement structure, the failure mechanism should be known. Knowing this failure mechanism can then aid in understanding the problems concerned with design and construction practices. The two main distress modes associated with BCO are cracking and delamination. The accepted cracking mechanism of overlays is based on empirical results or engineering judgment. Bonded concrete overlays are, for instance, meant to produce reflective cracking that will coincide with the cracks in the existing pavement. This, however, does not always happen. Experimental bonded concrete overlay sections under surveillance in Houston did not always provide reflective cracking. The currently assumed mechanism of crack formation is, therefore, not always applicable. Another field observation that influenced the long-term performance of bonded concrete overlays was the detection of delamination, as well as punchouts, occurring in overlaid structures on IH-610 in Houston. Cracking and delamination are, therefore, important parameters that should be investigated and controlled in the design and construction of bonded concrete overlays.

The above paragraphs show the status of bonded concrete overlays in the Interstate system and also some of the problems with the design of bonded concrete overlays.

1.2 PURPOSE OF THE STUDY

The main purpose of the study was to develop a design model for bonded concrete overlays, which involved characterizing failure mechanisms that cause delamination and cracking in bonded concrete overlays. By establishing the failure mechanisms, a design procedure could be developed to improve current design procedures as well as to improve the prediction of long-term performance of bonded concrete overlaid systems. This study was done in conjunction with another study done at The University of Texas at Austin, one investigating early-age performance of overlaid systems (Ref 57).

1.3 SCOPE OF THE STUDY

The objective of this study was to investigate current concrete overlay design procedures for concrete pavements. Factors influencing the long-term performance of bonded concrete overlays were determined, and an analysis factorial was formed for a sensitivity study of the different variables. Before doing any analysis, a finite-element method (FEM) program with an ability to model cracks and

delamination was compared with other theories to assure compatibility between the FEM program and existing theories. The most sensitive variables were used in the model development. The effects of the existing pavement, wheel loads, and environmental stress on overlaid systems were evaluated to obtain the sensitivity of variables for long-term performance prediction. These variables were also used in the report to develop the failure mechanism of bonded concrete overlays. The failure mechanism, with the stress variables, was used to develop a cost-effective design procedure that will adequately project the long-term performance of bonded concrete overlays.

The specific objectives were

(a) to model phenomena observed on overlays in Houston, with specific reference to the cracking behavior and delamination;
(b) to accurately analyze the behavior of bonded concrete overlays, incorporating temperature stresses as well as wheel load stresses;
(c) to develop a rational method for establishing when placement of a BCO is more favorable than either reconstruction or placement of an unbonded overlay;
(d) to develop an easily usable design procedure for bonded concrete overlays incorporating the above factors; and
(e) to accurately describe the long-term performance of bonded concrete overlays.

The method used to evaluate BCO is shown in Figure 1.1. The first part of the method involves certain field observations that are made to identify a specific problem. A statistical evaluation of field data and an analysis of the sensitive variables are then performed. The data obtained from the statistical analysis and the analysis of sensitive variables are then used to do the mechanistic modeling. Design equations are then developed, and they are used with the failure mechanisms and a long-term performance model in a design procedure.

1.4 SCOPE OF THE REPORT

Chapter 1 discusses the background, purpose, and scope of the report.

Chapter 2 describes design procedures and evaluates current bonded concrete overlay design procedures, with specific attention to the definition of failure and the fatigue approach used. The limitations of these various methods are discussed and critiqued.

Chapter 3 discusses the factors influencing the long-term performance of bonded concrete overlays, looking at the structural system and material properties and including a historical review of fatigue of concrete structures throughout the years. This is an important part of the report; it acknowledges the limited amount of research done in the area of concrete fatigue as well as the complexity of the problem. Finally, the loads influencing stress distribution in the pavement and the failure criteria for bonded concrete pavements are discussed.

Chapter 4 evaluates an FEM procedure to be used, by comparing it to existing theories. The FEM procedure is then used to evaluate the sensitivity of the long-term performance of BCO to variable factors.

Chapter 5 evaluates the field performance of BCO overlays in Houston to be used in calibrating the long-term performance prediction model.

Chapter 6 evaluates stress development in BCO, using wheel load as well as environmental stresses.

Chapter 7 discusses the development of an empirical-mechanistic design procedure for BCO. A design procedure for BCO, as well as a long-term performance prediction model, is proposed.

Chapter 8 discusses conclusions from this study with recommendations for future work.

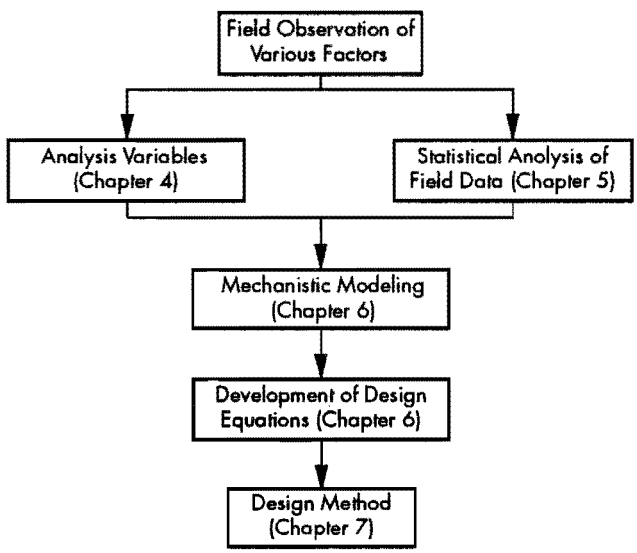

Figure 1.1 Chart showing conceptual layout of method followed to develop a design method for BCO

CHAPTER 2. PAVEMENT DESIGN

2.1 INTRODUCTION

The design of pavement and its long-term performance are important in the overall transportation system in the United States. The public expects good roads to get them from point A to point B. The public further expects these roads to be comfortable, safe, and economical. If engineers are to serve the community responsibly, these are factors they need to consider when designing a new pavement or a rehabilitation project. Another aspect of responsible engineering is research, such as that reported in this study, which is carried out for the purpose of improving existing procedures. However, before a design procedure can be developed, it is necessary to understand what a design procedure is, what design procedures are currently used, and what their limitations are. Knowing the current state of the art will help engineers develop and improve existing procedures. In this chapter, current procedures for the design of portland cement concrete pavements are discussed, as well as the design concepts and different methods of developing a design system. Finally, existing overlay design procedures are discussed and critiqued.

The three main purposes of this chapter are (1) to establish the position of this study in the overall transportation system, (2) to evaluate currently accepted overlay design methods, and (3) to discuss important conceptual problems.

2.2 DESIGN SYSTEM

In general, a design system is a system in which a certain facility is designed to perform adequately, for its intended purpose, over a given time. A design system consists of input, analysis, and output. The inputs include known parameters, geometric constraints, and factors that induce stresses in the system. For pavement structures, the inputs are comprised of the pavement structure geometry, material properties, and factors inducing stress. These factors are used within a certain analysis system to produce an output. By a process of synthesis, the output is a pavement structure that needs to be tested against constraints such as cost-effectiveness, safety, and long-term performance.

The model used within the design system is extremely important. The better the ability of the model to predict actual field behavior of the pavement, the more reliable the model and, therefore, the more cost-effective the resulting structure. The model depends on the development concept used and the concrete pavement system analyzed.

2.2.1 Design Concept

A design system can be modeled using field tests, a computer modeling, or both. They are conceptually different in approach when used in a design system development. Historically, empirical methods have been developed and used in pavement design. However, during the last decade a switch to a more mechanistic design approach has been made. Most of the mechanistic design approach methods use empirical methods to verify the design model, in order to model field behavior more realistically. Therefore, there are three methods for developing design systems for pavements; they use, respectively, an empirical, a mechanistic, and an empirical-mechanistic approach. These three methods are described below.

2.2.1.1 Empirically Developed Design Methods

Empirically developed design methods use field observations and conditions to model pavement behavior under certain environmental conditions and wheel loading. An example of such a method is the AASHO Road Test, which was conducted between 1958 and 1961, in which different types of pavement structures were tested under truck loading. From the data obtained, models describing crack development in concrete pavements were developed. Two problems exist in using an empirical approach. One is that the developed model is representative only of the area in which the test was done; extrapolation of the data to other climatic regions is questionable and reduces reliability. It would be extremely expensive to create a testing facility covering all types of materials and climatic conditions of a region as large and diverse as the United States, or even as Texas.

2.2.1.2 Mechanistically Developed Design Methods

Mechanistic design procedures use theory to predict stresses, strains, and deflections for a specific system. They provide a means of interpolation between different structures. The problem with a true mechanistic design procedure is the necessary characterization of material properties and long-term performance prediction. For the model to reliably predict stresses, strains, and deflections developed under induced in-service stresses, the material characteristics used in the model should be as close as possible to those under in-service conditions. Most of the time these characteristics are found using either laboratory testing or in-situ testing of materials to be used in the pavement system. Analytical programs for modeling fatigue of material are not available. Therefore, empirical results are needed to verify and modify design models.

2.2.1.3 Design Methods Developed Using an Empirical-Mechanistic Approach

From the above two paragraphs, it is evident that a true empirical model is expensive and produces results that are confined to one region, while a true mechanistic approach presents problems in materials characterization and long-term performance prediction. The logical step is to combine the two methods. A good example of this combination is the AASHTO Road Test rigid pavement design equation (Ref 1), in which a part of the equation was empirically developed while the rest was based on a mechanistic approach and reliability. Most models use mechanistic methods to calculate stress in a structure and use testing and true engineering parameters, such as tensile strength, to characterize materials. However, empirical methods are used for verifying fatigue or long-term performance models. An empirical-mechanistic model produces higher reliability when the same model is used for different systems and environmental regions. The primary reason for this is that empirical-mechanistic models use interpolation to arrive at design parameters, while purely empirical models use extrapolation. For example, the AASHO Road Test data are extrapolated within the AASHTO rigid pavement equation so that it can be used in areas with different environmental and soil conditions. Furthermore, materials characterization is improved by laboratory tests, and long-term performance prediction is improved by empirical tests, which verify the selected model.

2.2.2 Concrete Pavement Systems

The type of pavement system analyzed in the overall pavement design system is also important, because it will influence stress distributions and, therefore, the performance of the pavement. Three types of portland cement concrete pavement systems are currently used—namely, jointed concrete pavement (JCP), jointed reinforced concrete pavement (JRCP), and continuously reinforced concrete pavement (CRCP). The three systems are shown in Figure 2.1.

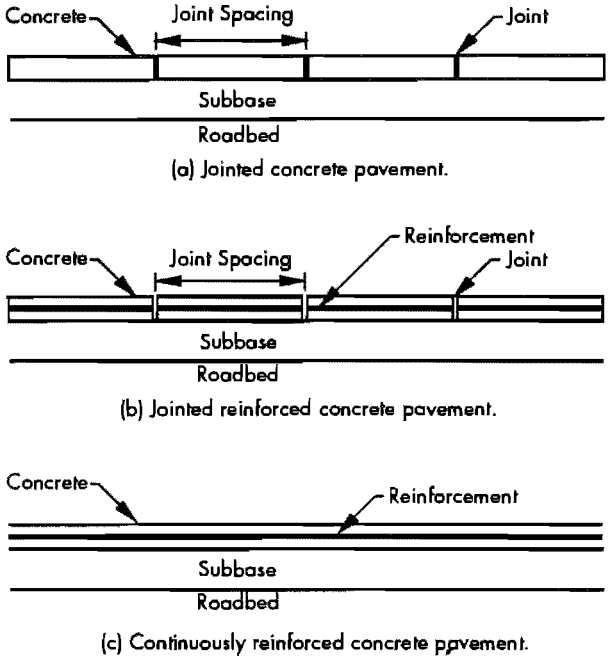

Figure 2.1 Concrete pavement systems

2.2.2.1 Jointed Concrete Pavement System

Jointed concrete pavement systems are unreinforced systems in which cracks are controlled by joints. The cracks are formed as a result of shrinkage, moisture movement, temperature changes, or a combination of the above. Joints are placed at specific locations to control cracking if it occurs. The AASHTO Design Guide (Ref 1) specifies a crack spacing, in feet, of not more than twice the pavement thickness measured in inches. Therefore, for an 8-inch pavement thickness, a maximum joint spacing of 16 feet is required. Another general guideline is that the ratio of slab width to length should not exceed 1.25. These guidelines are only general guidelines, because the joint spacing is a function of the material properties and of the environmental region in which the pavement is built. Some conditions may necessitate shorter or longer joint spacings than others.

2.2.2.2 Reinforced Jointed Concrete Pavement System

The cost of joint construction is extremely high owing to the required detail of the joint as well as to

construction problems. As a result, a reduction in the number of joints will reduce the construction costs. However, it should be noted that a reduction in the number of joints increases joint movement which, in turn, increases maintenance costs and makes rehabilitation more difficult. By introducing reinforcing into the system, the joint spacing can be increased, which results in the formation of cracks within the system. The percentage reinforcing in the concrete layer controls crack formation and pavement slab dimensions. The AASHTO Design Guide (Ref 1) uses joint spacing, steel working stress, and the friction factor between the slab and the subbase to calculate the required reinforcing percentage. Depending on the joint spacing, the crack will form in the center, at the third point, or, eventually, at specific intervals if the joint spacing becomes very large.

2.2.2.3 Continuously Reinforced Concrete Pavement System

In continuously reinforced concrete pavement, the joints are completely eliminated. This is the main difference between CRCP and JRCP. By increasing or decreasing the percentage of reinforcing within the system, the crack spacing and width can be controlled. The AASHTO guidelines (Ref 1) specify three limiting criteria: the crack spacing should be less than 8 feet but not less than 3-1/2 feet; the allowable crack width should not exceed 0.04 inch for extreme temperatures or 0.023 inch at freezing; and the maximum steel stress should be less than 75 percent of the yield point stress.

2.3 CONTINUOUSLY REINFORCED CONCRETE PAVEMENT DESIGN PROCEDURE

In the previous paragraphs the concepts behind different design methods and the different systems they serve were discussed. Any one of these methods can be used. This study concentrates on continuously reinforced concrete systems. The design of CRCP systems consists of a thickness design and a reinforcing design. The AASHTO Design Guide (Ref 1) procedure is well known. The thickness design is completed using the AASHTO rigid pavement equation

$$\log_{10}(W_{18}) = A + B + C$$

where

$$A = Z_R * S_o$$

$$B = 7.35 * \log_{10}(D+1) - 0.06 + \{\log_{10}[\Delta psi / (4.5 - 1.5)]\} / \{1 + [1.624*10^7] / [(D+1)^{8.46}]\}$$

$$C = (4.22 - 0.32 * p_t) * \log_{10}\{[S'_c * C_d * (D^{0.75} - 1.132)] / [215.63 * J*(D^{0.75} - (18.42 / (E_c / k)^{0.25})]\}$$

with

W_{18} = predicted number of 18-kip equivalent single axle load applications;

Z_R = standard normal deviate;

S_o = combined standard error of the traffic prediction and performance prediction;

D = thickness (inches) of pavement slab;

Δpsi = difference between the initial design serviceability index, p_o, and the design terminal serviceability index, p_t;

S'_c = modulus of rupture (psi) for portland cement concrete used on a specific project;

J = load transfer coefficient used to adjust for load transfer characteristics of a specific design;

C_d = drainage coefficient;

E_c = modulus of elasticity (psi) for portland cement concrete;

k = modulus of subgrade reaction (pci);

A = reliability part of the equation;

B = empirical part of the equation; and

C = mechanistic part of the equation.

With this equation and the known parameters, a thickness, D, can be calculated to show, at a specified reliability, structural failure after some amount of predicted traffic has passed over it.

The next step is to calculate the required percentage reinforcing. The AASHTO Guide considers three limiting criteria, as mentioned before. Nomographs are used in the guide for each of the three criteria. The specific equation for each criterion is shown below. Each one of these equations must be satisfied before the correct percentage of reinforcing can be specified.

$$\text{Crack Spacing} = \{1.32 * [1 + f_t/1{,}000]^{6.70} * [1 + \alpha_s/2\alpha_c]^{1.15} * [1 + \phi]^{2.19}\} / \{[1 + \sigma_w/1{,}000]^{5.20} * [1 + P]^{4.60} * [1 + 1{,}000Z]^{1.79}\}$$

$$\text{Crack Width} = \{0.00932 * [1 + f_t/1{,}000]^{6.53} * [1 + \phi]^{2.20}\} / \{[1 + \sigma_w/1{,}000]^{4.91} * [1 + P]^{4.55}\}$$

$$\text{Steel Stress} = \{47{,}300 * [1 + DT_D/100]^{0.425} * [1 + f_t/1{,}000]^{4.09}\} / \{[1 + S_w/1{,}000]^{3.14} * [1 + P]^{2.74} * [1 + 1{,}000Z]^{0.494}\}$$

where

f_t = concrete indirect tensile strength;
α_s = steel thermal coefficient;
α_c = concrete thermal coefficient;
ϕ = reinforcing bar or wire diameter;
σ_w = tensile stress caused by wheel loading;
P = percent reinforcing;
Z = concrete shrinkage at 28 day;, and
DT_D = design temperature drop.

Before the design can be completed, considerable effort is needed to obtain the different material variables, environmental parameters, and wheel loading.

2.4 CONTINUOUSLY REINFORCED CONCRETE PAVEMENT REHABILITATION

After construction and some years of service, an effective way of upgrading a CRCP is through rehabilitation. The following paragraphs discuss rehabilitation of concrete pavements and design procedures currently used.

The use of concrete for resurfacing is well known. Since the early 1900's, paving with portland cement concrete has been used as a rehabilitation method, with the main purpose being the extension of the lifespan of an existing pavement. The concrete pavement used at that time consisted of small concrete blocks, which one can think of as miniature jointed concrete pavement blocks. An example of this is the first all-concrete pavement constructed in the United States, at Bellefontaine, Ohio, in 1893 (Ref 2). The pavement was constructed in blocks about 5 feet square, and, although the surface was rough, it gave satisfactory results. Since that time, the science of pavement engineering has improved dramatically. Westergaard's stress equations and the subsequent improvements by others, as well as the later availability of the microcomputer, contributed to improvements in the use of concrete as a paving material. During the later part of the century, many design systems have been developed for rigid pavements, and, with the Interstate system in the U. S. reaching the end of its design life, the emphasis has changed from reconstruction to rehabilitation as a more cost-effective procedure.

2.4.1 Rehabilitation Procedures

Rehabilitation of CRCP depends on the state of the existing pavement, on cost-efficiency, and, in many cases, on the preferences that a designer might have. CRCP can be rehabilitated by the addition of either a portland cement concrete layer or an asphalt concrete layer to the pavement structure. Many different procedures have been developed by different agencies for overlay-thickness design. Most procedures provide a means for obtaining an overlay thickness by using a specific overlay design equation, such as the Corps of Engineers (COE)equation, with an equation such as the AASHTO rigid pavement equation, which is used to calculate the thickness for a new pavement for the expected traffic. This thickness is then used in the Corps of Engineers equation to obtain an overlay thickness. Figure 2.2 shows a typical overlay design procedure layout (Ref 3). The procedure starts with selecting the design criteria and obtaining condition surveys and deflection measurements. The condition survey and deflection measurements are used to select design sections and for materials characterization. Then the remaining life of each design section and the subsequent overlay thickness are calculated. Finally, a design thickness is selected.

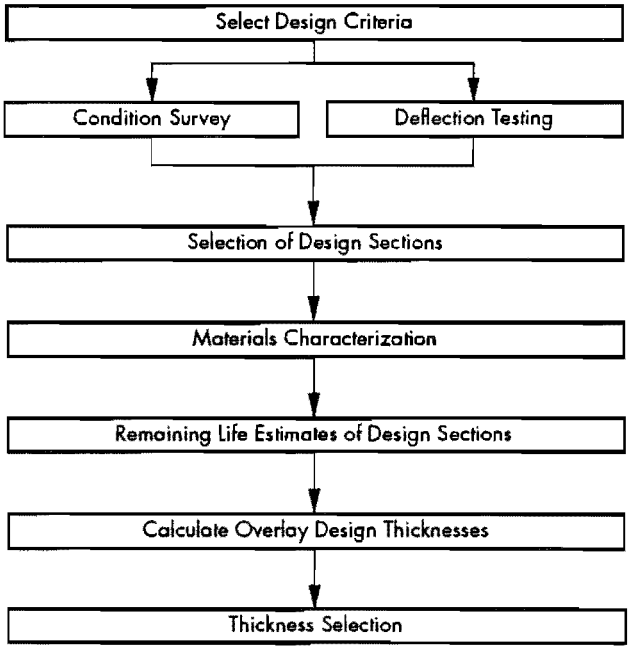

Figure 2.2 Flowchart of the Texas SDHPT overlay design procedure

In 1958, the Corps of Engineers developed an overlay design equation, primarily for airport runways and taxiways. Various other institutions have developed procedures of their own, and today design engineers can choose from among a wide variety of overlay design methods. Experience with concrete overlays for highway structures, such as jointed concrete pavements or continuously reinforced concrete pavements, is limited in the sense that the Interstate system is only now nearing the end of its design life, and many overlay test sections are, therefore, a maximum of five years old. Well-documented test sections in Houston are reaching their fifth year after construction.

Long-term evaluation data for portland cement concrete (PCC) overlays are, therefore, either nonexistent or based on accelerated testing procedures. The design procedures must therefore be developed using rigid pavement experience, theoretical procedures, or a mixture of the two. However, the use of rigid pavement experience creates a problem, because a rigid pavement structure differs from an overlaid system, where part of the structure has deteriorated to some extent.

2.4.2 Continuously Reinforced Concrete Pavement Overlay Design Concepts

The Corps of Engineers recognized that concrete overlays can be bonded, partially bonded, or unbonded. Each of these three systems will react differently to vehicle and environmental loads. Each one of the three systems is conceptually described in the next paragraphs.

2.4.2.1 Unbonded Concrete Overlays

Unbonded concrete overlays (see Figure 2.3) are overlays in which there is no bond between the existing pavement and the overlay. An asphalt layer is normally used as a separation layer to prevent bonding and serve as a stress relief course. This layer prevents the reflection of cracks or joints into the surface layer. The two concrete layers are therefore totally independent of each other. Because of the separation between the two layers, the maximum stress can occur in the overlay structure.

Therefore, unbonded concrete overlays are normally thicker than bonded concrete pavements and as thick as the existing pavement. An unbonded system is preferred over a bonded system when the existing pavement's remaining life is very short. The unbonded overlay can be constructed on the existing pavement with only minimal improvement of the existing pavement. Sometimes cracking and seating are used to create a uniform pavement structure before the overlay is added to form the unbonded concrete overlay shown in Figure 2.3.

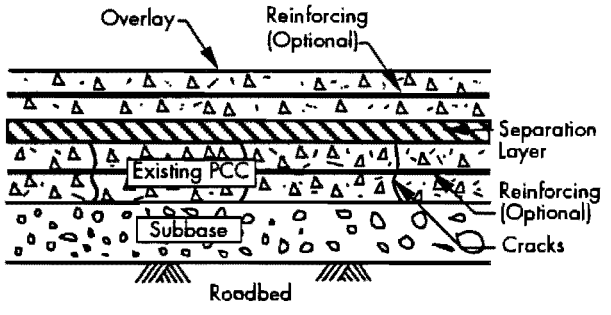

Figure 2.3 Unbonded concrete overlay

2.4.2.2 Partially Bonded Concrete Overlays

Partially bonded concrete overlay pavements (see Figure 2.4) are rarely used. The overlay is placed on the existing pavement without any specific preparation of the existing pavement surface. The pavement is partially bonded to the existing pavement, but the strength and uniformity of the bond are uncertain.

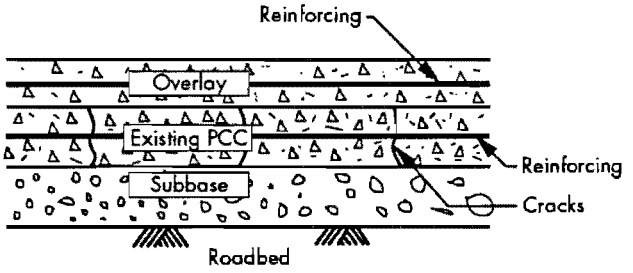

Figure 2.4 Bonded concrete overlay

2.4.2.3 Bonded Concrete Overlays

Bonded concrete overlays are overlays in which the surface of the existing pavement is specially prepared by techniques such as cold milling or shot blasting, and a bonding agent is used to assure good bond between the two layers. The performance concept is that the existing concrete pavement and the overlay will act as a composite structure to provide a much thicker pavement, which will improve rideability, and will also increase the remaining life of the existing pavement.

This study was mainly concerned with BCO on CRCP pavement, as mentioned before.

2.5 CURRENT DESIGN PROCEDURES FOR BONDED CONCRETE OVERLAYS

The previously developed overlay design procedures normally include equations for unbonded, partially bonded, and bonded concrete overlays. As mentioned before, many of these procedures exist. However, this study focused on bonded concrete overlays, and therefore most of the following discussion is concerned with bonded concrete overlays. Procedures developed by the Corps of Engineers, the American Concrete Institute, the Portland Cement Association, FHWA/Texas, AASHTO, and The University of Texas at Austin are discussed below.

2.5.1 Corps of Engineers (COE) Procedure

The Corps of Engineers (COE) procedure is the most widely used procedure.

2.5.1.1 Design Methodology

The Corps of Engineers (Ref 4) developed their PCC overlay procedure for the design of overlays for airport runways and taxiways. The U. S. Air Force and Federal Aviation Administration use this procedure in their rehabilitation designs also. The COE used accelerated test tracks to provide data to model the design of PCC overlays. Three models were developed—namely, for bonded, partially bonded, and unbonded PCC overlays. The following equations were developed:

(1) Bonded case:

$$h_o = h_n - h_e$$

(2) Partially bonded case:

$$h_o^{1.4} = (h_n^{1.4} - Ch_e^{1.4})$$

(3) Unbonded case:

$$h_o^2 = (h_n^2 - Ch_e^2)$$

where

h_o = concrete overlay thickness,
h_n = theoretical thickness if a new pavement were built,
h_e = existing pavement thickness, and
C = coefficient depending on the structural value of the existing pavement and ranging between 0.35 and 1.00.

The partially bonded and unbonded cases were subsequently changed (Ref 5) to incorporate the variation in flexural strength between the existing pavement and the new pavement structure.

2.5.1.2 Fatigue Consideration

This method assumes that the bonded overlay system will provide the same lifespan in number of load applications as a new pavement with thickness equal to the combined existing pavement and overlay thicknesses. The assumption inherent in the procedure is that, for bonded overlays, the existing slab is either in good structural condition or will be upgraded to good structural condition. Further, it assumes that the mechanism of failure for the overlaid system is that of a newly constructed pavement. Many other design methods are based on the same design philosophy.

If one evaluates the method used to develop these equations and compares it to its use for the design of highway overlays, the difference is significant; the accelerated test used for developing unbonded and partially bonded concrete overlays was done on a structure in which the thickness of the existing pavement varied from 6 to 10 inches, whereas the overlay thickness varied from 6 to 13 inches. One bonded overlay section was analyzed in which the existing pavement was 11 inches thick and had a 17-inch overlay. It is apparent that the bonded overlay pavement is extremely thick, especially when compared with what can be used for highway applications. Also, the number of applications in these test sections is much less than the number expected on concrete highways. The COE method defines failure as the application level, or coverage, at which cracking or structural breakup first occurs; this, from a fatigue standpoint, is an unacceptable criterion for highway overlays, especially for CRCP in which the pavement is expected to crack.

2.5.2 American Concrete Institute (ACI) Procedure

The ACI procedure is an example of the influence of the COE method on other institutions.

2.5.2.1 Design Methodology

The ACI method reported by subcommittee VIII of ACI Committee 325 (Ref 6) uses the Corps of Engineers procedure; that is, the same equations are used. The COE failure concept is therefore used. However, if the ACI rigid overlay design procedure is used to design the thicknesses needed in the overlay design equations, the fatigue equation changes to that used in the ACI rigid design method.

Because of the similarities between the ACI Report and the COE method, the ACI method is not discussed in detail here.

2.5.3 Portland Cement Association (PCA) Procedure

The PCA procedure also uses the COE equations, but it uses an improved version for bonded concrete overlays.

2.5.3.1 Design Methodology

The PCA procedure recognizes that the remaining life of the existing pavement will influence the performance of the overlaid pavement. Therefore, the design concept is to create an overlaid pavement that is structurally equivalent (Ref 7) to a new, full-depth pavement, incorporating the existing pavement condition.

The first step in the design procedure is to obtain a design thickness for a full-depth pavement using the PCA rigid pavement design method or any other rigid pavement design method. The main variables needed for this design are the future traffic needs and the subgrade properties, as well as various concrete properties. By using the JSLAB computer program, the PCA developed design curves using flexural strengths for the existing pavement as well as for the new pavement.

The edge condition was analyzed for a full-depth and an overlaid system. Graphs were developed

from this analysis by using the new pavement thickness, from which the existing-plus-resurfacing thickness can be obtained.

2.5.3.2 Fatigue Consideration

The fatigue evaluation depends on the design system used to obtain the thickness of a new pavement. If the PCA procedure is used, the fatigue assumptions are those incorporated in the method. These assumptions are, for instance, that a stress limit exists—i.e., an infinite number of applications at low stress levels—and that the limit is based on plain concrete tests. If the AASHTO method is used for new pavement thickness design, fatigue will be incorporated by the equations developed from the AASHO Road Test.

2.5.4 FHWA/Texas Procedure

2.5.4.1 Design Methodology

The FHWA/Texas design method (Ref 8) formed the basis for subsequent improvements by Schnitter (Ref 9), Taute (Ref 3), and Seeds (Ref 58) for specific application in Texas. The method introduces a systematic approach that includes deflection measurements and condition surveys as the basis for developing design sections and parameters. Specific parameters obtained from these surveys are sections with the same performance capability, or remaining life, and the material properties of the existing system. These values, with variables concerned with environmental conditions and traffic growth, are then used to obtain an overlay thickness to prevent fatigue cracking.

The thickness design is based on deflections obtained from the AASHO Road Test. These deflections and the computer program SLAB49, a stress analysis program, were used to determine k-values for different slab deflections. These k-values were used with the deflections and, again, SLAB49 to develop modulus of elasticity values related to slab deflections. In the development of the method, other factors, such as concrete that is mechanically broken up, and voids underneath the slab, were also considered. The accepted failure criteria were Class 3 and 4 cracking as defined at the AASHO Road Test. Class 3 cracking is defined as a crack opened, or spalled, at the surface to a width of 1/4 inch or more over a distance of at least one-half of the crack length, except that any portion of the crack opened less than 1/4 inch at the surface for a distance of 3 feet or more is classified separately. A Class 4 crack is defined as any crack that has been sealed. The fatigue equation was further modified to reduce scatter by evaluating the effect of slab pumping, equivalency factors, pavement type, and seasonal effects. A suitable thickness is obtained by calculating the stress in the concrete, using SLAB49 or the Westergaard or Pickett equations, and then calculating the number of 18-kip Equivalent Single Axle Loads (ESAL). This is the number of 18-kip ESAL necessary to get the particular pavement thickness to show Class 3 or 4 cracking. The thickness can then be increased or decreased until the predicted and the design 18-kip ESAL are equal. The method was incorporated into computer program RPOD1.

2.5.4.2 Fatigue Consideration

The whole design method is based on a fatigue concept to prevent Class 3 and 4 cracking in concrete pavements, which differs from that used by the previous methods. The method was later modified by Schnitter, in 1978 (Ref 9), by Taute, in 1981 (Ref 3), and by Seeds, in 1982 (Ref 58), and is considered to be an improvement of the method with respect to material characterization and fatigue life prediction of bonded concrete overlays. However, the verification of the fatigue model for overlaid pavements was done using asphalt overlays on concrete pavements.

2.5.5 A Mechanistic Design for Thin-Bonded Concrete Overlays

2.5.5.1 Design Methodology

This method was proposed by Bagate et al (Ref 10). The method was incorporated into a computer program called TBCO1. The Finite Element Method (FEM) program JSLAB is used as a subroutine to the main program.

The first step in the procedure is to back-calculate the in-situ material properties at mid-span and at cracks of the existing pavement, using elastic layered theory and Dynaflect deflection measurements. A k-value, including the structure up to the top of the base slab, is then calculated using the modulus of elasticity of the base and subbase obtained from deflection measurements taken in the center between two adjacent cracks, again using elastic layer theory. Using this k-value and the program JSLAB, maximum deflections are calculated for varying moduli of elasticity of the concrete, pavement characteristics, and Dynaflect loading configurations. From these computations, an adjusted between-crack concrete modulus is obtained using actual field deflections.

Using the initial ratio obtained for between-crack and at-crack moduli, as well as the adjusted between-crack modulus, an adjusted at-crack modulus is obtained. This modulus is used for so-called soft elements in the JSLAB program. The widths of these soft elements are increased in JSLAB until an overlap in computed and field deflections is obtained. From this information, a zone of influence of cracks can be obtained by plotting maximum

deflection versus the influence "zone." Various critical loading conditions are assumed and the maximum tensile stress is used in the fatigue equation.

2.5.5.2 Fatigue Consideration

The equation developed by Taute (Ref 3) is used in the program to calculate fatigue life. The equation was obtained using AASHO Road Test data for asphalt concrete overlays on concrete pavements. The program assumes the equation is applicable to concrete overlays. The failure criterion used is 50 feet of cracking per 1,000 square feet. The equation is

$$N = 43{,}000(f/\sigma)^{3.2}$$

where

- N = number of 18-kip ESAL repetitions,
- f = concrete tensile strength (determined by the splitting tensile test), and
- σ = maximum tensile stress in concrete.

The equation was obtained using AASHO Road Test data and layered theory.

2.5.6 AASHTO Procedure (Ref 1)

The AASHTO method follows the COE equations with a few variations.

2.5.6.1 Design Methodology

Serviceability-traffic concepts used in the general AASHTO design method are also used in the overlay design method. It uses life-cycle cost concepts to obtain cost-effective overlays. The guide also endorses nondestructive test methods for material characterization of in-situ pavement layer properties. The following equations are used for rigid concrete overlays on rigid pavements:

(1) Bonded case:

$$D_{OL} = D_y - F_{RL}(D_{xeff})$$

(2) Partially bonded case:

$$D_{OL}^{1.4} = D_y^{1.4} - F_{RL}(D_{xeff})^{1.4}$$

(3) Unbonded case:

$$D_{OL}^{2} = D_y^{2} - F_{RL}(D_{xeff})^{2}$$

where

- D_{OL} = concrete overlay thickness,
- D_y = theoretical thickness if a new pavement were built,
- D_{xeff} = existing pavement effective thickness, and
- F_{RL} = remaining life factor taking into account the remaining life of existing pavement before overlay as well as the remaining life of the overlaid system after the overlaid traffic has been reached.

The terminal PSI value of 2.0 at the end of the overlay life is suggested by the AASHTO Design Guide. Methods are proposed in the Guide for determination of the existing pavement effective thickness, as well as the remaining life of the existing pavement. Theoretical thickness, D_y, is the thickness calculated for a new concrete pavement that will last until the design overlay ESAL is obtained. The methods for determining most of the values are based on empirical tests.

2.5.6.2 Fatigue Consideration

Fatigue is considered in calculating the theoretical pavement thickness if the AASHTO pavement design method is used. The remaining life is obtained by deflection measurements, design traffic versus past traffic, the time period, serviceability rating, or a condition survey. All of these methods are very subjective. The AASHTO Design Guide failure definition is based on serviceability, therefore, fatigue failures are part of the inherent AASHTO equation and are not separately considered. The pavement can therefore be certified as failed according to the AASHTO design while it still has fatigue life left, and vice versa. Furthermore, the overlay thicknesses are based on the COE equation, which is again based on the first crack failure mechanism inherent in the COE equation.

2.6 CRITIQUE OF CURRENT DESIGN PROCEDURES

It is apparent from previous discussions that the concepts incorporated in the COE method are widely accepted, and it has become the most popular method used today. From the equations developed by the COE method, it can be seen that only partially bonded and unbonded cases consider the state of the existing pavement, whereas the bonded case assumes that the overlaid pavement is the same as a newly constructed pavement. However, the remaining life of the existing pavement is between 0 and 100 percent. The reduction of the remaining life of the existing pavement at the time of overlay will reduce the life expectancy, compared with that of a newly constructed pavement of the same thickness.

It is clear that the method is not applicable for highway overlay design, although it is good for airport pavements. No fatigue mechanism exists in the development of the equations that is applicable to highway design. If other design methods, such as the AASHTO method for rigid pavements, are used, the fatigue evaluation of the method will be incorporated into these equations. Most of the inherent fatigue equations in rigid pavement design methods do not consider the fact that two layers of concrete with different stiffnesses are bonded

together. In these analyses, the equations also do not anticipate the strength of bond between the layers or the stiffness of the existing pavement.

When the overlay design equation of the COE is used in conjunction with another rigid pavement design equation, two different fatigue approaches, one inherent in the COE equation and one inherent in the rigid pavement equation, are used.

The state of the art of long-term performance prediction for concrete pavements is therefore not conclusive. There is much variation among design methods, the assumptions used to develop the methods, and, specifically, the concept of failure between methods.

2.7 CONCLUSIONS

Pavement design is an important factor in the overall transportation system. Within the area of pavement design, two primary types of pavement systems exist: flexible and rigid. Within a rigid pavement system we have three main types of pavement structures—namely, jointed concrete pavements, jointed reinforced concrete pavements, and continuously reinforced concrete pavements. At the end of the pavement design life, three methods can be used to improve the pavement. The existing pavement can be upgraded by heavy maintenance or rehabilitation, such as overlay construction, or a new pavement can be built. If the selected option is rehabilitation, the designer can use either unbonded, partially bonded, or bonded concrete overlays.

This study focused on improving the design methods for bonded concrete overlays, and this chapter shows the position of this study in the overall transportation system. Furthermore, it looks at the currently used overlay design procedures.

This discussion gives background for the most widely used design equations, the Corps of Engineers overlay design equations. These equations are based on accelerated testing of overlays on airport pavements. Two problems exist in using these equations. First, they must be verified as being applicable to highway pavements. Second, the fatigue or long-term performance criterion of failure is inherent in the COE equations as well as in the rigid pavement design equation used. One criterion is used in the COE equation, while a totally different criterion is used in the rigid pavement design equation. The COE equation is based on first structural cracking, while the AASHTO Design Guide rigid pavement equation is based on Class 3 and Class 4 cracking. From this information, it can be concluded that it is not satisfactory to base long-term performance predictions on design equations, which are often used to model concrete overlays.

We can also conclude that, because most of the currently used equations are based on empirical testing, factors such as interface bond strength, crack spacing, and other structural features are not fully addressed by these equations. There are, therefore, features important in bonded concrete overlay design and performance that are not covered by the current design procedures.

In Figure 2.2, an overlay design procedure is shown. This discussion shows that in that overlay design procedure, improvements in the area of predicting the performance of the overlay as well as the method of thickness design, in which important factors are not considered, are needed. The next step is to identify those variables influencing the long-term performance of bonded concrete overlays and to incorporate the most sensitive variables into the design process.

CHAPTER 3. FACTORS INFLUENCING THE LONG-TERM PERFORMANCE OF BONDED CONCRETE OVERLAYS

3.1 INTRODUCTION

In the previous chapter the problems in the currently used bonded concrete overlay design procedures were discussed. If these are addressed and improved, then the cost-efficiency, performance, and safety of bonded concrete overlay systems can be improved. In order to effect empirical-mechanistic improvements, the factors influencing the long-term performance of bonded concrete overlays should be evaluated. From this evaluation, the most significant factors can be identified and used to improve the design and the long-term performance models of bonded concrete overlays.

The factors influencing the long-term performance can be divided into five broad categories—namely, structural geometry of the system, material properties within the system, induced stresses, fatigue behavior of concrete, and failure criteria. Figure 3.1 shows a layout of the five categories.

A particular pavement structure has certain material properties and wheel- and environment-induced stress systems. For a given structure, the combination of material properties and the induced stresses will influence the fatigue strength of the system. During dynamic loading, the material properties and stresses within the pavement system change as cracks form, concrete fatigues, and loss of load transfer occurs. All these factors will increase the rate of deterioration of the pavement. A loss of load transfer can, for instance, create stress concentrations in the overlaid layer or can change an interior loading case to an edge-loading case.

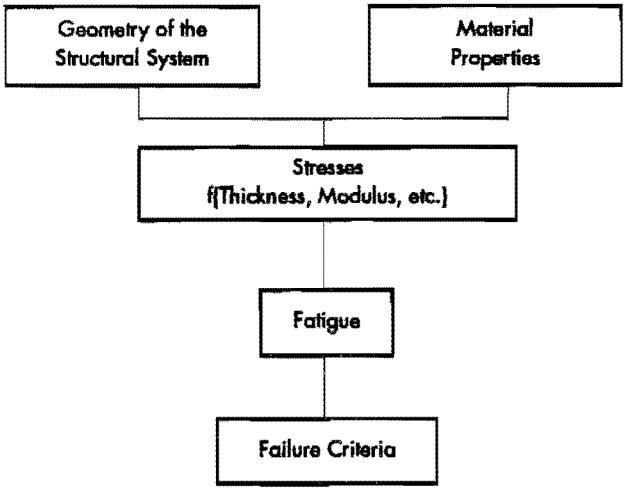

Figure 3.1 Categorical layout of factors influencing long-term performance of bonded concrete overlays

The system is said to have failed when the selected failure criterion is reached. The failure criterion is not fixed to a specific system, such as loads or material properties. It is normally selected by engineers using sound engineering judgment and various design guides or codes. It is necessary to discuss the existing failure criteria for concrete pavements as well as for bonded concrete overlays. These criteria are important because different criteria can give different design lives to the same pavement structure.

At the AASHO Road Test (Ref 11) fatigue testing was done on full-scale pavements. These pavements included specific structural systems, material properties, and wheel- and environment-induced stresses, and were evaluated using a specific failure criterion. The Corps of Engineers also did some full-scale fatigue testing on airport pavements with systems and criteria different from those used at the AASHO Road Test. These full-scale tests were used to develop empirical fatigue equations. The experimental factorial used was normally quite small because of the large costs involved in full-scale testing.

The results obtained from these tests are therefore very specific to the system from which they were obtained, and extrapolation of the results to other systems should be done with care. Each of these equations was therefore developed for a different system or with a different failure criteria. The AASHTO equation for rigid pavement systems, the Corps of Engineers equations developed for overlays on airport pavements, and the tests done by Kesler and others (Ref 12) were each developed to obtain specific concrete fatigue properties.

Different fatigue curves are obtained, owing to the nature of the test and failure criteria assumed. Figure 3.2 (page 13) compares four fatigue equations for thickness versus number of applications, using an

elastic modulus-reaction of subgrade ratio of 100,000 and a concrete flexural strength of 600 psi. Considerable variability exists between these curves, which change as the properties used in the analyses change. These equations are also based on different failure criteria. The ARE equation is based on 50 feet of cracking per 1,000 square feet, while the others are based on the present serviceability index.

The knowledge gained from the tests previously mentioned can be used to develop a fatigue equation for bonded concrete overlays. Before such an equation can be developed, the various factors influencing the long-term performance of bonded concrete overlays should be considered because of the difference in structural layout of an overlaid pavement versus a normal concrete pavement. This chapter, therefore, considers factors that influence the long-term performance of bonded concrete overlays. These factors can then be used in a sensitivity analysis to obtain the most significant variables, which will then be used in the development of a bonded concrete pavement design model.

3.2 STRUCTURAL SYSTEM

The structural system covers the physical layout of the bonded concrete overlay system. Figures 3.3 through 3.5 illustrate the various factors that influence the long-term performance of the system. Each of these factors is discussed in the subsequent paragraphs. Most of these factors influence the pavement displacements and, therefore, the stresses within the pavement which can cause structural damage and eventually lead to fatigue failure. Figure 3.3 illustrates the factors inherent in the existing pavement system (before the overlay is placed) that will influence the long-term performance of the bonded concrete overlay.

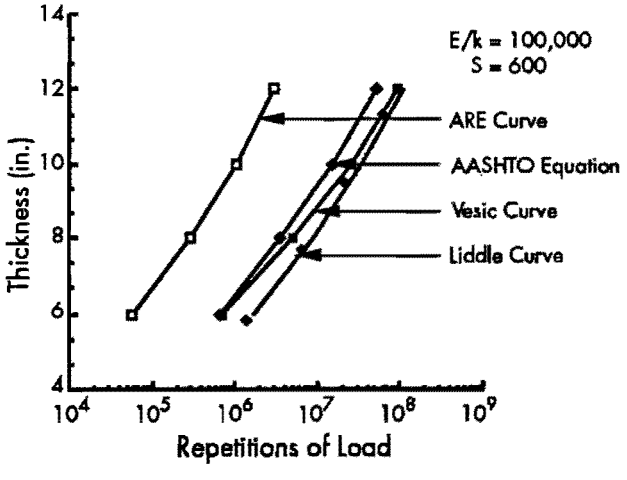

Figure 3.2 Comparison of different fatigue equations

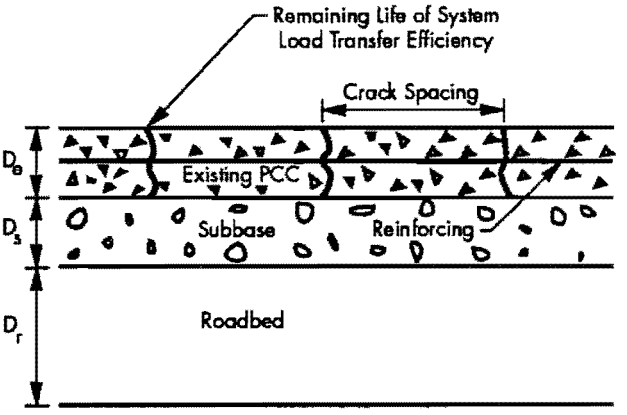

Figure 3.3 Existing structural systyem factors that will influence the fatigue life of bonded concrete overlays

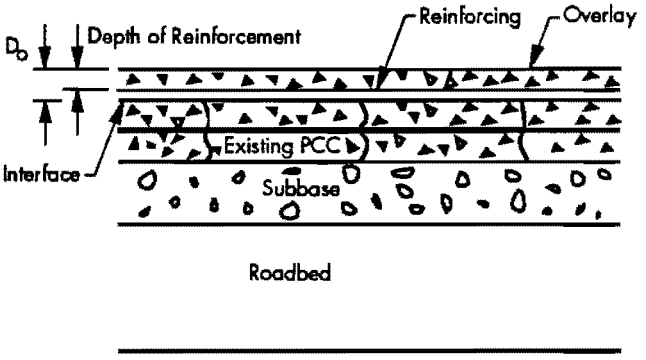

Figure 3.4 Overlay factors that will influence the fatigue life of bonded concrete overlays

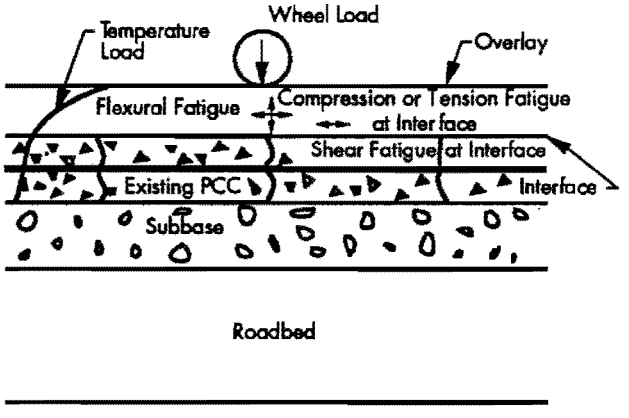

Figure 3.5 Loads influencing fatigue life

The purpose of the bonded concrete overlay is to strengthen the existing system. The thicknesses of the layers in the existing system influence stress development in the overlay. The amount of reinforcing present, the number of existing cracks, and the load

transfer efficiency at the crack are also very important, as is the remaining life of the existing system. Figure 3.4 shows the factors within the overlay that influence the long-term performance of the system: the thickness of the overlay, the quality of the bond between the existing pavement and the overlay, the percentage reinforcing, and the construction procedure.

Figure 3.5 shows the influence of the loading on the pavement. Fatigue loading creates stresses within the pavement that cause flexural fatigue. However, at the interface weak zone (caused by the bond between old and new concrete) compression, tensile, or shear fatigue failure may occur, as the result of wheel loading or environmental conditions.

3.2.1 Existing Pavement System

3.2.1.1 Layer Thicknesses

The different layer thicknesses of the system to be overlaid are important to the long-term performance, because they influence the stresses that will develop in the concrete layers under wheel loading. These thicknesses, with the various material properties, are variables that need to be addressed in a stress analysis. In the overlay design procedure, the existing pavement layers are normally fixed because the layers were constructed many years before the overlay design and construction. The roadbed thickness can vary and can be finite or infinite. The depth of a solid layer underneath the concrete pavement influences the deflections considerably. The closer the solid layer is to the concrete pavement, for the same system, the lower the stresses. However, the subgrade material between the pavement and the solid layer could be weaker because of trapped water. This can increase the chances of pumping. Depending on the analysis program used, the thickness of layers can be modeled into either a modulus of subgrade reaction or an actual thickness. By changing these thicknesses, the variation in stresses can be calculated.

3.2.1.2 Percentage Reinforcing

The purpose of the reinforcing in the pavement is to control environmental stresses, i.e., to control cracks if they occur. It also serves as a partial load transfer device at the crack. The condition of the reinforcement at the time of overlay placement is, therefore, important. If it is rusted through, the effect it has on load transfer, as well as on the crack width, will be nonexistent. The governing stress at the crack changes from an interior stress condition to an edge stress condition. Both these factors will influence stress development in the overlaid system.

3.2.1.3 Remaining Life of Existing Pavement

The remaining life and the subsequent load transfer ability of the existing pavement influence crack formation in the new overlay. With repeated loading the manner in which these cracks propagate is important. If the remaining life of the existing pavement is low, the existing pavement condition may be reflected into the overlay, resulting in premature failure. There are many methods for calculating the remaining life. The AASHTO Design Guide (Ref 1) discusses methods for making this important calculation.

3.2.1.4 Cement-Treated Base

The existing concrete pavement is normally evaluated by calculation of its remaining life, as described above and in the AASHTO Design Guide. However, the cement-treated base is also exposed to fatigue loading, which results in a reduction of stiffness. The weakening of this layer caused by fatigue stresses can be important and may be modeled by decreasing the cement-treated base (CTB) layer stiffness.

3.2.1.5 Crack Spacing in Existing Pavement

The crack spacing in the existing pavement is also an important factor. With very closely spaced cracks, an old rigid pavement may react more like a flexible pavement than a rigid pavement. The larger the crack spacing in the existing pavement, the more the pavement behaves as a JCP with reduced load transfer. The crack spacing will influence the stress development as well as the crack propagation within the overlay pavement.

3.2.2 Overlay

The existing pavement is part of the boundary conditions that exist when the overlay is placed. As the overlay strength increases, the development of cracks is very similar to the occurrence of cracks in the existing pavement.

3.2.2.1 Construction

Studies completed and underway at The University of Texas at Austin show that the first few days, especially the first 18 hours, can be extremely important for the sound development of the overlaid system. Delamination was found in one test section on the South Loop of IH-610 in Houston within the first 34 hours.

Sound construction techniques include concrete placement to specifications including good compaction, correct preparation of the interface, good curing, frequent monitoring of the environmental factors

influencing strength development of the concrete, and adjustments if needed. These factors are necessary to reduce early-age delamination, in order to increase the long-term performance of the system as a unit.

3.2.2.2 Interface Bond

Delamination occurs at the interface because of the 'weak' zone created during construction. It is, therefore, important to create a clean rough surface to provide good bond. Not only is good shear bond necessary, but so is tension bond. Studies at The University of Texas at Austin have evaluated different interface materials and construction techniques that will create good bond strengths in shear and tension.

3.2.2.3 Overlay Thickness

The overlay thickness will change the stress levels obtained and, therefore, will also change the long-term performance of the system. The thicker the overlay, the less influence the existing pavement has on the long-term pavement performance. It was mentioned in previous chapters that the Corps of Engineers equation is based on an accelerated test in which the overlay thickness was 17 inches over 11 inches of good existing pavement. A thin bonded overlay on an 8-inch pavement with normally higher stress levels will act differently in its distress development, compared with the previous tests with thick overlays.

3.2.2.4 Percentage Reinforcing

The percentage reinforcing in the overlay will reduce crack propagation and deterioration. The position of the reinforcement may also be an important factor and should be investigated. On a test section with a 4-inch overlay on an 8-inch existing pavement in Houston, the reinforcement was placed at the bottom of the overlay (at the interface). This procedure has provided excellent performance and was based on fatigue tests of small-scale slabs and extensive bond testing.

3.2.2.5 Crack Spacing in Overlay

The overlay crack spacing is dependent on the environmental conditions, and type of material and reinforcing, as well as on the interface bond strengths and applied loads. It is further dependent on the early-age performance of the overlay. Shrinkage and temperature differentials cause cracking before the overlay is opened to traffic. The development of these cracks is important in long-term performance because of the interaction with the existing pavement, which will have different stiffnesses at cracks versus uncracked areas. This difference in stiffnesses, together with specific crack spacing in the overlay, can reduce load transfer ability at cracks very quickly and cause punchouts, spalling, or other types of distress.

3.3 MATERIAL PROPERTIES

Portland cement concrete, reinforcing bars, and other construction materials are normally subject to certain specifications. These specified material properties are then used in modeling the materials in the system being analyzed. For bonded concrete overlays, material properties influence the stress development within the structure, which in turn affects the long-term performance of the pavement structure. The most important properties used in pavement stress analyses are modulus of elasticity, Poisson's ratio, coefficient of thermal expansion, compression strength, shear strength, tensile strength, reinforcing yield strength, and interface shear and tension strength.

3.3.1 Modulus of Elasticity

Temperature and wheel load stresses are a function of the modulus of elasticity of the concrete. For the composite overlaid system, the ratio of the modulus of the existing pavement concrete and that of the overlay concrete is also important because the stress levels will change as the ratio changes. The subbase and roadbed modulus values are also important for modeling the existing support of the new pavement.

3.3.2 Coefficient of Thermal Expansion

This property varies for concrete made of different aggregates and is important in stress calculation because of temperature differentials. For the overlaid structure these values are extremely important for obtaining stress within the concrete. The importance of this parameter is discussed later when the influence of subgrade and roadbed temperatures on the concrete surface layers is analyzed.

3.3.3 Poisson's Ratio

Poisson's ratio is the ratio of unit lateral strain to unit longitudinal strain. Varying this property may vary calculated stress values. Suggested Poisson's ratios for concrete and subsurface materials vary, and this variation must be analyzed to evaluate its influence on stress values in the model used.

3.3.4 Interface Shear and Tension Strength

The interface is a "formed weakened plane" and delamination of this weakened plane depends on the bond and shear strength between the existing pavement and the overlay material.

3.3.5 Reinforcing Yield Strength

The type of reinforcing bars used, specifically their yield strength, can be a factor in the design. Reinforcing is normally used as a crack control device and can increase fatigue life if it keeps cracks well spaced and with small widths.

3.3.6 Curing Temperature

The curing temperature is normally used to calculate temperature differentials within a rigid pavement. Curing temperature is not well defined. Some designers (Ref 13) believe it is the temperature at final set. Many others have different ideas. However, the curing temperature should be that temperature at which the concrete starts developing strains as it is starting to resist loads. This concrete temperature will then start to follow the daily temperature cycle as it absorbs or loses heat from or to the environment. However, at the early stages this change of concrete temperature in phase with the environment cannot be mathematically explained, owing to influences that may retard this phenomenon, in which the concrete temperature is in phase with ambient temperature.

3.4 FATIGUE OF CONCRETE

In the previous paragraphs the material properties influencing the long-term performance were discussed. Although concrete fatigue strength is stress dependent and, therefore, also a material property, it is also dependent on the induced loading. Therefore, it is handled as a separate factor.

Webster's New World Dictionary defines fatigue in several ways. One definition is "to weary with labor or exertion." Another, and a more appropriate definition for fatigue in concrete, is "the tendency of a material to break under repeated stress." The fact that fatigue is present in portland cement concrete is well known. After van Ornum performed compression fatigue tests on beam and bond specimens, he concluded (Ref 14) that "certain observed peculiarities in tests of concrete led to the conclusion that brittle engineering materials (such as stone, brick, mortars, concrete and others), of which cement mixtures are a 'fair' type, possess the property of progressive failure or 'gradual fracture,' which becomes complete under the repetitions of load well within the ultimate strength of the concrete." However, the mechanism of fatigue failure, the variables affecting it, and the projection of fatigue life are uncertain in many instances.

A wide variety of opinions about this are available in papers and research reports, primarily because, as Murdock (Ref 15) pointed out, research into fatigue of concrete has been very sporadic. Previous research studies were concerned only with a problem needing immediate attention, which created information on fatigue in a very uncorrelated way. Most of the research was done on axial and bending fatigue of concrete. One of the few tensile fatigue tests was done in 1898, by De Joly (Ref 15). Some researchers assume that tensile fatigue is closely related to bending fatigue, which may have increased the reluctance of researchers to continue research on tensile fatigue. Axial tension testing is also difficult to perform in the laboratory, which makes it natural to prefer flexural fatigue testing. In concrete pavements, we are mostly concerned with bending fatigue, but axial and shear fatigue should also be kept in mind. In bonded overlays a "weak zone" exists at the interface, which may deteriorate as the result of axial and shear fatigue loading.

Before discussing the anticipated mechanism of failure in portland cement concrete and the factors influencing fatigue in concrete, two definitions should be mentioned. It was long believed that concrete has a so-called fatigue limit. The fatigue limit of concrete is the percentage of the static ultimate tensile strength of the concrete at which the amount of repetitions will not cause failure. Some researchers have found (Ref 14) that concrete does not have a fatigue limit. Another definition used in discussing fatigue of concrete involves the fatigue strength. The definition varies among different researchers but states basically the percentage of the static ultimate strength at which the specimen will fail, after, for example, 10 million cycles. The data from fatigue testing are normally expressed in a so-called S-N curve. This shows the relationship of stress ratio (stress at test/static tensile strength) versus the log of the number of cycles to failure. Figure 3.6 shows a typical S-N curve. This curve is used here to discuss various factors influencing fatigue of portland cement concrete. It has been modified and adjusted for various experiments.

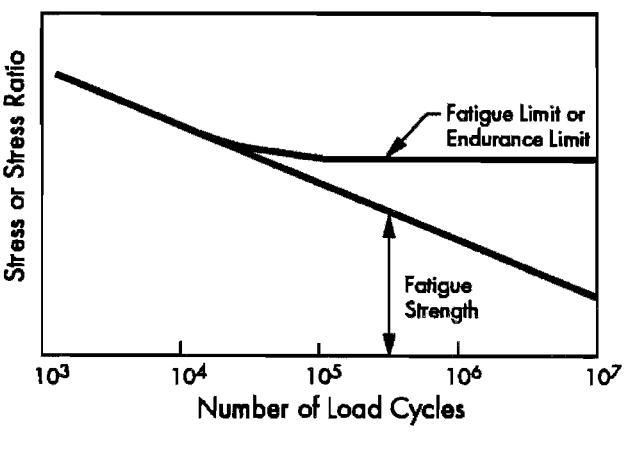

Figure 3.6 Conceptual stress ratio versus log of number of cycles

Knowledge about fatigue of concrete is needed to provide adequate and economical designs of new pavements as well as overlays. It is also needed to improve the knowledge of engineers and to help with interpreting full-scale testing experiments, such as the AASHO Road Test. It is, furthermore, needed to evaluate the remaining life of existing concrete pavements to decide when and whether or not to reconstruct or overlay an existing pavement. Table 3.1 shows the factors important in discussing fatigue of concrete structures. In addition, previous studies of CRCP performance in Texas have revealed that when the rate of failures/year/mile exceeds a value of three, the rate increases rapidly. This value can also be used as a limit that represents the fatigue life of the concrete that is being consumed at a rapid rate.

Table 3.1 Factors influencing concrete fatigue (Ref 14)

Fracture Mechanics	Macro Cracking
	Micro Cracking
Factors Influencing Fatigue of Concrete	Range of Loading
	Varying Load History
	Stress Gradients
	Load History
	Definition of Fatigue Limit
	Frequency and Speed of Loading
	Age
	Air Content
	Water-Cement Ratio
	Aggregate Type
	Moisture Condition

3.4.1 Concrete Fracture Mechanics

Before discussing the factors influencing the fatigue life of concrete, the fracture mechanism of concrete at the macroscopic and microscopic levels is discussed.

An accurate characterization of fatigue behavior is extremely difficult and very expensive to define through experimental research. Using finite-element methods to model dynamic or fatigue loading is difficult, because there is no universally accepted fatigue mechanism and failure condition.

However, researchers have noted several facts influencing the failure and fatigue mechanisms. Doyle, Kung, Murdock, and Kesler (Ref 16) studied flexural behavior of a cement and fine aggregate matrix using pre-placed coarse aggregates as well as voids. They concluded (Ref 18) that residual stresses caused by shrinkage of mortar around a single, comparatively rigid, unbonded inclusion have no significant effects on either static or fatigue strength. They also concluded that static and fatigue failures initiate in the bond between coarse aggregate and the mortar matrix when the modulus of elasticity of the aggregate is greater than that of the matrix. Neal, Kung, and Kesler (Ref 18) increased the complexity of the experiment mentioned above to investigate the effect of aggregates in close proximity to each other. They concluded that fatigue failure begins at the bond between the coarse aggregate and the mortar matrix and apparently is not influenced by the elastic modulus of the coarse aggregate. In addition, residual stresses caused by shrinkage of the mortar matrix around particles of coarse aggregate are not great enough to influence static or fatigue strength of the specimen or to influence the failure plane.

Antrim (Ref 17) tested cement paste in axial compression as well as on the paste diluted with aggregates. He concluded that, for cement paste, failure occurs because of the formation of small cracks. The formation of the small cracks depends on the water-cement ratio of the paste and the presence of shrinkage stresses in the paste. These crack patterns are slower to develop in concretes with high water-cement ratios, owing to a more flexible paste, which can readjust itself to delay the buildup of stress concentrations. This is also true for concretes with different water-cement ratios, according to Antrim. The fatigue failure occurs as a result of the development of small cracks which, as for the cement paste, are dependent on the water-cement ratio.

Fracture of a concrete matrix can occur (1) where the cement paste is fractured, (2) if the aggregate is cracked, (3) at the bond between aggregate and cement matrix, or (4) when there is a combination of these. Many investigators also conclude that the mechanism of fracture is the same for fatigue and static loading. The fracture of concrete is well described by Kesler (Ref 12). The fractures develop from macrocracks, and the size of macrocracks is increased by microcrack propagation.

3.4.1.1 Macrocracking Propagation

Concrete is not a homogeneous material, which makes the fracture process a more complex phenomenon. When concrete is first placed, hydration, shrinkage, and other factors act to increase stress, which becomes so high that some areas in the matrix are stressed to the limiting strength of the matrix, if the matrix is adequately restrained within the structure. These stresses are normally larger than the average shrinkage, environmental, and applied load stresses. If the stress is larger than the limiting stress, macrocracks are formed. Macrocracks can also be formed by sufficiently large applied loads. At the tips of these macrocracks, high stress concentrations are created that initiate microcracks to relieve the matrix from high tensile stresses. This will continue until the energy input is insufficient to create new microcracks. It appears that there is some limit to the

energy absorption, which is uniformly distributed over the cracks. This energy is stored until there is a sufficient energy supply to initiate further propagation of cracks. Crack propagation of these macrocracks follows microcracks that are favorably oriented. Because it is easier for the macrocracks to propagate into microcracks than to create a new crack, other cracks will normally be a certain distance away. Thus, the mechanism of fracture at the macroscopic level involves the propagation of macrocracks through the paste matrix or aggregate-paste interface from microcracks at the tip of the crack. Repeated stress creates additional energy, which in turn develops internal damage from which crack growth is initiated.

3.4.1.2 Fracture at the Microscopic Level

There is considerable evidence to show that microcracks occur in concrete when it is loaded (Ref 19). Kesler (Ref 12) states that the fracture at the microscopic level appears to be directly related to the interaction between primary and secondary bonds present in the matrix. The secondary bonds will fail first because of the lower strength and will try to create a stress state compatible with the applied load. Primary bonds, such as van der Waal's forces, are overstressed but, if the loading is low enough, the stability within the matrix will be restored. However, the energy input at certain loads may be high enough to cause the further development of macrocracks and eventually result in failure. The total crack surface exceeds the area of the main crack surface and the total surface energy is greater than the energy required to form only the main crack. Tests show that fracture initiates at the aggregate matrix bond (Ref 20). It initiates from the aggregate-mortar interface because of the presence of a pre-existing crack or what will be a crack at first loading.

3.4.2 Factors Influencing Fatigue Life of Concrete

With time, researchers have carried out studies concerning many factors that were assumed to affect the fatigue strength of concrete. Some assumptions proved valid, whereas others proved to be not significant. Many of these factors affect the fatigue life of concrete in a way similar to the way in which they affect the static ultimate strength. To help understand the concept of fatigue, the most important factors are discussed, with more emphasis on their influence on fatigue life than on their historical development.

3.4.2.1 Range of Loading

The definition of fatigue strength, as discussed before, was developed for test specimens loaded in either compression, tension, or flexure until failure. A value of 55 percent of the static ultimate strength for fatigue strength is very common in the literature. If the range of loading is changed, the number of repetitions until failure is also changed. This behavior is illustrated best by the so-called "Modified Goodman Diagram," shown in Figure 3.7, which is valid for only 2 million cycles. The Goodman diagram is well known for its use in connection with the fatigue of metals, but Grab and Brenner, as discussed by Murdock (Ref 15), modified the diagram for concrete compressive loading. The diagram illustrates the effect of loading range on concrete fatigue by relating fatigue strength to the maximum and minimum stresses to which the concrete is subjected.

The diagram is entered on the left, with the minimum stress, which is, for example, 1,700 psi. One then moves horizontally to the 45-degree line, proceeds vertically to the upper curve, and moves horizontally to the left-hand side of the diagram. The value, which is 2,260 psi for the case in Figure 3.7, is the maximum stress value the concrete can be subjected to in order to reach 2 million cycles before failure. The diagram was developed using compression testing on about 100 specimens, of which some were loaded to more than 2 million cycles before failure. The stress range is (1 – 1,700/2,260), which is 0.25. The maximum stress level is (2,260/2,550), which is 0.88.

The effect of the range of stress is also apparent from Figure 3.8, which shows the relation between stress range, R, and the number of cycles to failure, n_u, for constant maximum stress levels.

For stress levels below the sustained load strength of concrete, the relationship between R and

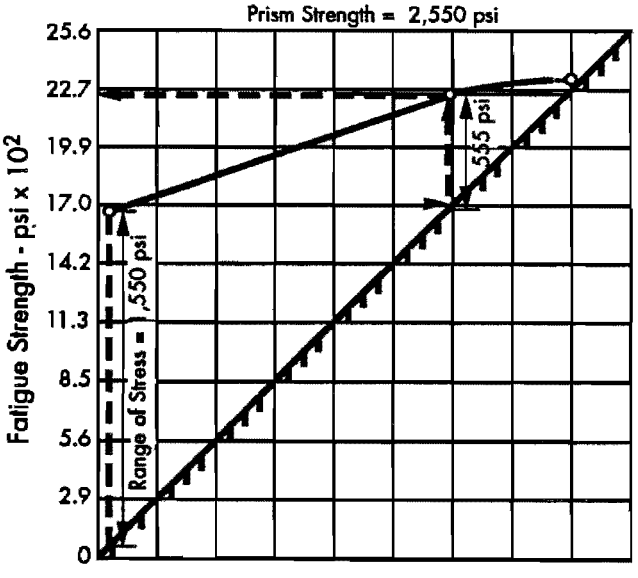

Figure 3.7 Modified Goodman diagram (Ref 15)

n_u should approach the horizontal axis asymptotically to give an n_u of infinity for an R value of 0. That is, however, not the case for basically all stress levels for R smaller than 0.5. At these stress levels the maximum stress is well above the sustained load strength. In this case, the time for which the specimen has to sustain the loading becomes more important than the number of cycles before failure. Therefore, a further reduction in the value of R does not result in a significant increase in cycles to failure. Therefore, it appears from the figures that the fatigue strength is dependent on the range of applied stress and increases as the range of stress is reduced.

The Modified Goodman Diagram was also developed for fatigue testing of concrete for 10 million cycles, as shown in Figure 3.9.

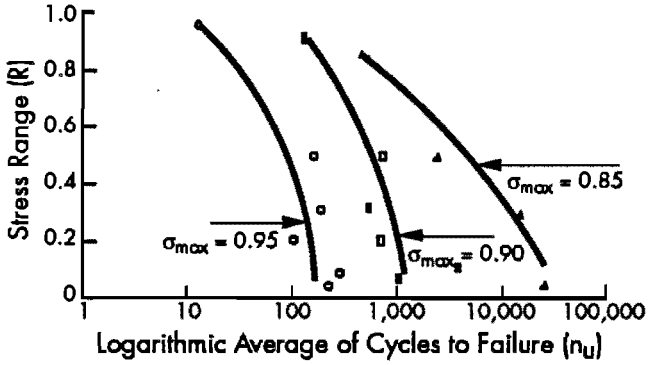

Figure 3.8 Relationship between stress range and number of cycles to failure for different maximum stress levels (Ref 33)

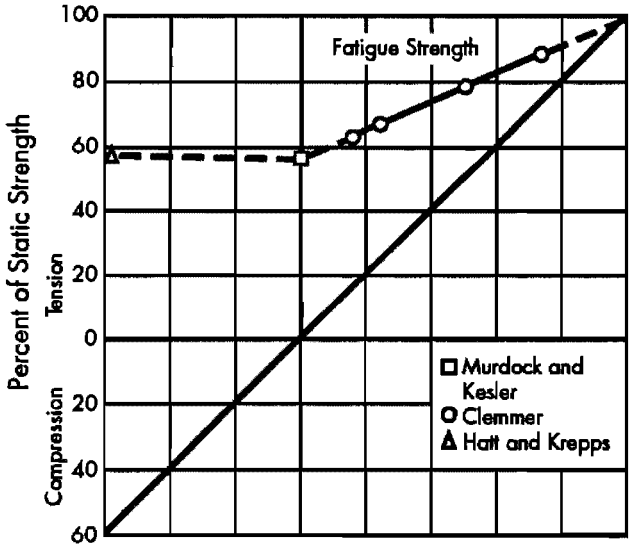

Figure 3.9 Modified Goodman diagram showing the effect of range of loading on the fatigue limit of plain concrete under repeated flexural loading (Ref 16)

For flexural loading, Murdock and Kesler (Ref 15) concluded that the range of stress does effect fatigue response and that a greater fatigue strength may be obtained if the range of stress is reduced, which is similar to conclusions made from compression fatigue tests.

Award and Hilsdorf (Ref 21), after testing some 300 test specimens, came to the following conclusion, which sums up the effect of range of stress on concrete fatigue very well: when concrete is subjected to high repeated compressive stresses, a decrease in either the maximum stress level or the stress range results in an increase in the number of cycles to failure, which is also true for flexural stresses, according to other researchers such as Murdock (Ref 15). The increase in failure cycles with decreasing stress range becomes insignificant at high maximum stress levels and small stress ranges. Also, the failure strains of concrete under repeated loads increase with decreasing stress level or decreasing range of loading. Award and Hilsdorf subsequently developed an analytical procedure to predict fatigue properties of concrete for various stress ranges and stress rates.

3.4.2.2 Varying Load History

Some tests have been done (Ref 22) using varying flexural stresses. Three different loading systems were used. First, a specimen was loaded with a number of cycles at a given stress, and the stress was then increased and kept up until failure. Second, a specimen was loaded with a number of repetitions at a high stress level, and the stress was then reduced and maintained until failure. The third load system was a combination of these two systems. The specimens were loaded until failure with alternating high and low stress levels. The results showed that specimens subjected to a low stress level and then a higher stress level until failure showed a shorter fatigue life than specimens loaded at the high stress level throughout the tests. A brief period of high stress level loading followed by a lower stress level resulted in a longer fatigue life than that of a specimen loaded at the lower stress level throughout. The effect of the third loading condition is discussed later, when Miner's hypothesis is introduced.

According to Holmen (Ref 23), loading histograms with lower minimum stress levels seems to cause a compounding of load effects and is therefore more damaging. The presence of small amplitudes in the loading histogram seems to reduce the sequence effects. Small amplitude loading is therefore favored.

3.4.2.3 Stress Gradients

Ople and Hubbes (Ref 12) found that the stress gradient has a significant effect on the fatigue strength of concrete in compression. They found the

static ultimate strength of a non-uniformly stressed specimen to be approximately 17 percent greater than when the stress is uniformly distributed. They suggested that the fatigue strength of uniformly stressed specimens be used as the lower limit for flexural members in which compression stresses control.

3.4.2.4 Load History

Van Ornum (Ref 24) concluded that for compression members the stress-strain curve varies with the number of load repetitions as the convex upward curve gradually straightens under repeated loading and eventually becomes concave upward near failure. The degree of concavity indicates how near the test was to approaching failure. The total effect was noted only for those specimens stressed above the so-called fatigue limit. Research showed that repeated loading at a level less than the load that will cause failure at 10 million cycles increased the static and fatigue strengths of concrete (Ref 12). Clemmer (Ref 14) noted that beams subjected to a certain load history could resist a greater number of applications of load at an increased stress intensity as long as the first stage of loading was below some critical value. It was also found that rest periods increased the fatigue strength of concrete. It was found (Ref 15) that rest periods of between one and five minutes could be beneficial. However, the rest periods on highways during peak hours are lower than two minutes. In general, it was found that, for a given probability of failure, rest periods permitted a greater number of applied cycles of loads but that the probability of failure at a given stress level and at a given number of cycles of load was reduced if rest periods were introduced in the loading cycle.

3.4.2.5 Definition of Fatigue Limit

Earlier studies showed the existence of a fatigue limit. Mills and Dawson (Ref 15) found the fatigue limit for compression members to be 50 percent of the static ultimate strength of concrete. Van Ornum failed, in 1903, to produce a fatigue limit on 2-inch concrete cubes. Clemmer found this limit to be between 51 and 54 percent for concrete in flexure. Kesler (Ref 14) did some testing at the University of Illinois and did not find a fatigue limit, which is also known as an endurance limit. An example of this "limit" is shown in Figure 3.6. Subsequent tests proved that no fatigue limit exists up to 10 million cycles and it is now assumed that no fatigue limit exists for concrete in compression or flexural tension up to 10 million cycles of loading.

3.4.2.6 Frequency and Speed of Loading

Concrete specimens in compression tests showed no significant effect of the speed of testing; however, very low frequencies of applications of load resulted in somewhat smaller fatigue strengths. For flexural fatigue of concrete, Kesler found that the influence of the speed of testing is not significant for the range of frequencies he used (Ref 25). He recorded tests in which the frequency of loading was changed from 70 to 900 cycles per minute and found no significant difference. Frequencies of less than 10 cycles per minute may, however, result in slightly lower fatigue lives.

3.4.2.7 Age of Concrete

Older concrete specimens exhibit higher elastic properties than green concrete which increase its ability to resist stress. Age and curing, therefore, have a huge effect on concrete. Aged, well-cured concrete has more fatigue life than concrete that is inadequately cured and aged. Raithby and Galloway (Ref 26) reported a substantial increase in fatigue endurance with age. Their tests ran over a three-year period. They also reported that a lean mix produces earlier fatigue failure than higher-quality concretes.

3.4.2.8 Air Content

In a review of fatigue research, Murdock concluded that the fatigue response of concrete compression members, in terms of static ultimate strength, is independent of air entrainment. He came to the same conclusion for flexural fatigue in concrete. Other research has contradicted these findings. Klaiber and Lee (Ref 27) did tests on concrete specimens at five different levels of air entrainment. They concluded that the fatigue strength of concrete in flexure is reduced as the air content increases. As the air content increases, the failure of concrete increasingly occurs at the aggregate and cement-paste interface. Therefore, failure around the aggregate, rather than through the aggregate, predominates. Limestone and gravel aggregates were used in their experiments. They also found that, for similar air contents, the failure surface for gravel tends to be at the gravel-cement interface, whereas for the limestone concrete the cracks went through the limestone aggregate.

3.4.2.9 Water/Cement Ratio

There is a slight but insignificant decrease in fatigue strength for concrete compression members, and there are corresponding increases in water/cement ratio (w/c). Klaiber and Lee (Ref 27) found that flexural fatigue w/c ratios of 0.4 to 0.6 showed no difference in fatigue strength. The fatigue strength is, however, decreased for a low w/c ratio, for example., 0.32.

3.4.2.10 Aggregate Type

It was mentioned in a previous paragraph that the failures of gravel and limestone are different, in

the sense that limestone tends to fail through the aggregate, and a gravel aggregate fails at the aggregate-cement interface. For compression members, most researchers concluded that aggregate type did not affect the fatigue strength of the concrete significantly. Klaiber and Lee (Ref 27) found that, for flexural concrete specimens at high stress levels, the gravel specimens performed better in fatigue than did limestone specimens. However, at lower stress levels there seemed to be no significant difference between the two aggregate types. They also concluded that differences in fine aggregate content did not influence the fatigue performance of the concrete.

3.4.2.11 Moisture Condition

Raithby and Galloway tested beams in flexure at different stages of drying out. They found that oven-dried specimens gave better fatigue results, as shown in Figure 3.10.

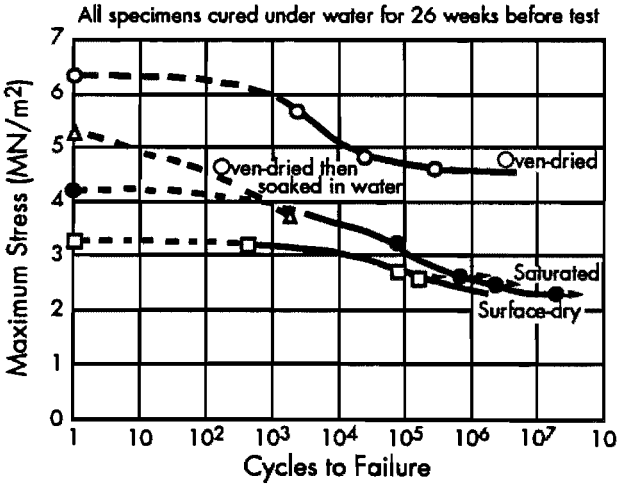

Figure 3.10 Effect of moisture condition on fatigue of concrete (Ref 26)

Saturated, surface-dry specimens gave the worst performance. The reason for this phenomenon was not specifically investigated, but it is possible that a dried out specimen is much stronger, due to the closeness of particles. The van der Waals forces in concrete depend on the inverse of the squared distance between particles: the closer together the particles are, the stronger the van der Waals forces, and, therefore, the higher the energy input required to initiate cracking.

These findings agree with those of Kesler and Chang (Ref 28), who conclude that specimens of increased moisture content exhibit a somewhat lower fatigue strength than specimens tested dry.

3.4.2.12 Conclusions

It can be concluded from the above summary that various factors influence the fatigue of concrete. The data available on the fatigue of concrete, as applicable to highways, are very limited. The frequency of loading and number of applications until failure, of the data available, falls outside the inference base of highways. It is, therefore, difficult to use the data directly with portland cement concrete pavements.

3.5 STRESSES IN THE PAVEMENT SYSTEM

The stresses in the pavement can be caused by the environment (which includes temperature, moisture, and shrinkage) and by wheel loading.

3.5.1 Wheel Loading

Wheel loading is the most important dynamic load on a pavement system. The AASHTO Design Guide (Ref 1) uses an 18,000-lb load as datum load and converts all other loads to 18-kip equivalent single axle loads (ESAL). The influence of overloading on pavement performance is enormous, and the influence on a thin bonded concrete layer should be analyzed. Wheel loading also varies significantly between light cars and heavy trucks, which can carry loads up to a specified legal limit.

It was mentioned before that varying loads has an impact on the fatigue life or performance of concrete structures. With pavements, this variability is extremely difficult to evaluate or to simulate. On any major highway the loading imposed on the pavement by cars and trucks varies significantly. Of the two, trucks are more important, and the effect varies because trucks are not always loaded to the legal limit and some are overloaded. Depending on the freight carried, the weight can vary between the unloaded truck weight and the operating value. Therefore, although the weight influences the long-term performance, it is normally converted to 18-kip ESAL, which was the legal load at one time. The variability in the loads is, therefore, accounted for by converting the weight to one load case. The conversion is done by using either stress or deflection, which are indications of the damage done on the pavement, as the criterion.

The variation in weight may contribute to the fact that the fatigue lives of concrete pavements are often underestimated. For instance, the South Loop of IH-610 in Houston, Texas, is approximately 30 years old. With the enormous growth in vehicle usage of this highway during that time, the pavement probably reached its design traffic load long ago. However, major rehabilitation projects were started only in 1986.

3.5.2 Temperature Stresses

Temperature differentials cause the concrete to curl, either up or down. Stresses are developed because of this curling, which is the result of a

temperature differential between the top and the bottom of the concrete pavement. These stresses can either increase or decrease the stress within the pavement when a wheel loading occurs simultaneously with the temperature stress. This will depend on the time of day as well as the season. A further influence on concrete stress can be the temperature differential within the subgrade and the stresses resulting from this movement.

Temperature loading is not only a daily variation; it also varies with the season. This makes the curing temperature, previously discussed, very important, especially when the existing concrete pavement was placed in, say, winter and the overlay in summer. This will induce different temperature differentials, which in turn will induce different movements in each layer. These movements will effect stress development and subsequent crack propagation within the system.

3.5.3 Shrinkage and Moisture

Drying shrinkage is the reduction in volume of concrete caused by the loss of water. To reduce the shrinkage at an early age it is important to provide enough water for hydration of the cement paste. Together with drying shrinkage, moisture changes in the concrete result in differentials, which can cause stress variations. It is extremely difficult to establish the magnitude of these stresses.

However, it was found by Janssen (Ref 30) that significant drying shrinkage can be expected to only a shallow depth of the pavement. For his sets of conditions the stress exceeded the strength of a concrete specimen for 3/4 of an inch into the concrete. A typical moisture distribution is shown in Figure 3.11.

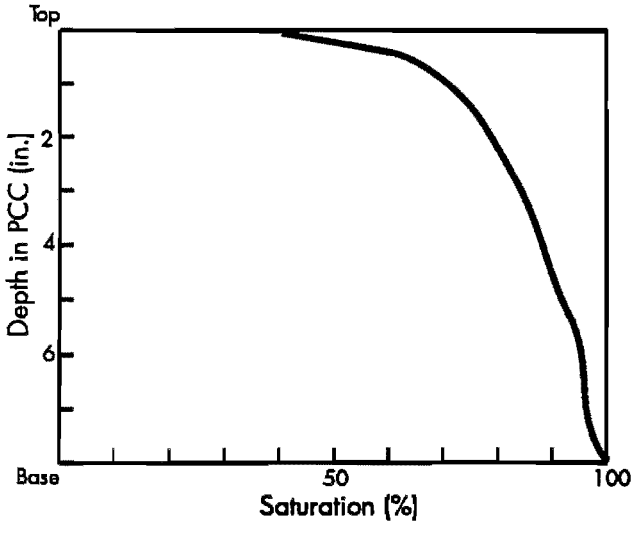

Figure 3.11 Moisture distribution in concrete (Ref 30)

From this discussion, it is concluded that the effects of temperature contraction and expansion cause more full-depth cracks than movements resulting from moisture changes. Moisture changes will create high tensile stresses in the top surface, which will create hairline cracks. These cracks acts as stress relievers, which, by forming a weakened zone, reduce shrinkage stresses caused by moisture, which in turn reduces curling stresses. This is especially true for well-cured concretes with water/cement ratios below 0.45, where not much excess water is available. For modeling purposes, the shrinkage can be part of the temperature distribution, which will increase the differential if upward curling exists or decrease the differential if downward curling exists.

3.5.4 Range of Stress

Range of stress is another important parameter discussed earlier. For rigid concrete pavements, the range of stress will vary from the stress induced by temperature stress to an upper stress, which is a combination of temperature and load stresses. This range can be incorporated in any model, but again it is based on legal limit loads and variability is ignored. Current highway fatigue equations were empirically developed; they include the factor of range of stress. If an existing fatigue equation is used, the effect of range of loading can be ignored.

3.6 FAILURE CRITERIA

The failure criteria are important, because they are the basis of design. The point of failure is the time the structure is either unsafe to use or has adverse effects on the users of the facility. For overlays, the extent of the problem is increased because of different types of fatigue. The different types are discussed in the following paragraphs.

3.6.1 Types of Fatigue in Bonded Concrete Overlays

Four types of fatigue may exist in the system. It may be either flexural or compression fatigue of the pavement, and compression, tension or shear fatigue at the interface between the overlay and the existing pavement. This is conceptually shown in Figure 3.12.

3.6.1.1 Flexural Fatigue (σ_F)

The normal loading expected on highways and other road systems is wheel loads from cars and trucks. This loading condition creates tensile stresses within the structure, which can lead to fatigue failure, caused by the repetitive nature of the loading. The number of loads expected during the pavement lifetime is, therefore, an important parameter. The AASHTO Design Guide uses 18-kip equivalent single axle loads (ESAL) as the design parameter. The further reduction of fatigue in the existing pavement as

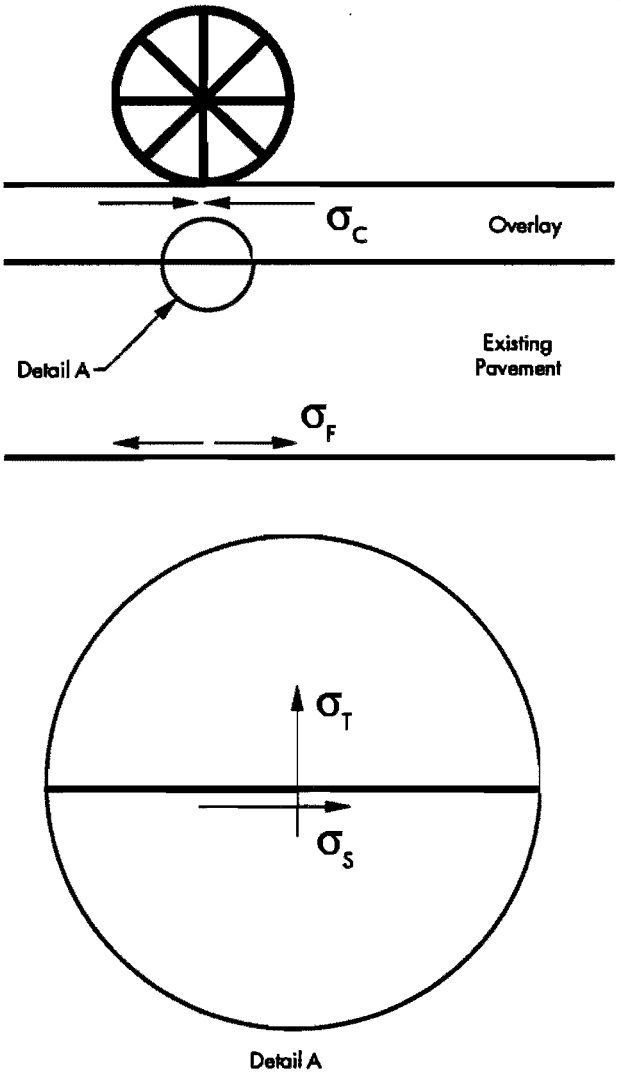

Figure 3.12 Layout of fatigue stresses in an overlaid system

well as in the overlay should be investigated. It was mentioned before that the higher the stress range of loading, which is the highest versus the lowest stress level, the shorter the fatigue life. Overloaded trucks and heavily loaded vehicles are, therefore, the main loads causing damage to the road system. Environmental stresses could be added to the wheel loads to obtain the total stress in the pavement. The repetitiveness of temperature loading is less frequent than wheel loads because the loading follows the ambient temperature. The magnitude of temperature loads is therefore more important than the dynamic effect. Loads induced by moisture add to or reduce the temperature effect.

3.6.1.2 Compression Fatigue (σ_C)

An unknown factor in the overlaid system is the effect of compression fatigue in the overlay. Compression fatigue tests have been done on concrete before, but not on specimens with an interface layer within the specimen. This could be a failure mechanism as the overlaid system reaches its design life.

3.6.1.3 Shear Fatigue (σ_S)

Another problem with repetitive loading is shear fatigue at the interface. Very few, if any, shear fatigue tests have been run on specimens. Shear fatigue can reduce the effective shear strength and eventually cause delamination and punchouts.

3.6.1.4 Tension Fatigue (σ_T)

Tension fatigue at the interface can be caused by environmental loads. Although the effect will not be as extensive as that of shear and compression fatigue at the interface, it may supplement the forces creating shear and compression fatigue when the interface is in tension caused by temperature and a passing load creates a shear or compression fatigue, thus reducing the compression force at the interface.

3.6.2 Failure Mechanism

Each of the above-mentioned fatigue failures can have its own failure mechanism. It is normally assumed that flexural fatigue causes failure in concrete pavements. This, in effect, states that failure will always result from transverse cracking followed by longitudinal cracking and punchouts for CRCP. However, because of the different fatigue types in bonded concrete overlays, failure can also occur as the result of a combination of horizontal cracks at the interface and transverse or longitudinal cracking. The failure mechanism also consists of the factors influencing fatigue life that were described previously. If the failure mechanism is known, the failure criteria can be established.

3.6.3 Failure Criteria

With the previous section in mind, a single unique fatigue failure mechanism for thin bonded concrete overlays may not be present; the failure may be a result of one or more mechanisms. The development of these failure criteria is part of this study and is discussed after a detailed analysis of the overlaid section using a finite-element program.

The failure criterion that agencies across the United States used for developing overlay equations varies. The Corps of Engineers definition of failure is "first appearance of a crack due to wheel loads" (Ref 4). The AASHTO Design Guide uses the same equations for PCC overlays as for new pavements and,

therefore, should apply the same criteria. However, in the thickness design used in the AASHTO rigid equation, there is an equation in which the failure criteria used are Type 3 and 4 cracking, as defined before. The FHWA/Texas procedure also uses Type 3 and 4 cracking as failure criteria. This method, which was modified by Taute, and a mechanistic model proposed by Bagate used a fatigue equation developed by Taute. The failure criteria for this equation is 50 feet of cracking per 1,000 square feet of pavement.

It is, therefore, apparent that different failure criteria have been used in the past. It is, however, important to know what the failure mechanism is before a failure criterion can be established.

3.7 CONCEPT OF DAMAGE

Damage in concrete, especially considering the material variability, is difficult to establish. It is easy to recognize that damage is progressive. The more loads applied, or, in the case of highways and roads, the more applications, the more the damage. How the damage and the number of applications, or load, vary with each other and whether the variation is linear, quadratic, or some other function is unknown. There are also a number of values or parameters needed to evaluate the induced damage. The type of loads, the magnitude, their frequencies, and the total number of applications are needed. The fatigue strength, or number of applications the given material can take before failure, should be known. From the previous sections, it is evident that a correlation between different stress levels and ranges is necessary because they are important parameters when the fatigue strength of concrete is analyzed.

3.7.1 Miner's Hypothesis

To evaluate the amount of damage in concrete pavements, most engineers use Miner's hypothesis for considering varying stress levels. Many engineers use it because no useful alternative exists. Before discussing research that has been done to evaluate Miner's hypothesis, the hypothesis itself is discussed.

In his paper proposing Miner's hypothesis (Ref 31), Miner explicitly states the following assumptions:

(1) The loading cycle is sinusoidal.
(2) The total amount of work that can be absorbed produces failure (under the further assumption that no work-hardening of the material occurs).
(3) The relationship between various stress ratios (ratio of minimum stress to maximum stress) is approximately as shown in Figures 3.13 and 3.14. Figure 3.14 consists of test data as well as R values derived from Figure 3.13.
(4) The inception of a crack, when observed, constitutes failure.

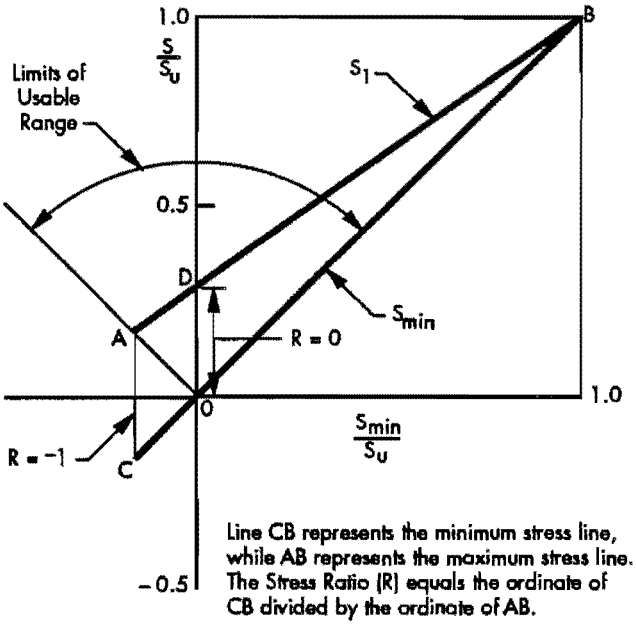

Figure 3.13 Modified Goodman diagram

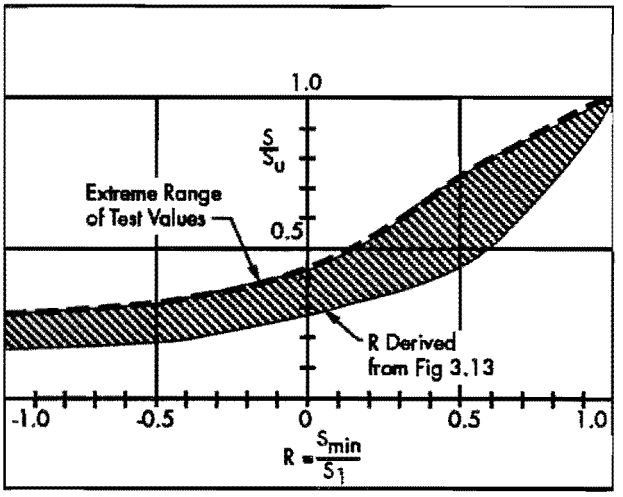

Figure 3.14 Plot of stress versus ratio of minimum to maximum stress in loading cycle showing agreement between straight line from Figure 3.13 and test results

These assumptions are followed by the following limitations to the hypothesis:

(1) Only aluminum alloys were studied in the experimental verification.
(2) Only maximum stresses above the stress at which fatigue failure occurs at 10^7 cycles are to be considered.

Miner reasoned that, if W is the net work or energy absorbed at failure and w_1 is the work done in n_1 cycles, then w_1/W is equal to n_1/N_1, where N_1 is the number of cycles to failure for the stress level at which the n_1 cycles are run. The same equation

holds for a second set of cycles at a different stress level and the total amount should be equal to one, because the work done in each of the stress level cycles should be equal to the total work absorbed at failure W. Therefore,

$$w_1/W + w_2/W + \ldots\ldots + w_n/W = 1 .$$

Substituting this for the number of cycles gives

$$n_1/N_1 + n_2/N_2 + \ldots + n_n/N_n = 1$$

or, in simpler terms, the summation of

$$\Sigma n_i/N_i = 1 .$$

The concept is illustrated in Figure 3.15. The model proposed is called a linear damage model because of the assumption that fatigue damage accumulates linearly. It assumes that the damage is proportional to the stress level and the number of cycles of load. Miner concluded the following:

(1) The concept of cumulative damage holds true for Alclad 24S-T aluminum alloy and probably for the other high-strength alloys.
(2) The hypothesis provides a simple practical means for analyzing fatigue problems.
(3) The hypothesis should be experimentally investigated for steels and other materials to determine its range of usefulness.

Miner's hypothesis was developed for aluminum alloys and is directly used by engineers in the design of concrete pavements. The following paragraphs consider this fact.

Hilsdorf (Ref 15) compared results of tests in which a low and a high stress level were used on the same specimen. One series of test specimens was loaded at a low stress level for a number of applications and then at a higher level until failure. The next series was done by first using a high stress level for a number of cycles and then a lower stress level until failure. In the third series, the high and low stress levels were alternated until failure. For both the first two series of tests, Miner's hypothesis was found to be in error. In the first series the stress level required to produce failure was less than what was predicted, and in the second series the stress level was larger than that predicted.

Kesler (Ref 12) developed design curves that included a probability of failure (see Figure 3.16). This modification gave reasonable results, but it was based on limited experimental data.

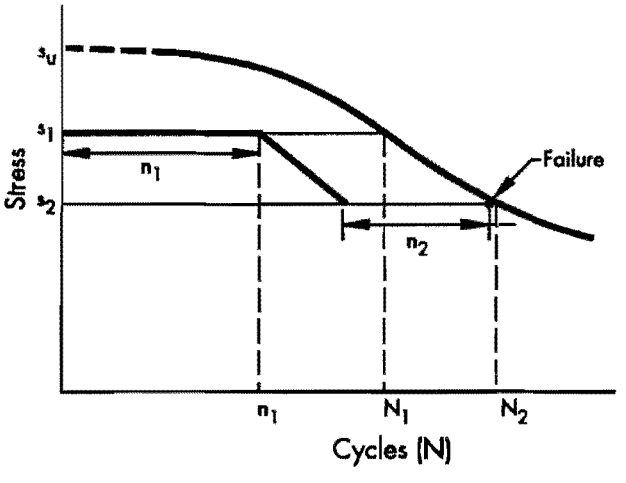

Figure 3.15 Typical S-N curve explaining Miner's hypothesis

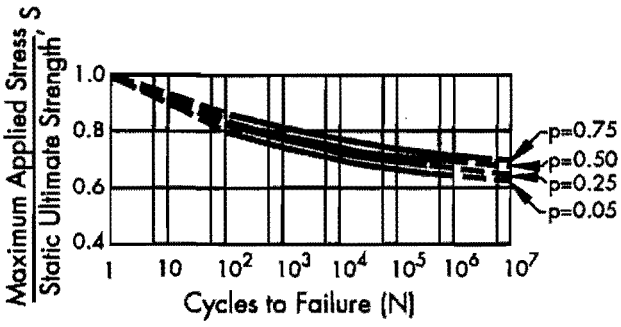

Figure 3.16 Design curves for use with Miner's hypothesis

3.7.2 Experimental Research Evaluating Miner's Hypothesis for Portland Cement Concrete

Holmen concluded that variable loading – specifically, varying amplitude loading – seems to be more damaging than estimated by Miner's hypothesis and attributed this to the sequential effects present in variable loading. Ballinger (Ref 29) did some tests to evaluate the effect of variable loads on the fatigue of concrete and to test Miner's hypothesis. He concluded that Miner's hypothesis represents cumulative damage to plain concrete caused by variable load in a reasonable manner.

Some researchers tried to enhance Miner's hypothesis, but in general the hypothesis is mostly used in its original format, as proposed by Miner. As mentioned before, Kesler added a probability of failure to obtain better results when using Miner's hypothesis. Holmen introduced an interaction factor, which is a function of loading parameters (Ref 23). More recently, Chung (Ref 32) proposed a damage model in which the energy dissipation capacity of a member, instead of the number of cycles to failure, is used to define damage.

In this work, Miner's hypothesis in its original format is used because it is the best method available at this time.

3.8 CONCLUSIONS

It is apparent from the above discussion that many variables influence the long-term performance of bonded concrete overlays. The important factors obtained from the above discussion are listed in Table 3.2. Other factors that were discussed in the previous paragraphs and that are not listed in Table 3.2 are the deterioration of the cement-treated base, construction, bond, air content, aggregate type, shrinkage and moisture, range of stress, and varying loads.

Deterioration of the cement-treated base, aggregate type, and air content can be modeled by using various moduli of elasticity values. Construction parameters are assumed to be of good quality, and a sound overlay is placed before traffic loading. Shrinkage and moisture can be modeled with the temperature distribution. Finally, range of stress is evaluated using different loads. However, the specific influence will be established by using methods developed in the literature. This is necessary because the method of modeling overlays in analysis programs is static and, therefore, is not a dynamic modeling. Variation in loads varied with the range of stress as well as the concrete damage model, such as Miner's model, and therefore is evaluated through accepted methods of predicting damage.

It is concluded that the factors listed in Table 3.2 are all important in the long-term performance of bonded concrete overlays. It is further concluded that current fatigue testing results are normally at much lower levels of application than the number of applications on highways and that the rest periods between tests are also sometimes higher than the time period between cars and trucks following each other on highways.

The reliability of estimating fatigue life of the bonded overlay with the discussed tests is, therefore, reduced. Another area in which a lack of information exists includes the compression, shear, and tensile fatigue at the interface between existing pavements and bonded concrete overlays. Finally, it can be concluded that Miner's hypothesis is not representative of concrete behavior in some instances. However, it is the only method widely accepted and is also used in this work.

The factors discussed in this chapter can now be used in a sensitivity analysis to obtain the most sensitive variables in the overall system.

Table 3.2 Summary of factors influencing long-term performance of bonded concrete overlays

Structural System	**Existing Pavement Structure**	Thickness:	Roadbed
			Subbase
			Surface Layer
		Reinforcing %	
		Remaining Life	
		Crack Spacing	
	Overlay Structure	Thickness	
		Reinforcing %	
		Reinforcing Position	
		Crack Spacing	
Material Properties	Elastic Modulus:	Roadbed	
		Subbase	
		Surface Layer	
		Overlay	
	Thermal Coeff:	Roadbed	
		Subbase	
		Surface Layer	
		Overlay	
	Poisson Ratio:	Roadbed	
		Subbase	
		Surface Layer	
		Overlay	
	Shear Strength:	Existing Pavement-Overlay Interface	
		Existing Pavement-Subbase Interface	
	Tensile Strength:	Existing Pavement-Overlay Interface	
		Existing Pavement-Subbase Interface	
		Overlay	
	Reinforcing Bar Yield Strength		
Fatigue	Flexural Compression at Interface Shear at Interface Tensile at Interface		
Loading	Wheel Loading Environmental Stresses		
Failure Criteria	Based on Cracking, Punchouts, Serviceability?		

CHAPTER 4. METHODOLOGY FOR A REDUCTION OF VARIABLES INFLUENCING LONG-TERM PERFORMANCE OF BCO

4.1 INTRODUCTION

In Chapter 2, the design of bonded concrete overlays, currently used design procedures, and their limitations are discussed. In Chapter 3, the factors influencing the long-term performance are discussed. These factors may all influence a design system, as discussed in Chapter 2. If all the factors were to be analyzed, a huge analysis factorial would have to be filled. This would be an extremely expensive operation due to the fact that a finite element method is used to analyze the factorial. Furthermore, some of the variables might not be sensitive to the performance of overlays in influencing the cost-effectiveness of the system. In this chapter, all the variables discussed in the previous chapter are evaluated and if necessary used in a sensitivity study.

The finite element method program used to do the sensitivity analysis is also used to model the influence of cracks and different interface shear and tension stresses between the existing pavement and the overlay. Cracks and interface zones can be modeled using so-called slip elements. The FEM program used was developed by Texas Tech University in coordination with the Center for Transportation Research at The University of Texas at Austin. It has been developed as a plane strain analysis program which simulates loadings, such as temperature stresses in a pavement. The program can be used directly for the calculation of temperature stresses, because it is a two-dimensional problem, which assumes that the distribution of temperature within the concrete is the same from one edge of the pavement to the other edge. It is easy to understand that this is not true for wheel loading on a pavement, which is a three-dimensional, or axi-symmetric, problem. Since this work covers long-term performance analysis of bonded concrete overlays, it necessitates the use of wheel loads in the analysis.

The purpose of this chapter is, first, to evaluate stresses calculated using the FEM program by comparing them to stresses calculated using established analysis methods, under wheel loading. The different analysis programs used to compare the FEM model are discussed. An evaluation of the comparison between the methods is made and used in a comparison with the stresses calculated using the FEM program. Then a methodology for the reduction of variables influencing the long-term performance of bonded concrete overlays is discussed. Finally a sensitivity analysis is completed using the finite element method discussed above.

4.2 FINITE-ELEMENT ANALYSIS PROGRAM COMPARISON TO OTHER THEORIES

4.2.1 *Comparison Methods*

Three analysis methods are used in the stress comparison. The first uses the Westergaard equations (Ref 33), the second the layered theory program ELSYM5, and the third the finite-element method program. The first two methods are compared with each other and the method which best reflects the actual behavior of the concrete pavement is selected. That method is then compared with the finite-element method.

4.2.1.1 Westergaard

Westergaard developed his equations during the 1920's. The same equations are still used today although they have been modified by Pickett and Ray (Ref 34) and many others. Westergaard assumed that the concrete slab acts as a homogeneous isotropic elastic solid in equilibrium and that this solid is supported by reactions that are vertical only. These vertical reactions are a measure of the subgrade stiffness and are called the modulus of subgrade reaction. Therefore, the influence of friction or shear stress between the concrete and the subbase is neglected. Westergaard also concluded that the important stresses are not affected by the modulus of subgrade reaction. Values in a range of 50 to 200 lb/in.^{3} produced no significant difference in the important stresses needed in the pavement analysis. Westergaard's original interior stress equation for ordinary theory is given by

$$\sigma_i = \{[3\ (1+\mu)\ P] / [2\pi h^2]\}\ \{\log_e (l/a) + 0.6159\} \quad (4.1)$$

where

σ_i = interior stress,
P = wheel load,
μ = Poisson's Ratio,
h = concrete slab thickness,
a = radius of loaded area,
l = $([Eh^2]/[12\ (1-\mu^2)k])^{0.25}$,
E = elastic modulus of the concrete slab, and
k = modulus of subgrade reaction.

The Westergaard equations and the subsequent changes by others are still being used because they represent a simple and quick procedure for calculating stress. In an analysis where stresses calculated using the Westergaard equations were compared to stresses calculated using a finite-element program (Ref 35), it was concluded that the Westergaard solution to the calculation of stresses in concrete pavements is still valid. From the above discussion, it is concluded that, if stresses calculated using the plane strain finite-element program compare favorably with stresses calculated using the Westergaard solutions, the FEM can be accepted as an analysis tool.

4.2.1.2 ELSYM5

ELSYM5 is also used in the analysis, because it uses layered theory as a basis, which is different from the slab theory used in the Westergaard equations. ELSYM5 and other layered theory programs such as CHEVRON15 were developed mainly for the analysis of asphalt concrete pavements. ELSYM5 is used here in the comparison to evaluate its use in calculating stresses in portland cement concrete pavements.

4.2.2 Evaluating the Modulus of Subgrade Reaction

For a three-layered system, the k-value depends on the layer moduli and the thicknesses of the base and the concrete layer. Eisenmann (Ref 36) developed an equation for calculating the k-value using Odemark's theory of equivalencies for the calculation of bending stresses in two- and more-layered systems. For this study, a three-layered system is used. When an overlay is added a four-layered system is used. However, the two concrete layers can be considered as a single layer.

The equations developed by Eisenmann consists of two parts: effective thickness is calculated and then the k-value. The equations are

$$h^* = 0.83h_1(E_1/E_3)^{1/3} + c(h_2)(E_2/E_3)^{1/3} \quad (4.2)$$

and

$$k = E_3/h^* \quad (4.3)$$

where

h_1 = Portland cement concrete thickness in millimeters,
h_2 = cement-treated-base thickness in millimeters,
E_1 = portland-cement-concrete modulus in newtons/millimeter squared,
E_2 = cement-treated-base modulus in newtons/millimeter squared,
E_3 = roadbed modulus in newtons/millimeter squared,
c = 0.83 for cement-treated base course and 0.9 for bituminous-treated base coarse, and
h^* = effective thickness.

The same type of relationship was developed for untreated base-course systems. This work concentrates on treated base-course systems, since most concrete highways are constructed using a treated base course.

4.2.3 Comparison of Westergaard and ELSYM5

Using the method shown above for obtaining a modulus of subgrade reaction from an elastic layered system, a k-value was obtained for a variety of structural systems and stresses were calculated for each system using the three different methods. Table 4.1 is a summary of the stresses and deflections calculated.

Three different concrete thicknesses and two subbase thicknesses were used. An infinite roadbed thickness was assumed for calculating stresses in ELSYM5. In calculating the k-value it was also assumed, within the calculation, that the roadbed was of infinite thickness. The stresses calculated using an infinitely thick roadbed are higher than the stresses calculated if a rigid base exists below the pavement system, depending on the depth below the pavement system.

Using the values tabulated in Table 4.1, Figures 4.1 to 4.3 were prepared; they may be used to evaluate the correlation between the two stress calculation methods.

Figure 4.1 shows the stress values for the two methods and the 24 structural systems analyzed. Analyses 1 through 8 are for an 8-inch-thick concrete pavement, analyses 9 through 16 are for a 12-inch-thick concrete pavement, and analyses 17 through 24 are for a 16-inch thick concrete pavement.

Figure 4.1 shows that ELSYM5 gives much lower stress values for a system than Westergaard does. It can also be seen from Figure 4.1 that, as the concrete thickness increases, the difference in stress between Westergaard and ELSYM5 decreases.

This is also evident from Figure 4.2, where the stress differences between the slab theory program and ELSYM5 are significant, especially for thinner

Table 4.1 Stress and deflection values of Westergaard, and ELSYM5 analysis for different structural systems

Stress Comparison Using:							Westergaard Analysis				ELSYM5	
No.	h1 (in.)	h2 (in.)	E1 (ksi)	E2 (ksi)	E3 (ksi)	k (psi)	Int (psi)	Defl (in.)	Edge (psi)	Defl (in.)	Int (psi)	Defl (in.)
1	8	6	5,000	400	20	360	179	0.004	209	0.014	120	0.005
2	8	6	5,000	400	40	908	161	0.002	176	0.009	110	0.003
3	8	6	5,000	800	20	339	180	0.004	211	0.014	90	0.004
4	8	6	5,000	800	40	854	162	0.003	178	0.009	84	0.003
5	8	12	5,000	400	20	290	183	0.004	217	0.016	96	0.004
6	8	12	5,000	400	40	730	165	0.003	184	0.010	92	0.002
7	8	12	5,000	800	20	263	185	0.005	220	0.016	66	0.004
8	8	12	5,000	800	40	662	167	0.003	187	0.010	63	0.002
9	12	6	5,000	400	20	261	93	0.003	117	0.009	67	0.004
10	12	6	5,000	400	40	859	85	0.002	103	0.006	61	0.002
11	12	6	5,000	800	20	250	94	0.003	118	0.009	55	0.003
12	12	6	5,000	800	40	630	85	0.002	103	0.058	50	0.002
13	12	12	5,000	400	20	222	95	0.003	120	0.010	57	0.003
14	12	12	5,000	400	40	560	86	0.002	105	0.006	53	0.002
15	12	12	5,000	800	20	206	95	0.003	121	0.010	43	0.003
16	12	12	5,000	800	40	519	87	0.002	106	0.006	40	0.002
17	16	6	5,000	400	20	205	58	0.002	76	0.007	43	0.003
18	16	6	5,000	400	40	517	53	0.001	68	0.004	38	0.002
19	16	6	5,000	800	20	198	58	0.002	76	0.007	37	0.003
20	16	6	5,000	800	40	499	54	0.002	68	0.004	33	0.002
21	16	12	5,000	400	20	180	59	0.002	77	0.007	38	0.003
22	16	12	5,000	400	40	454	54	0.001	68	0.004	34	0.002
23	16	12	5,000	800	20	169	59	0.002	78	0.007	30	0.002
24	16	12	5,000	800	40	427	54	0.001	69	0.002	27	0.002

pavements. A further observation from Figure 4.2 is that the variability in range of stress is much higher for the thinner pavement section than for the thicker pavement section within each model.

For an 8-inch-thick concrete pavement the stress difference is about 40 psi, versus about 20 psi for the 16-inch-thick concrete pavement for the Westergaard analyses. Since most overlaid pavements will be thicker than 10 inches, probably 12 inches or more, the influence of subgrade support on the stress is not big and stress calculations can be concentrated around the concrete layers instead of around the support layers. The inference base used for these layers was a subbase modulus ranging from 400 to

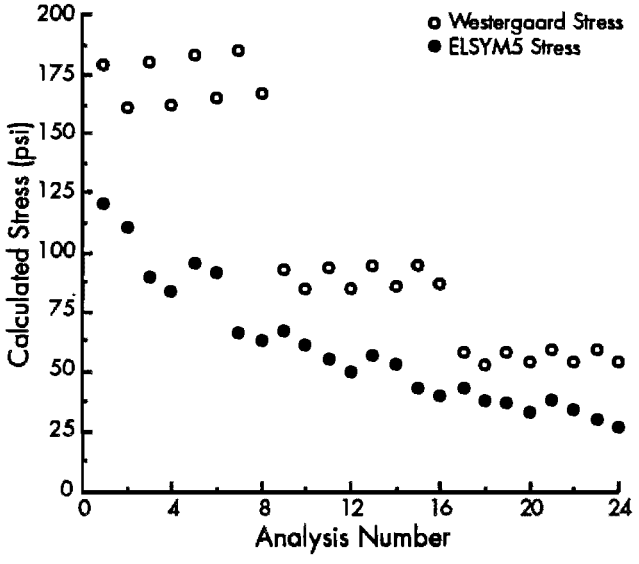

Figure 4.1 Comparison of calculated stres values from Westergaard and ELSYM5 for different structural systems

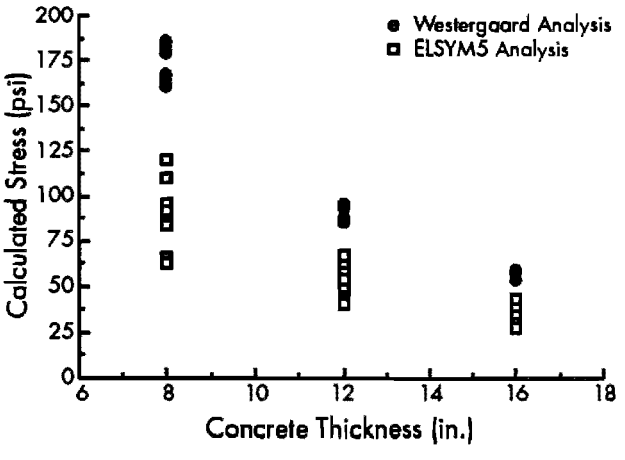

Figure 4.2 Comparison of calculated stress values from Westergaard and ELSYM5 for different structural systems

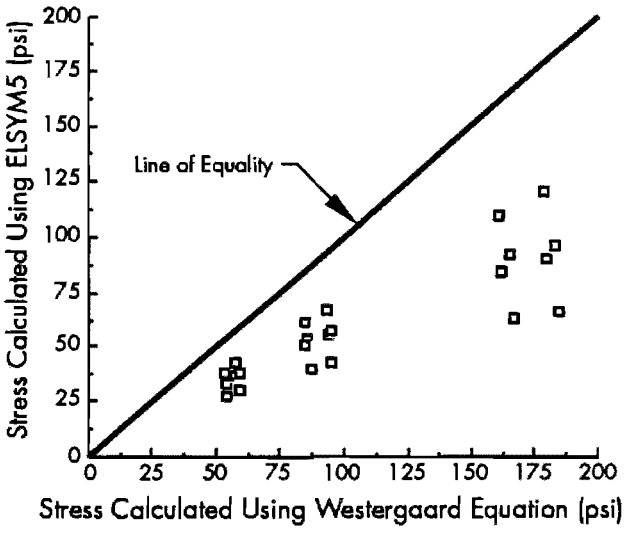

Figure 4.3 Comparison of Westergaard and ELSYM5

800 ksi and a roadbed modulus ranging from 20 to 40 ksi.

Figure 4.3 shows a comparison of the Westergaard stress calculations and those made with ELSYM5. It is evident from this figure that ELSYM5 produces lower stresses for rigid pavement systems than Westergaard does. When these stresses are used in fatigue calculations, they will produce significantly longer fatigue lives than the Westergaard equations will produce.

It should be mentioned that if a k-value is calculated for a subbase-roadbed system using ELSYM5, and stresses between the two theories are compared based on the ELSYM5 k-value, stresses compare favorably.

It can be concluded from this that the Westergaard equation can be used as an analysis method for obtaining values to compare with the FEM stresses because the results show good correlation with other rigid pavement methods and the method has proved through the years to be a reliable way of calculating stress. If the fictive thickness k-value method is used, Westergaard stresses are larger than ELSYM5 stresses.

4.2.4 Analysis of Westergaard Results

Before a comparison was made between results from the FEM and the Westergaard equation, the Westergaard stresses in Table 4.1 were analyzed to set up a comparison factorial. By investigating Table 4.1 it can be seen that the biggest factor in changing stress values is the concrete pavement thickness. In other word, the concrete stiffness is one of the most important parameters in stress calculation. It is evident from Table 4.1 that the lower layers, and therefore the k-value, do not influence the stress calculation significantly. Furthermore, the subbase thickness does not change the stress significantly, either. The thicker the pavement system, the narrower the range between maximum and minimum stresses. The stress calculation for thicker pavements will therefore be more reliable if we assume that the Westergaard equation is valid.

We concluded then that the main parameter causing stress is the thickness of the stiff PCC surface layer in the pavement. Therefore, it was concluded that in a stress comparison between Westergaard and the FEM model the modulus of the subbase layers can be kept constant. The modulus was selected at the lower values of 400 ksi for the cement-treated base and 20 ksi for the roadbed. Because the upper layer stiffness has the largest influence, on stress, the modulus of the PCC layer is also analyzed in the Westergaard-FEM comparison. From this discussion, it can be concluded that the upper layer thickness and modulus values are the most important factors in stress calculations.

4.2.5 FEM Analysis

The FEM analysis was completed using a system which is also used in the evaluation of the influence of wheel and environmental loading on the performance of bonded concrete overlays. Figure 4.4 shows a layout of the section to be analyzed for values to be compared with Westergaard's.

Because this analysis is a plane strain analysis we need to obtain a method for transferring the FEM data to realistic data, such as those obtained from a Westergaard analysis. Due to the fact that the plane strain problem and axi-symmetric problem are two totally different systems and the mathematics explaining them was developed for two different sets of conditions, a mathematical relationship between the two was not easily obtainable. The only way to reduce the data to realistic data was by changing the analysis width in the FEM program. This is shown in Figure 4.5.

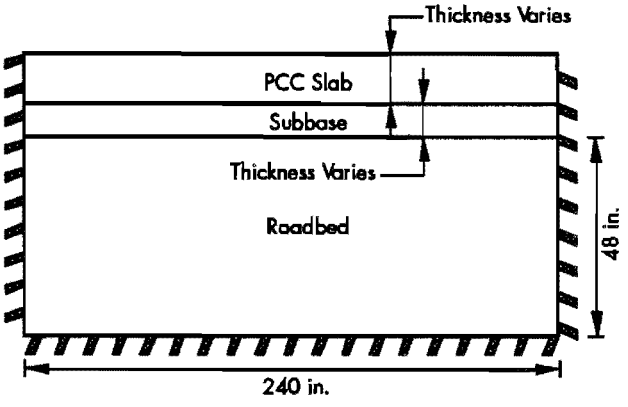

Figure 4.4 FEM analysis system layout

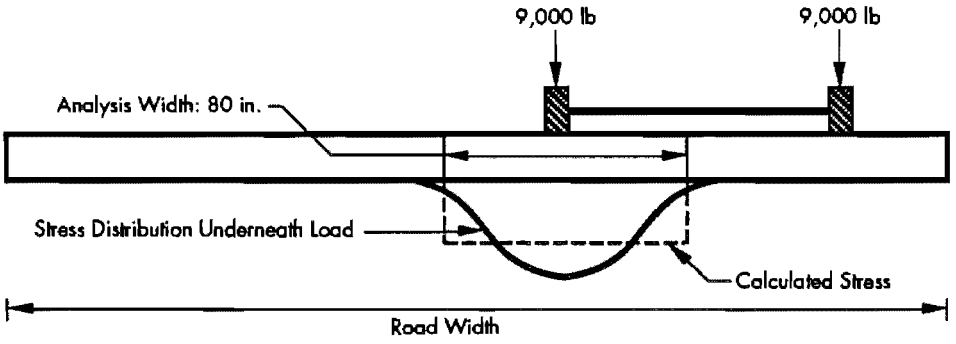

(a) Analysis width equal to 80 inches

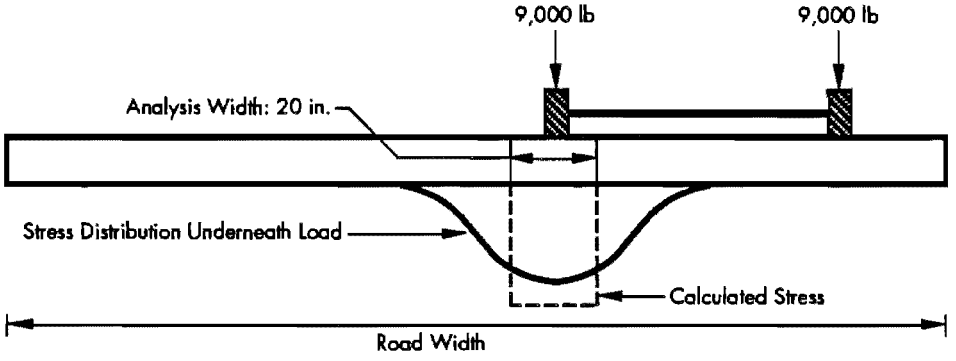

(b) Analysis width equal to 20 inches

Figure 4.5 Influence of different analysis widths

If stresses are calculated using the width in Figure 4.5(a), they will be much less than the stresses developed using the analysis width in Figure 4.5(b). By using a few different widths, a comparison of the FEM stress and the Westergaard stress can be obtained and a thickness to be used in the analysis, which will provide stresses similar to the Westergaard stresses, can be prescribed. Although this procedure is not perfectly accurate it is a reasonable alternative to the exact solution. The exact solution would involve changing the FEM model to an axi-symmetric program, which would be much more expensive to develop as well as to use, because the computer time would be increased significantly.

Four variables are analyzed and the calculated results are compared to Westergaard stress results. The four variables are the PCC surface layer thickness and stiffness, the subbase thickness, and the width of analysis. The lower layer's Poisson's ratio was held constant at 0.4, and the modulus values used were 400 ksi for the cement-treated subbase and 20 ksi for the roadbed. The PCC layer Poisson's ratio was held constant at 0.2.

4.2.6 FEM Comparison to Westergaard Analysis

The comparison factorial analyzed is shown in Table 4.2, as are the stress results obtained for each analysis width. The factorial was only partially filled. However, the results do convey the results needed for the wheel load analysis. The data are explained using Figures 4.6 through 4.8.

From the table, it is evident that there is no specific width of FEM model analysis which will produce equivalent Westergaard stresses. From the table, it can be seen that the best width to use for an 8-inch-thick pavement lies between 20 and 40 inches. However, for 12 and 16-inch-thick pavements, that width lies between 40 and 80 inches. In order to compare the FEM results with realistic stress values, a width that will approximately produce realistic results must be selected and a method found to change the results into equivalent Westergaard stresses.

Figure 4.6 shows a plot of FEM calculated stress versus analysis width for three different modulus values. The Westergaard stress for each modulus

Table 4.2 FEM versus Westergaard factorial and stress results

			Wastergaard		FEM Analysis Results					
h1	h2	E1	Int.	Deflec.	Width,b=80		Width,b=40		Width,b=20	
(in.)	(in.)	(ksi)	(psi)	(inch)	Bot	Deflec.	Bot	Deflec.	Bot	Deflec.
8	6	3,000	166	-0.0047	64	-0.0029	125	-0.0058	246	-0.0115
8	6	4,000	174	-0.0042	71	-0.0027	140	-0.0054	276	-0.0107
8	6	5,000	179	-0.0039	77	-0.0026	153	-0.0051	301	-0.0110
8	12	3,000	171	-0.0053						
8	12	4,000	178	-0.0048						
8	12	5,000	183	-0.0044	68	-0.0024	134	-0.0048	261	-0.0095
12	6	3,000	88	-0.0030	43	-0.0022	86	-0.0043	169	-0.0085
12	6	4,000	91	-0.0027	48	-0.0020	95	-0.0039	187	-0.0078
12	6	5,000	93	-0.0025	51	-0.0018	102	-0.0036	201	-0.0072
12	12	3,000	89	-0.0032						
12	12	4,000	92	-0.0030						
12	12	5,000	95	-0.0027	49	-0.0018	96	-0.0035	188	-0.0070
16	6	3,000	55	-0.0022	31	-0.0016	62	-0.0033	123	-0.0065
16	6	4,000	57	-0.0020	34	-0.0015	68	-0.0029	134	-0.0058
16	6	5,000	58	-0.0019	36	-0.0013	72	-0.0027	142	-0.0053
16	12	3,000	56	-0.0024						
16	12	4,000	57	-0.0021						
16	12	5,000	59	-0.0020						

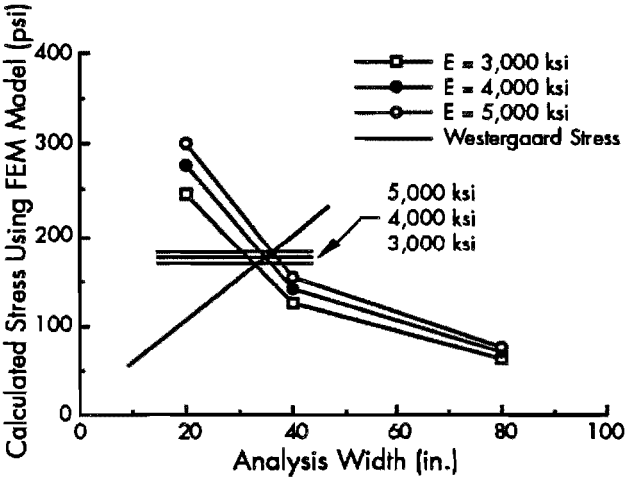

Figure 4.6 FEM stress comparison of 8-inch-thick pavement versus Westergaard stresses

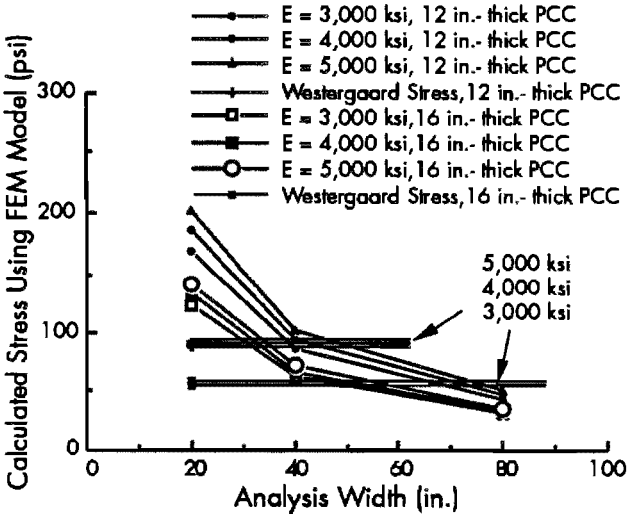

Figure 4.7 FEM stress versus Westergaard values for 12-inch and 16-inch pavements

value is also shown and a straight line can be drawn through the three points. These values are very close to each other and range from 166 psi to 179 psi. From the figure it can be seen that an analysis width between 32 and 37 will produce results similar to the Westergaard results. This figure is drawn for only the 6-inch subbase, and from Table 4.2 it can be seen that, although the Westergaard stress is not influenced by subbase thickness, the FEM stress is. However, a 12-inch-thick subbase is thicker than those used in practice.

Furthermore, the subbase thickness is 6 inches on test sections under surveillance in Houston by the Center for Transportation Research. Keeping this in mind, together with the fact that increasing the thickness can reduce stresses in the concrete layers, it is

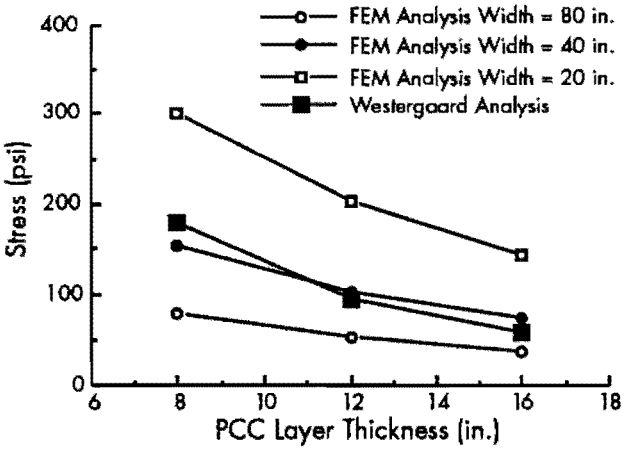

Figure 4.8 Stress versus PCC surface layer thickness for different analysis widths

concluded that we can leave out this variable and concentrate on a 6-inch-thick subbase. This will produce maximum stresses from the FEM analysis while the conversion to Westergaard's analysis will produce a stress which, according to the Westergaard analysis, is the same as that for a thicker subbase.

In Figure 4.7 the comparison graphed in Figure 4.6 for an 8-inch-thick pavement is shown for 12-inch-thick and 16-inch-thick pavements. Again straight lines can be fitted through the Westergaard stress values, but the slopes are much smaller than the slope of the same line in Figure 4.6.

From Figures 4.6 and 4.7 it can be concluded that as the pavement thickness increases the effect of the elastic modulus of the top layer is reduced. For an 8-inch-thick pavement, an analysis width of 35 inches should provide adequate results while an analysis width of about 40 to 55 inches should provide adequate results, for a 12- to 16-inch-thick pavement. This is evident in Figure 4.8.

In order to predict Westergaard stresses from the FEM stresses more accurately a regression equation incorporating all the important variables was developed. The regression equation is

$$\text{Wester} = 0.755h_2 + 0.00336E + 0.0102\text{FEM} + 0.0234b + 9805/h_1^2 \quad (4.4)$$

where

Wester = Westergaard equivalent stress (psi),
h_2 = subbase thickness (inch),
E = modulus of elasticity (ksi),
FEM = calculated finite element stress (psi),
b = analysis width (inches), and
h_1 = PCC thickness.

This equation gives an extremely good correlation, with an R^2 value of 99.96 percent. It can therefore be used to calculate equivalent Westergaard stresses from the FEM stresses, but it should be remembered that it is applicable only to the system analyzed in the FEM analysis. If the roadbed thickness is increased from 48 to 60 inches, this equation may change.

4.2.7 Conclusions

From this we can conclude that the plane strain FEM can be used to predict axi-symmetric strains for the system that will be analyzed. For pavements from 12 to 16 inches thick, an FEM analysis width of 50 inches will produce realistic stress values, while an FEM analysis width of 35 inches will provide adequate results for an 8-inch-thick pavement. Equation 4.4 can be used to predict Westergaard stresses from FEM stresses.

4.3 REDUCTION IN FACTORS INFLUENCING WHEEL LOADING STRESSES BEFORE SENSITIVITY ANALYSIS

In Chapter 3, the factors influencing the long-term performance of bonded concrete overlays were discussed. It was concluded in that section that a sensitivity analysis is needed to reduce the number of variables analyzed. This will reduce computer costs and also make the final results more practical if used for design purposes. However, some variables can be intuitively changed to remain constant or can possibly be ignored.

In Chapter 3, three main areas were identified in the factors influencing long-term performance. These factors included (1) the existing pavement system, (2) the overlay layer, and (3) the material properties. Reduction in variables considered important in wheel loading analysis are discussed below.

4.3.1 Existing Pavement System

The percentage reinforcing in the existing pavement can be held constant at 0.6 percent because it has been common practice to require a minimum percentage of steel of 0.6 percent in the United States (Ref 37).

It was previously concluded that PCC layer thickness is the most important factor in calculating stress. Therefore, it was concluded that the moduli of elasticity of the lower layers as well as their thicknesses can be held constant for good comparison of the FEM program with Westergaard equation results.

The remaining variables need to be analyzed using a sensitivity analysis.

4.3.2 Overlay

All the variables concerned with the overlay should be analyzed using a sensitivity study because of the uncertainty of their influence on the structure.

4.3.3 Material Properties

Several material property variables can be eliminated to reduce the number of variables. Poisson's ratio for the lower layers can be held constant for wheel loading, for the reasons given before.

The thermal coefficient of the layers can also be held constant, especially for the lower layers. It is, however, known that siliceous river gravel and limestone have different thermal coefficients (Ref 38). It was found that the thermal coefficient of limestone is 0.000006 and that of silicious river gravel is 0.000008. This effects only temperature loads and, therefore, a constant parameter will be assumed for all layers when wheel loads are analyzed.

The modulus of elasticity is also important. To reduce the variables more, modulus values for the subbase and roadbed can be held constant for wheel loading. The steel yield stress can be held constant because Grade 60 steel is very commonly used in pavements.

From laboratory results, it was found that the tension strength at the interface between the existing pavement and the overlay is approximately one-half of the shear strength; Table 4.3 shows the results. When using PCC grout, the tension strength is about 40 percent of the shear strength while the tension strength is about one-half of the shear strength when epoxy or latex modified grout is used. If this finding is used, the tension strength can be modeled using half the shear strength, and, if we assume the same relationship between a cement treated base and existing pavement, we can reduce the shear and tension strength variables from four to two.

4.4 REDUCTION IN VARIABLES FOR ENVIRONMENTAL STRESSES BEFORE SENSITIVITY ANALYSIS

The most important factors in stress calculation using temperature are the coefficient of thermal expansion and the modulus of elasticity. Shrinkage and moisture stresses can be modeled using a temperature differential in the FEM program. Before a reduction in variables for temperature stresses could be considered, it was necessary to evaluate the temperature distribution through the soil and the influence of the various parameters on stresses in the PCC layer of the pavement

4.4.1 Investigation of Soil Temperature Distribution and Thermal Properties

The temperature distribution within a soil structure is extremely difficult to evaluate due to variability between soils, organic material within soils, moisture content, and so on. This investigation was conducted to evaluate the temperature distribution within a soil, its thermal properties, and the sensitivity of variation in these parameters to the outcome of

Table 4.3 Shear and tension strengths for various bonding agents, textures, and surface temperatures

Texture	Surface Temp. (Fahr.)	Stress Type	Bonding Agent			
			Latex	Epoxy	PCC Grout	No Grout
Light Shot Blast	50-60	Shear	676	890	183	627
		Tension	222	346	170	247
	70-100	Shear	735	505	412	232
		Tension	171	339	167	276
	125-140	Shear	552	589	675	523
		Tension	120	327	170	181
Heavy Shot Blast	50-60	Shear	793	921	435	582
		Tension	239	352	283	245
	70-100	Shear	754	338	653	679
		Tension	250	245	172	197
	125-140	Shear	520	705	504	607
		Tension	229	351	211	192
Cold Mill	50-60	Shear	655	878	613	272
		Tension	281	320	327	216
	70-100	Shear	501	311	899	691
		Tension	258	282	287	230
	125-140	Shear	611	637	800	442
		Tension	290	267	259	172

the results of an FEM analysis. The results obtained from this investigation were used to reduce or add variables to the sensitivity study of factors influencing the long-term performance of BCO.

A literature search provided several papers covering temperature distribution within a soil structure to some extent. Many of these articles are based on research done in the agricultural area, while a few of the papers discuss temperature distribution beneath portland cement concrete or asphaltic concrete. However, many of the results are inconclusive or specific only to a certain type of soil or area. The type and form of the temperature distribution curve are, however, approximately the same.

4.4.1.1 Factors Affecting Soil Temperature

Many factors influence soil temperature distribution. Crawford (Ref 39) cited Bouyoucos, who divided these factors into two broad classes: intrinsic and external. Intrinsic factors are all the factors within the soil structure, whereas external factors are those outside of the structure. He categorized the factors as intrinsic and external, as listed in Table 4.4.

Bouyoucos stated that the intrinsic factors which most often become unbalanced and cause temperature differences are latent heat of fusion of ice, latent heat of evaporation of water, ground surface cover, ground surface color, and topographic position. He found that it was impossible to analyze the interrelation of external factors. The only external factor influencing soil temperature directly is air temperature. The rest of the factors more or less cancel each other out. Absorption of solar energy from the sun is also an important factor; it causes the soil surface temperature to be higher than the mean air temperature directly above it. Crawford (Ref 39) cited Bauer, who stated that soil temperature is primarily dependent on the radiant energy from the sun. Based on this, explanations for other factors follow naturally. For example, a low relative humidity will reduce soil temperature due to higher evaporation of moisture from the soil, which tends to cool the soil down.

Another important factor is rainfall. While opinions about the effect of rainfall differ between researchers (some think the influence is overestimated), it appears that rainfall does have a modifying effect on soil temperature. On modern highways the effect of rainfall is controlled to some extent. Shoulders and efficient drainage control the extent to which rainfall will effect the internal soil temperature. Rainfall also influences another important intrinsic factor: the soil moisture content. The soil moisture content can influence other intrinsic factors, such as specific heat properties of soils, because the specific heat of water is five times greater than that of dry sand.

Crawford (Ref 39) also cited Keen, who mentioned that dry sand also has a low conductivity. Moisture increases the grain contact and, therefore, increases the overall conductivity; however, the specific heat also increases, which makes the total temperature increase small. In another study, de Gijt et al (Ref 40) cited Richards, who found from studies done in Australia that temperature gradients measured led to the assumption that thermal moisture underneath sealed pavements is negligible for specific conditions. He made the unverified statement that any thermal transfer of moisture will probably lead to safer structural conditions.

From the above discussion, it can be seen that soil temperature distribution is a complex phenomenon. Although it has been the topic of many research papers, there are many areas of soil temperature distribution yet to be investigated. The factors involved in this phenomenon, many of which are not discussed here, form a closely interrelated system, and some may influence the soil temperature more than others. And, while the notion that they do

Table 4.4 Factors influencing soil temperature distribution (Ref 39)

Intrinsic Factors	External Factors
Specific Heat	Air Temperature
Radiation	Wind Velocity
Organic Content	Precipitation
Evaporation	Sunshine
Specific Gravity	Dew Point
Absorption	Barometric Pressure
Texture and Structure	Relative Humidity
Nature of Surface	
Thermal Conductivity	
Moisture Content	
Concentration of Salts in Solution	
Topographic Position	

affect each other is easily understood, it is on the other hand extremely difficult to isolate the factors in order to determine exactly their precise influence on the temperature within the soil. It is, however, apparent that the most important fact to keep in mind is not how much these factors change the temperature distribution of the soil but what their influence on the thermal properties of the soil is. This is important in highway engineering work and may effect the properties of the soil used in the design. When an analysis procedure of any kind is used to calculate the stresses in the pavement structure, the movement due to temperature change in the vertical and horizontal directions, the change in thermal properties due to temperature, and its influence on the stress in the pavement structure above it are important.

4.4.1.2 Thermal Properties of Soils

An understanding of the thermal properties of soil is important in many different fields. Temperature change can create volume changes and pore water pressure variations in saturated soils. When a pavement-soil structure is analyzed, the movements of underlying soils are an important part of that analysis. Under fully drained conditions and constant confining pressure, a volume of water will drain out from a saturated soil as a result of a temperature increase. Drained triaxial tests have shown that significant permanent volume decreases may occur during initial temperature increases. The most important factors controlling pore water pressure changes appear to be the thermal expansion of the pore water, the compressibility of the soil structure, and the initial effective stress. All these factors depend on the soil temperature, which in turn depends on the thermal properties.

Thermal Conductivity

The thermal conductivity of soil is the quantity of heat that will pass through a unit area of unit thickness in unit time under a unit temperature gradient. It is normally measured in British thermal units transmitted per hour through one square foot of soil, one inch thick, per degree of Fahrenheit difference between the two surfaces. The thermal conductivity of soils varies with moisture or water content. The effect of moisture on conductivity is shown in Figure 4.9.

Thermal Diffusivity

Thermal diffusivity is the thermal conductivity divided by the specific heat times density. Specific heat is the amount required to raise the temperature of a unit weight of soil by one degree. The effect of moisture content on the thermal diffusivity is also shown in Figure 4.9.

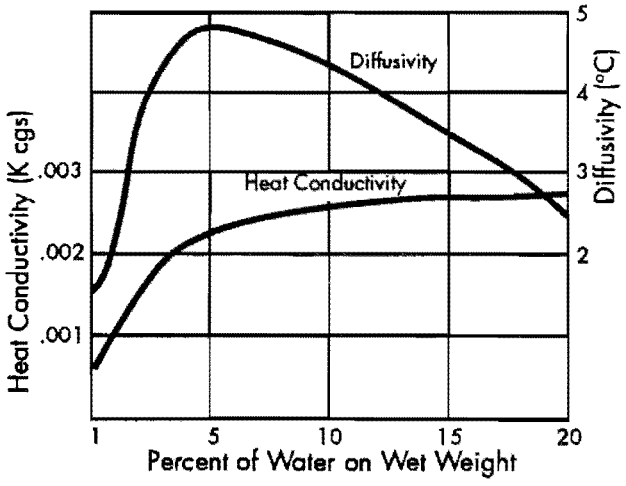

Figure 4.9 Effect of moisture content on the thermal behaviour of a coarse quartz powder (Ref 39)

Heat Capacity

The volumetric heat capacity is equal to the specific heat of the soil times the density. Moisture will change the heat capacity of the soil. A coefficient of thermal expansion will vary as the heat capacity varies, or, in other words, different expansion or contraction values are obtained when the thermal conductivity and the diffusivity of the soil change.

The influence of change in temperature and subsequent change in volume on stresses in the concrete pavement is important, especially in a finite element analysis. The vertical load-carrying capacities of soils, and the subsequent deflections, are well documented. Engineers use either an elastic modulus or a modulus of subgrade reaction, otherwise known as a spring constant. Little attention has been given to the expansion or contraction of soils (with the exception of expansive clays) in the horizontal direction. One of the thermal properties most often used in civil engineering is the coefficient of thermal expansion. A coefficient of thermal expansion for a soil depends primarily on (1) the coefficient of thermal expansion of the soil components, (2) the amount of water, and (3) the volumetric strain due to physico-chemical effects.

The total volume change in the soil depends on the state the soil is in—for example, drained or undrained. If the soil is drained, no pore pressure buildup will exist, while an undrained soil will produce pore pressures. Campanella et al (Ref 41) proposed the following equation for the total volume change in soil due to temperature:

$$(\Delta V_m)_{\Delta T} = \alpha_s V_m \Delta T + (\Delta V_{st})_{\Delta T} \qquad (4.5)$$

where

α_s = thermal coefficient of cubicle expansion of mineral solids,
V_m = volume of soil,
ΔT = temperature difference, and
ΔV_{st} = temperature induced volume change due to change in interparticle forces, which requires some reorientation or relative movement of soil grains for the soil structure to carry the same effective stress.

For undrained conditions, pore water pressures may develop during temperature changes. The sum of the separate volume changes of the soil constituents due to temperature and pressure changes must equal the sum of the volume changes of the total soil mass due to both temperature and pressure changes.

The effects of the volume changes of a soil mass depend, therefore, on many factors. For drained soils, significant volume changes can occur during initial volume changes due to reorientation of particles within the soil mass, which is a consolidation effect. Furthermore, the higher the temperature, the lower the void ratio. Undrained tests showed that an increase in pore water pressures results from an increase in temperature and that the pore water pressure decreases as the temperature decreases. Table 4.5 shows elastic modulus values and thermal coefficients of expansion for various materials (Ref 42). As mentioned above, the volume change of a soil depends on the thermal expansion of various parts within the soil. Table 4.5 also gives an idea of the variance in the thermal coefficient of expansion of different materials.

The coefficient of thermal expansion for the soil is a combination of the thermal coefficient of the material, the density of the material, and the moisture content. Expanding and contracting can densify the soil structure. No exact coefficient of thermal expansion exists, therefore, for a soil structure. The coefficient will change as the moisture, temperature, and density of the soil change, and in accordance with the condition of the soil, drained or undrained.

Table 4.5 Material properties of rocks

Materail	Elastic Modulus (x 10^6, psi)	Linear Thermal Coefficient (x 10-6)
Chert	3.1 - 18.0	6.0 - 7.2
Quartize	3.2 - 10.2	6.2 - 6.9
Sandstone	2.9 - 4.0	6.3 - 6.6
Basalt	11.4 - 13.9	3.9 - 5.9
Granite	7.6 - 9.8	2.8 - 5.3
Limestone	5.1 - 12.6	1.8 - 5.4
Dolomite	2.5 - 10.0	4.0 - 5.0

All these variables are, therefore, dependent on moisture change. With variation in properties, which is evident in pavement structures undergoing high seasonal changes, an analysis of the sensitivity of stresses within the top layers of a pavement structure to subsurface expansion and contraction may provide a guide to what a reasonable coefficient of expansion should be. Before analyzing a soil-pavement structure, a temperature distribution is needed for that structure. The temperature distribution within a soil structure is discussed in the following section.

4.4.1.3 Temperature Distribution of Soils

The temperature distribution of soils has been studied intensively by many researchers. Moreover, in evaluating soil temperatures at certain depths, many different methods have been used, including the use of a temperature cone, where a penetration device is pushed into the soil and temperatures are then obtained at different depths (Ref 40).

The distribution of the soil temperature is dependent on many factors, some of which are mentioned above. A few other important factors include soil color and soil cover, of which concrete pavements are a good example. Figure 4.10 shows the difference between the temperature distribution underneath a concrete slab and the distribution for the same soil under the shoulder.

In their various studies on the penetration of temperature into soil, researchers have reported various conclusions. Goetz and Muller (Ref 43) studied distributions of temperature in Moraine raw soil and concluded that the thermal profile consists of a thermally active upper zone between the soil surface and 12 inches, a transition or boundary layer with nightly temperature reversion between 12 and 20 inches, and a thermally passive lower zone between 16 and 40 inches. Forbes, cited by Crawford (Ref 39), observed a decrease in temperature range with increase of depth below the surface. He found that, for a variety of soils, the temperature range at 24 feet was about 1/5 to 1/10 of what it was at 3 feet. Richards, cited by Mitchell (Ref 44), published results of a study of temperatures underneath a sealed pavement. The maximum observed temperature gradient over a depth of 10 to 15 cm was 0.3°C/cm. He, finally, concluded that daily air temperature variations had little effect on subgrade soil changes.

Not many values are available describing the temperature variations underneath various types of soil covers. Fang (Ref 46) produced the figure shown in Figure 4.11 for a rigid pavement system from

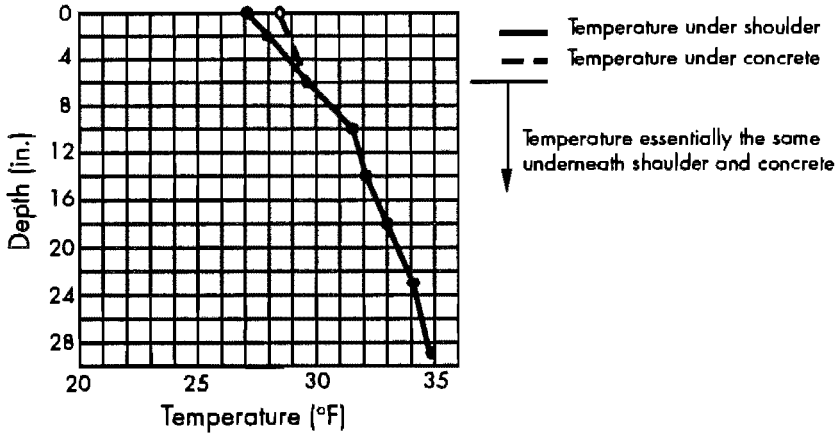

Figure 4.10 Subsurface soil temperature underneath 6-inch concrete slab and the shoulder (Ref 45)

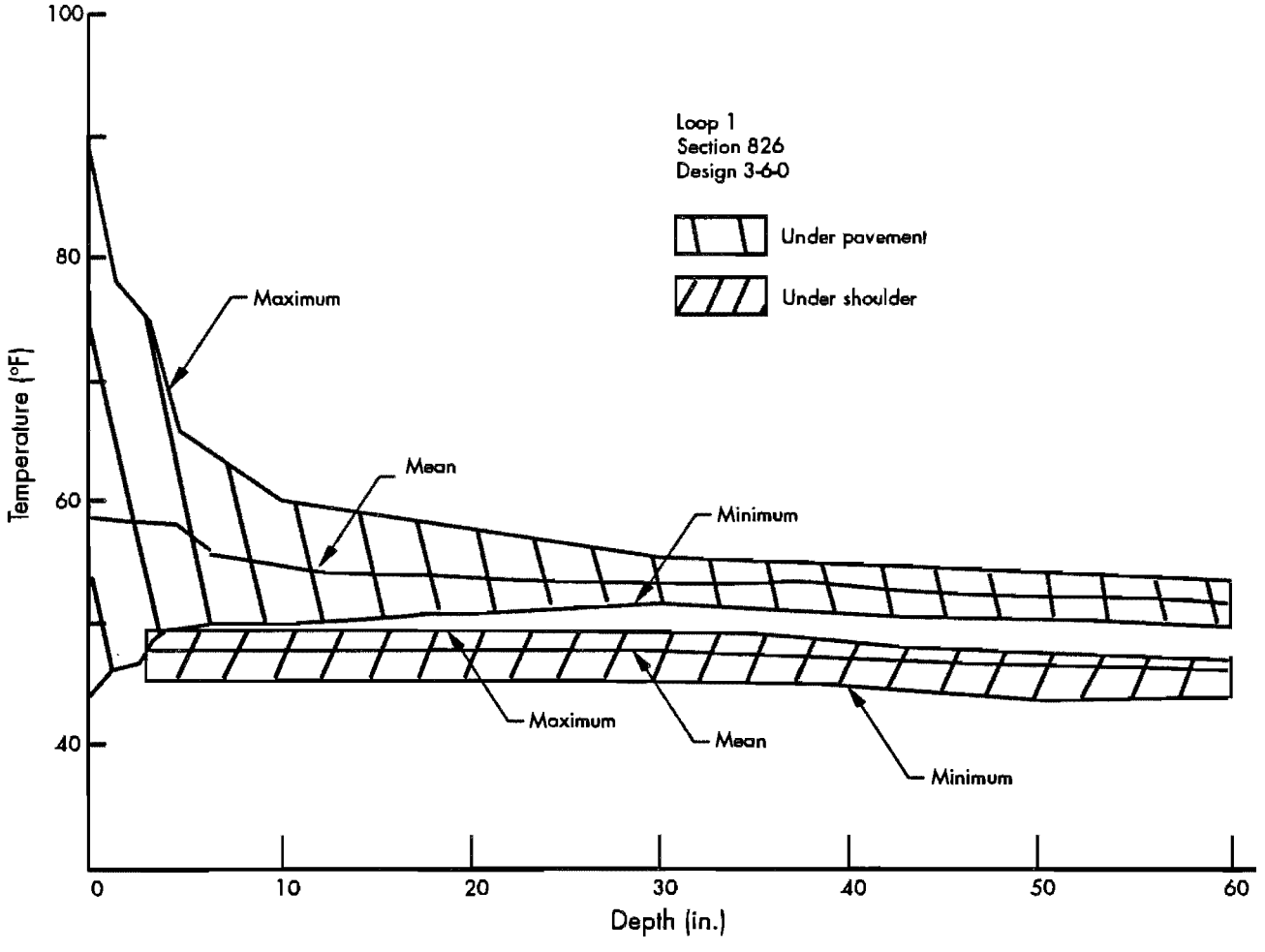

Figure 4.11 Temperature variations in soil-pavement system from AASHO Road Test (Rigid Pavement) (Ref 46)

results obtained at the AASHO Road Test. It indicates a difference in soil temperature underneath the pavement versus underneath the shoulder.

The variations in daily air temperature have little effect on the soil temperature. The final depth of actual influence depends on the cover thickness and the heat capacity of the cover materials. Although the temperature distribution of the soil will not vary much with daily temperature variations, it will be affected by seasonal variations in air temperature. The temperature in the soil lags behind the air temperature by a certain time. The time period of temperature lag between air and soil temperature will vary with different materials. It is difficult and expensive to research this problem and no data were found covering this specific problem.

Many models are available for describing soil temperature distribution. These models vary significantly in ease of operation and, therefore, some are much more involved than others. Two examples are given below.

4.4.1.4 Models Describing Soil Temperature

Two models are shown in this section. The purpose in discussing these models is to show how different these models—both developed to describe soil temperature—can be. They include an involved equation as well as a very simplified equation modelling the soil temperature distribution. The first model discussed was published by Sodha, Bansal, and Seth (Ref 47) and is extremely involved, as can be seen from the following equation. The mean ground temperature at time t and depth x is given as

$$T(x;t) = \sum_{m=0}^{\text{infinity}} B_m \cdot \exp(-\eta x) \cdot \cos(m\omega x - \eta x - \phi) \quad (4.6)$$

where

B_m = $(a^2_{mo}+b^2_{mo})^{1/2}/(\eta^2/c^2+(1+\eta/c)^2)^{1/2}$,
h = $(mW/2\alpha)^{1/2}$,
α = thermal diffusivity,
c = h/k,
h = heat transfer coefficient from ground surface to surroundings,
k = thermal conductivity,
a_{mo} and b_{mo} = coefficients, and
ω and ϕ = variables from Fourier transform.

Luthra, Saluja, and Amar (Ref 48) proposed the following, much less involved, equation:

$$T(x;t) = T_m + T_a \cdot e^{-rx} \cdot \sin(2\pi/p(t-t_o)-rx) \quad (4.7)$$

where

T_m = mean surface temperature,
T_a = temperature amplitude,
r = $(\pi/\alpha p)^{1/2}$,
α = thermal diffusivity,
p = period,
t = time, and
t_o = time interval between the middle of a designated month and the date when the surface temperature is equal to mean soil temperature.

Sodha et al used Equation 4.6 to investigate the variance of the temperature distribution. They found the temperature distribution to be a decreasing function of depth, becoming a small constant at a depth 10 inches below the surface. Luthra et al concluded that it is difficult to obtain mathematical expressions that adequately describe the variations of soil temperatures at various depths with time. However, they also felt that, by using approximations and adjusting coefficients using actual field measurements, useful relationships could be established.

4.4.1.5 Soil Temperature Distribution Effects on Portland Cement Concrete Pavement Stresses Using FEM

Using the knowledge gained from the previous discussions, an analysis of a soil-pavement structure with a Finite Element Method program was made. The input for soil thermal properties is a coefficient of thermal expansion. It is evident from the literature search that there are no specific data available for such a coefficient for soils. The modulus of elasticity of soils is well researched, especially in pavement engineering. By using thermal coefficients of 0.000001 and 0.000006 and a 16-degree temperature drop, it was found from the FEM analysis that the change in stress in the portland cement concrete layer is zero or extremely small. The change in stress does, however, influence the stress inside the soil structure significantly. There are therefore a few important factors to remember when doing an FEM analysis using a thermal coefficient of expansion for the soil:

(1) The thermal coefficients of soils are ill-defined. Using a value which can be only a best estimate is not scientifically correct.
(2) Using a decrease in temperature of 16 degrees Fahrenheit showed extremely high tensile stresses, in the order of 50 to 135 psi, which is unreasonable for most soils.
(3) Temperature changes affect pore water pressures and the expression can be related to the thermal expansion of the soil components, physico-chemical effects, and the compressibility of the soil. This is difficult to

model in a system where only a modulus of elasticity and a coefficient of thermal expansion are used.

(4) The stresses in the soil are not as dependent on time as portland cement concrete is, but depend much more on the induced load system and the level of saturation. The state of stress in the soil may change between any two time periods. This change may be due to a new load that is applied or to a temperature increase or decrease. An increase in temperature may change the state of stress but not necessarily the volume. That is, the pore water pressure may increase, but the increase in stress is not caused by an overall expansion of the soil structure. Modelling the different states of stress using a coefficient of linear expansion must be done with care, especially since no data are available to compare results with.

(5) Following from point 4 is the fact that, if we compare the stress state in the concrete five years after construction, we still use the curing temperature at construction as the base temperature. For soils, that is not the case because stress development depends not on a base temperature but on the temperature the soil is currently exposed to.

From the above discussion, it is apparent that using a thermal coefficient in modelling soil stresses is not an effective way of modelling. Richards (Ref 49) concluded that, for Australian conditions, soil and pavement temperatures have a significant effect on pavement performance, insofar as they affect the load-spreading properties of bituminous layers or cement- or lime-treated bases. This can be modelled by changing the modulus of elasticity, which will directly influence the stress within the pavement due to wheel loads. Murayama (Ref 49) used Osaka clay to obtain relationships for elastic constants versus temperature and found the constants to decrease with an increase in temperature. The FEM model can therefore predict change in stress in the pavement system by simply changing the modulus of elasticity.

4.4.2 Conclusions

The following conclusions are made from the above discussion concerning the sensitivity analysis:

(1) Due to the fact that soil temperature changes do not influence temperature stresses in the upper layers of the pavement structure significantly, it is concluded that a coefficient of linear expansion of 0.00001/°F should be used in the analysis.

(2) Due to unrealistic results in soil stresses when a high drop in temperature within the soil is used, it is concluded that the soil temperature change should be kept to zero.

4.5 SUMMARY OF VARIABLES AND ANALYSIS LEVELS NEEDED

For use in designing the analysis or experimental factorial, the important variables not eliminated from the analysis, the necessary analysis levels, and an identification parameter for each variable are shown in Table 4.6. Three levels are used to aid in the establishment of a curve or trend within a variable.

In Table 4.7 the variables listed in Table 4.6 are shown with the low, medium, and high values to be evaluated in the sensitivity analysis. In previous chapters it was concluded that the PCC layer thickness is important and therefore it is not necessary to evaluate the existing PCC and overlay layer thicknesses.

Even with the reduction in the number of variables and analysis levels, it can be seen that the analysis factorial will still be extremely large, which makes it impractical and also very expensive. Therefore, the planned sensitivity study will establish the effect of each variable on the maximum stress development in the pavement. For the sensitivity study, low, medium, and high values are given to each variable. The high values are always used as the basis of comparison. In this way, the most important variables are obtained and can be used in the wheel and temperature loading evaluation of the BCO, together with the variables which should be used in a mechanistic design procedure.

4.6 SENSITIVITY ANALYSIS USING FEM

In this study a traditional sensitivity analysis (Ref 50) was performed using the values shown in Table 4.7. The procedure of the sensitivity analysis is discussed in the following sections.

Table 4.6 Variables to be analyzed in the sensitivity analysis

Variable	Identification Parameter	Analysis Level
Existing Pavement Thickness	De	3
Poisson Ratio Existing Pvt.	$\mu\varepsilon$	3
Poisson Ratio Overlay	μo	3
Remaining Life	Rl	3
Crack Spacing Existing Pvt.	Cs	3
Overlay Thickness	Do	3
% Reinforcing Overlay	Rb	3
Position Reinforcing	Rp	3
Elastic Modulus Existing	Ee	3
Elastic Modulus Overlay	Eo	3
Thermal Coef. Existing	$\alpha\varepsilon$	3
Thermal Coef. Overlay	αo	3
Shear Str. Exist.-Overlay	Se-o	3

Table 4.7 Values of variables for sensitivity analysis

Variable	ID	Measured in	Value		
			Low	Medium	High
Existing Pavement Thickness	De	inch	8	10	12
Poisson Ratio Existing Pvt.	με	constant	0.15	0.2	0.25
Poisson Ratio Overlay	μo	constant	0.15	0.2	0.25
Remaining Life	R1	psi	0	50	Uncracked
Crack Spacing Existing Pvt	Cs	feet	3	5	Infinite
Overlay Thickness	Do	inch	2	4	6
% Reinforcing Overlay	Rb	%	0.4	0.6	0.8
Position Reinforcing	Rp	Position	Top	Middle	Bottom
Elastic Modulus Existing	Ee	ksi	3,000	4,500	6,000
Elastic Modulus Overlay	Eo	ksi	3,000	4,500	6,000
Thermal Coef. Existing	αε	/°F	0.000004	0.000006	0.000008
Thermal Coef. Overlay	αo	/°F	0.000004	0.000006	0.000008
Shear Str. Exist.-Overlay	Se-o	psi	0	100	200

4.6.1 Analysis Procedure

The high values in Table 4.7 are used for the basic system. This basic system is then compared to an analysis in which the low and medium values are changed one at a time. For instance, an analysis of the existing pavement modulus of elasticity is done comparing an analysis using the high set of values to an analysis in which only the low value is used and then one in which only the medium value is used. Not only will these three analyses show if significant differences exist, but they will also show if any mathematical trends exist. The same analysis procedure is completed for the other variables.

Various comparisons can be made using either deflection comparisons, tensile stress comparisons, or interface shear or interface tensile stress comparisons. The normal tensile stress comparison is used in this analysis because the fatigue performance depends mainly on the tensile stress within the concrete.

Table 4.8 shows the analysis number which are used in Tables 4.9 and 4.10. The remaining life and crack spacing were done separately with a smaller data file to reduce computation time. Analyses were also made separately for wheel loads and environmental stresses so that the factors important in each could be established.

Figure 4.12 shows a typical section used in the analysis. The maximum stress results are compared with each other.

Table 4.8 Analysis numbers of streses for use in Tables 4.9 and 4.10

Variable	ID	Analysis Number		
		Low	Medium	High
Existing Pavement Thickness	De	*	*	
Poisson Ratio Existing Pvt.	με	2	3	
Poisson Ratio Overlay	μo	4	5	
Overlay Thickness	Do	*	*	
% Reinforcing Overlay	Rb	6	7	1
Position Reinforcing	Rp	8	9	
Elastic Modulus Existing	Ee	10	11	
Elastic Modulus Overlay	Eo	12	13	
Thermal Coef. Existing	αε	14	15	
Thermal Coef. Overlay	αo	16	17	
Shear Str. Exist.-Overlay	Se-o	18	19	
Remaining Life	R1	21	22	20
Crack Spacing Existing Pvt.	Cs	23	24	

* Indicates variables accepted to influence stress values

Table 4.9 Wheel load stress analysis results

#	Concrete Stress Through Pavement Section														Max. Intf. Stress	
	Node															
	389	388	387	386	385	384	383	382	381	380	379	378	377	376	σ	τ
W1	-36	-31	-28	-26	-26	-28	-28	-18	-5	6	13	20	35	49	-0.88	8.26
W2	-37	-31	-28	-27	-27	-28	-28	-15	-3	7	13	19	33	47	-0.91	8.29
W3	-37	-31	-28	-27	-27	-28	-28	-16	-4	6	13	19	34	48	-0.90	8.69
W4	-37	-31	-27	-25	-23	-23	-23	-19	-6	5	12	20	35	50	-0.90	8.75
W5	-37	-31	-27	-25	-25	-25	-25	-19	-6	5	12	20	35	49	-0.89	8.72
W6	-37	-31	-28	-26	-26	-27	-28	-18	-5	6	13	20	35	49	-0.89	8.68
W7	-37	-31	-28	-26	-26	-27	-28	-18	-5	6	13	20	35	49	-0.89	8.68
W8	-35	-31	-38	-19	-12	0	12	-39	-17	4	13	20	35	47	-0.88	8.26
W9	-36	-31	-28	-26	-26	-28	-28	-18	-5	6	13	20	35	49	-0.88	8.26
W10	-35	-30	-28	-29	-32	-38	-44	-4	2	10	14	19	17	17	-1.30	9.95
W11	-45	-34	-27	-22	-18	-16	-14	-19	-5	6	12	17	35	51	-1.02	9.18
W12	-31	-26	-24	-23	-24	-24	-24	-14	-8	0	9	19	32	45	-1.01	9.88
W13	-42	-32	-25	-20	-14	-11	-7	-27	-11	2	11	19	34	49	-0.95	9.17
W14	-36	-31	-28	-26	-26	-28	-28	-18	-5	6	13	20	35	49	-0.88	8.67
W15	-36	-31	-28	-26	-26	-28	-28	-18	-5	6	13	20	35	49	-0.88	8.67
W16	-36	-31	-28	-26	-26	-28	0	-18	-5	6	13	20	35	49	-0.88	8.67
W17	-36	-31	-28	-26	-26	-28	0	-18	-5	6	13	20	35	49	-0.88	8.67
W18	-41	-19	0	12	24	30	37	-65	-41	-20	-1	18	37	58	0.00	0.00
W19	-36	-31	-28	-26	-26	-27	-28	-18	-5	6	13	20	35	49	-0.88	8.67
	Node															
	126	125	124	123	122	121	120	119	118	117	116	115				
W20	-55	-41	-30	-19	-9	-17	-1	13	20	28	36	44			5.60	1.46
W21	-53	-40	-29	-19	-9	-16	-2	12	19	26	33	42			5.59	1.46
W22	-53	-40	-29	-19	-9	-16	-2	12	19	26	33	42			5.59	1.46
W23	-43	-32	-23	-15	-8	-15	-4	6	10	16	22	28			5.40	4.41
W24	-53	-40	-29	-19	-9	-16	-2	12	19	26	33	42			5.59	1.46

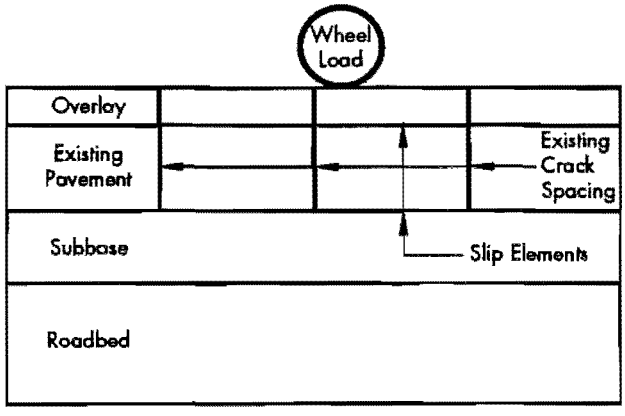

Figure 4.12 Typical section used in the analysis

4.6.2 *Sensitivity Analysis Results*

Table 4.9 show the results from the wheel load analysis. The environmentally induced stress evaluation is shown in Table 4.10. In Table 4.9, the **W** indicates wheel loading, and in Table 4.10 the **T** indicates environmental stress calculations. The numbers correspond to the analysis numbers in Table 4.8. Both tables show normal stresses for each node in psi as well as the maximum interface shear (s) and tension (t) stresses in psi. Figure 4.13 shows the layout of the nodes used for the largest portion of the factorial.

For both cases, analysis numbers 1 to 19 were computed using a data set different from that used to compute analysis numbers 20 to 24. The data set used for analysis numbers 20 to 24 was smaller, to reduce analysis time and, therefore, computer analysis costs.

Table 4.10 Environmental induced stress analysis results

#	Concrete Stress Through Pavement Section														Max. Intf. Stress	
	Node															
	389	388	387	386	385	384	383	382	381	380	379	378	377	376	s	t
T1	628	630	632	633	634	636	639	649	641	637	636	636	636	634	-0.15	11.60
T2	629	630	632	633	633	635	638	574	565	561	561	561	560	559	-0.15	9.49
T3	628	630	632	633	634	636	638	609	601	596	596	596	596	595	-0.14	10.48
T4	552	555	556	558	559	561	564	649	641	637	636	636	636	634	-0.15	11.63
T5	588	590	592	593	594	596	599	649	641	637	636	636	636	634	-0.15	11.62
T6	634	634	635	635	635	636	637	646	640	638	637	637	637	637	-0.10	11.40
T7	631	632	633	634	634	636	638	648	641	637	636	637	636	635	-0.12	11.50
T8	628	630	632	633	634	636	639	649	641	637	636	636	636	634	-0.15	11.60
T9	628	630	632	633	634	636	639	649	641	637	636	636	636	634	-0.15	11.60
T10	632	632	633	633	633	633	634	318	318	318	317	317	317	317	0.15	0.21
T11	633	632	630	628	624	625	624	501	485	477	476	476	475	474	-0.17	11.56
T12	333	633	330	326	326	311	296	547	606	639	643	642	644	649	-0.43	12.37
T13	475	632	471	469	466	466	464	655	643	637	636	636	635	633	-0.20	11.69
T14	632	331	633	634	634	634	634	317	317	317	317	317	317	317	-0.23	15.06
T15	627	473	632	633	634	636	639	489	481	477	476	476	476	474	-0.15	8.81
T16	308	632	312	313	314	316	319	649	641	637	636	636	636	634	-0.15	11.61
T17	468	630	472	473	474	476	479	649	641	637	636	636	636	634	-0.14	11.61
T18	647	310	633	628	624	621	619	636	636	637	637	638	638	639	0.00	0.00
T19	628	470	632	633	634	636	639	649	641	637	636	636	635	634	-0.15	11.61
	Node															
	233	232	231	230	229	228	227	226	225	224	223	222				
T20	635	635	635	635	635	635	635	635	635	635	635	635			-0.02	0.01
T21	32	49	66	81	96	102	109	79	114	151	193	237			-5.18	1.17
T22	32	49	66	81	96	102	109	79	114	151	193	237			-5.18	1.17
T23	11	8	4	2	-1	-2	-3	9	1	-6	-12	-19			2.00	0.19
T24	32	49	66	81	96	102	109	79	114	151	193	237			-5.18	1.17

4.6.3 *Discussion of Results*

The results show specific variables which should be included in a stress analysis of bonded concrete overlays. It was previously noted that the thickness of the overlay and existing pavement influences the stress within the pavement when wheel loading is considered. Pavement thickness does not influence maximum environmental stresses induced in the system. The variables influencing stress for wheel and environmental loading are shown in Table 4.11. These variables significantly change either the maximum stress at certain points within the concrete or the distribution through the concrete section. The level used in the analysis factorial, completed in a later chapter, is also shown for each variable. Using these variables, a design equation for stresses in bonded concrete overlays could be developed as part of the design procedure for bonded concrete overlays.

Table 4.11 Factors influencing long-term performance of BCO

Factors Influencing Stress Values in BCO			
Environmental	Level	Wheel Loading	Level
Modulus: Existing	2	Modulus: Existing	3
Modulus: Overlay	2	Crack Spacing	2
Thermal Coef Existing	2	Overlay Thickness	3
Thermal Coef Overlay	2	Existing Pvt. Thickness	3
Crack Spacing	2		
Overlay Thickness	3		
Existing Pvt Thickness	3		

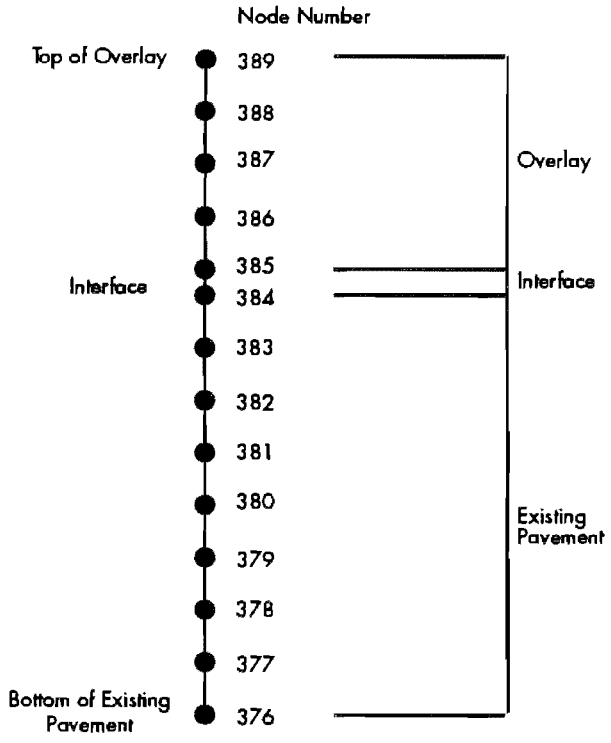

Figure 4.13 Layout of nodes shown in Tables 4.9 and 4.10

4.7 CONCLUSIONS AND RECOMMENDATIONS FOR ANALYSIS

From this chapter, it can be concluded that the modulus values of the existing pavement and overlay, the thermal coefficients of existing pavement and overlay, and the crack spacing all significantly influence stresses due to environmental conditions. Stresses due to wheel loads are significantly influenced by modulus value of the existing pavement, crack spacing, overlay thickness, and existing pavement thickness. These variables should be used in the development of a design equation for bonded concrete overlays.

CHAPTER 5. ANALYSIS OF FIELD PERFORMANCE OF BONDED CONCRETE OVERLAYS IN HOUSTON

5.1 INTRODUCTION

The factors identified in Chapter 4 are accepted as the most important variables in defining stress within the pavement. However, these factors do not evaluate the fatigue performance due to traffic loading and environmental conditions. Field data are needed, in conjunction with the variables in Chapter 4, to evaluate the stresses in BCO caused by wheel loading and the environment.

In order to evaluate the performance of the pavement, empirical data are needed to evaluate the long-term performance of bonded concrete overlays and these data should be tied in with the stress equations to complete the design model. Field data are normally very difficult to interpret and the variables necessary to explain the variability are not obtained in every case. However, the field data are, normally, the only means for establishing the long-term performance of a pavement.

In this chapter, field data from two different areas are analyzed to establish the factors which influence cracking and delamination the most. These test sections are in Houston and are under surveillance by the Center for Transportation Research. The locations are shown in Figure 5.1. The factors obtained from this analysis will be used with the stress variables discussed in the previous chapter to develop the design model.

5.2 SURVEY PROCEDURES

Most survey procedures done on test sections in Houston include a visual condition survey, to establish longitudinal crack length, number of transverse cracks, and delaminated areas. Transverse and longitudinal cracks were logged on paper from which the number of cracks and the lengths have been obtained. Delamination can be detected only by using sounding techniques or radar. On test sections in Houston, reinforcing bars were used to "sound" the pavement. The bars were dropped from about 6 inches above the pavement surface. A solid sound indicated a non-delaminated area, while a hollow sound, like the sound in a cave when the cave side is hit with a stone, indicated a delaminated area.

The surveys were also normally accompanied by falling weight deflectometer readings at various intervals. The falling weight deflectometer readings give an indication of the modulus values of the different layers in the system. These deflection measurements are highly dependent on the rainfall before the measurements (Ref 51) and the time of day or season the measurements are taken, as well as the load used to take the measurements. It is known that during the afternoon in the summer the pavements are expanded and may be in compression at cracks, which will produce a lower deflection than when measurements are taken during the morning, when it is cooler and the cracks may be open. The same explanation for transverse and longitudinal cracking exists when the overlay is placed. On test sections in Houston, cracks were spotted at an early age only during the cool morning hours.

The variability in time of the measurement, as well as the variability between different surveyors causes errors in the data collection process which are difficult to eliminate, especially for research projects which extend for long periods, during which surveyors change and the environmental factors are not exactly the same for each survey.

5.3 CRACKING AND DELAMINATION SURVEYS OF 2- TO 3-INCH BONDED CONCRETE OVERLAY

Five test sections were built in 1983 on the South Loop of Interstate Highway 610 in Houston. These sections consisted of three 2-inch sections, of which one was reinforced with wire fabric, one was reinforced with fibers, and the other was not reinforced. The other two sections were 3-inch sections, of which one was reinforced with wire fabric and the other with fibers.

5.3.1 Previous Surveys

Different surveys were performed from 1983 to 1990. A before-overlay construction condition survey was completed in May 1983. After-overlay condition surveys followed in February 1984, November 1984, and May 1985. These data were analyzed by Bagate (Ref 52). The various surveys included deflection

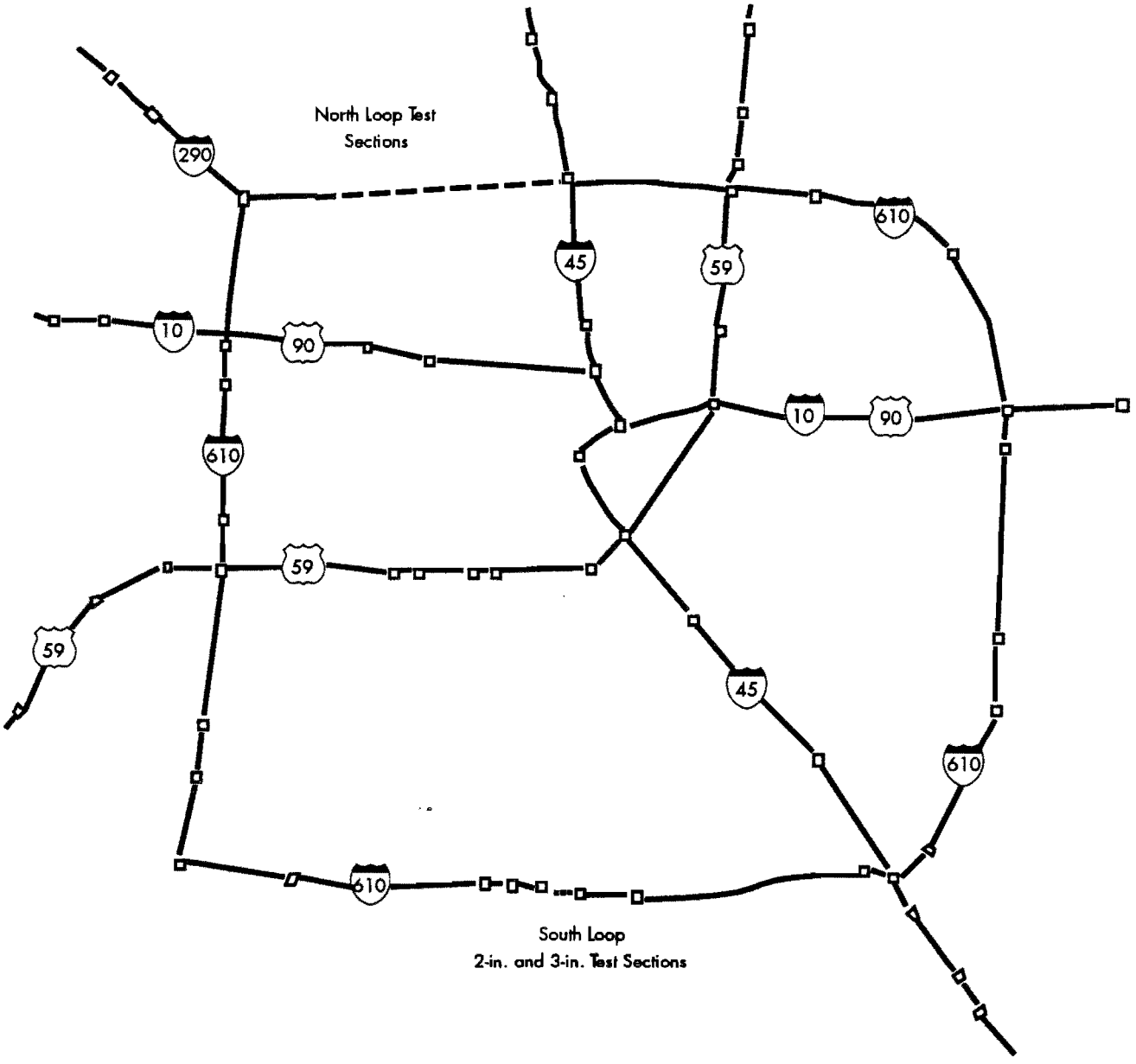

Figure 5.1 Test sections surveyed in Houston on North and South Loops of Interstate Highway 610

measurements. A further survey of Lanes 3 and 4 was completed in April 1990, evaluating transverse and longitudinal cracking as well as delamination. No delamination was found in any area.

5.3.2 Survey Results

The results for Lanes 3 and 4 are shown in Table 5.1 for transverse and longitudinal cracking. The results show cracking from the before-construction survey and the February 1984, November 1984, and April 1990 surveys.

5.3.3 Statistical Analysis of Results

The results shown in Table 5.1 were used in an analysis of variance for transverse as well as longitudinal cracking. The results of the statistical analysis for transverse and longitudinal cracks are shown in Table 5.2.

For transverse cracking, the model selected accounts for 81 percent of the variability, which is the the model sum of squares divided by the corrected total sum of squares. The square root of the number of transverse cracks per 100-foot section was modeled and the residuals plotted favorably. Only the

Table 5.1 Summary of transverse and longitudinal cracks on 2-inch and 3-inch test sections of South Loop IH610, in Houston

	Number Transverse Cracks							
	5/1/1983*		2/1/1984		11/1/1984		4/1/1990	
Section	Lane 3	Lane 4	Lane 3	Lane 4	Lane 3	Lane 4	Lane 3	Lane 4
2 in. NR	76	64	33	25	53	48	54	56
2 in. R	75	77	49	47	87	78	130	110
3 in. R	77	79	38	28	76	64	85	44
3 in. F	82	69	1	8	21	21	13	11
2 in. F	34	30	0	4	8	6	0	0
	Total Length Longitudinal Cracks (ft)							
	5/1/1983*		2/1/1984		11/1/1984		4/1/1990	
Section	Lane 3	Lane 4	Lane 3	Lane 4	Lane 3	Lane 4	Lane 3	Lane 4
2 in. NR	121	65	94	34	160	89	20	135
2 in. R	24	64	29	61	29	147	75	175
3 in. R	152	60	23	48	23	52	47	170
3 in. F	183	141	0	0	3	117	33	70
2 in. F	122	72	0	4	14	4	0	0

* Before Overlay
NR - No Reinforcing
R - Reinforced with Wire Fabric
F - Fiber Reinforced

Table 5.2 ANOVA for transverse and longitudinal cracks

ANOVA for Transverse Cracking					
Source	DF	Sum of Square	Mean Square	F-Value	PR > F
Model	11	52.30	4.75	7	0.0002
Error	18	12.23	0.68		
Corrected Total	29	64.53			
Source	DF	Sum of Square	F-Value	PR > F	Significant
Reinforcing	1	0.570	0.84	0.3719	No
Section	1	8.525	12.55	0.0023	Yes
Time	2	0.018	0.01	0.9871	No
Thickness	1	6.565	5.25	0.0343	Yes
Reinforcing * Time	2	0.826	0.61	0.5554	No
Section * Time	2	1.686	1.24	0.3126	No
Thickness * Time	2	0.795	0.59	0.5671	No
ANOVA for Longitudinal Cracking					
Source	DF	Sum of Square	Mean Square	F-Value	PR > F
Model	3	8.21	2.74	7.4	0.0010
Error	26	9.62	0.37		
Corrected Total	29	17.82			
Source	DF	Sum of Square	F-Value	PR > F	Significant
Thickness	1	0.743	2.01	0.1682	No
Reinforcing	1	7.316	20.36	0.0001	Yes
Time	1	0.673	1.82	0.1898	No

thickness and section were significant. The type of reinforcing and the section are correlated with each other. When the sections are omitted from the analysis, the reinforcing becomes highly significant. The conceptual model from the transverse cracking analysis is

Number of Transverse Cracks = f(Section, Thickness)

The model for longitudinal cracking explains 64 percent of the variability in longitudinal cracking. Again a square root model was used and the residuals plotted favorably. The reinforcing is the only factor significant at the 5 percent level. With interactions, 95 percent of the variability is accounted for but no significance is found. In a T-test between the April 1990 and November 1984 data collections no significant increases were found in transverse or longitudinal cracking. The conceptual model for longitudinal cracking is

Length of Longitudinal Cracking = f(Reinforcing).

From this analysis, it can be concluded that reinforcing type, thickness, and type of pavement are important in transverse crack development in bonded concrete overlays. Only the type of reinforcing influences the formation of longitudinal cracking. Environmental factors during construction could also influence the formation of longitudinal cracking, but these measurements were not taken during construction.

Another factor from the experimental results which is important in the analysis of bonded concrete overlays is that different reinforcing procedures produce different crack spacing. Table 5.3 indicates the before-overlay and after-overlay crack spacings for the five sections analyzed. For non-reinforced sections, the crack spacing was higher than for the before-overlay crack spacing. Results for wire reinforced sections were not significantly different for after and before-overlay crack spacing, while fibers significantly increased crack spacing.

Wire reinforced sections are normally reinforced with the same percentage reinforcing as the existing pavement section, and the concrete will react the same as the original pavement did. This increases the probability of reflective cracking, which is evident from Table 5.3, in which the average crack spacing, between before and after-overlay data is not significantly different. Non-reinforced sections have no restraint due to reinforcing and can have higher crack spacing, than the existing pavement before overlay. Fiber-reinforced sections are a totally different material, as can be seen from the average crack spacing comparison.

5.4 CRACKING, DEFLECTION, AND DELAMINATION SURVEYS OF 4-INCH BONDED CONCRETE OVERLAY ON THE NORTH LOOP OF IH-610 IN HOUSTON

Ten test sections were constructed on the outside lane of the IH610 North Loop during December 1985 and January 1986. A study was made by the Center for Transportation Research to evaluate these test sections. The objectives of this study (Ref 51) were to identify several sections that showed variations in the original pavement condition and in materials used for the overlay, to observe and record actual materials used for the overlay, to observe the behavior of parameters before and after overlay, and to evaluate the field data. Some important conclusions made from this study should be mentioned before follow-up surveys are analyzed. Five surveys were completed in this study, of which two were before-overlay surveys (22 May 1985 and 3 December 1985) and three were after-overlay surveys (4 February 1986, 13 January 1987, and 19 March 1987). Traffic data were obtained from traffic counters located near the test sections. The method of calculating the 18-kip ESAL is discussed in the next chapter.

From this study, it was concluded that bonded concrete overlays significantly reduced the pavement

Table 5.3 Before and after-overlay average crack spacing

Section	Avg Before-Overlay Crack Spacing (ft)	Avg After-Overlay Crack Spacing (ft)
2-in. Nonreinforced	2.3	3.0
2-in. Reinforced	1.8	1.4
3-in. Reinforced	2.3	2.7
3-in. Fiber Reinforced	2.4	10.9
2-in. Fiber Reinforced	4.9	45.7

After-overlay crack spacings were calculated as the average of November 1984 and April 1990 crack spacings due to no statistical difference between the two.

deflection, that the bonded concrete overlays reestablished load transfer at cracks, that the existing pavement condition did not influence the overlay performance as long as existing distress was repaired before overlay, and that good shear strength was developed at the interface in all the sections, especially in the fiber and limestone sections.

These conclusions need to be kept in mind when the follow-up analysis is completed.

5.4.1. Previous Surveys

A previous study was done on the outside lane in the eastbound direction. Due to the difficulty of traffic control on the outside lanes and the detection of delamination in the interior lanes, sections across from the initial study were identified in the westbound and eastbound directions for the two lanes next to the median in each direction. Condition surveys during March 1987, March 1988, and March 1990 were undertaken by the Center for Transportation Research. The data provided the opportunity to evaluate transverse and longitudinal crack development as well as to evaluate the effect of delamination and to establish its progression. Unfortunately, before-overlay data were not available on these test sections. The effect of the existing pavement can, therefore, not be modeled with certainty.

5.4.2 Survey Results

No longitudinal crack survey was made in March 1988. The dataset consists of many variables which are used to explain some of the variability in transverse and longitudinal crack development and in delamination. The specific variables in the dataset are direction, lane, percent delamination per 100-foot section, number of transverse cracks per 100-foot section, length of longitudinal cracks per 100-foot section, time since construction, traffic since construction, reinforcing type, aggregate type, areas with and without grout, and various construction measurements, such as concrete temperature, humidity and evaporation during construction, and the maximum and minimum temperatures during the first day after construction.

5.4.3 Statistical Analysis of Results

The statistical analysis of the data is divided into four parts. First, some material properties are back-calculated to evaluate the concrete modulus of elasticity as well as the roadbed modulus to assure compatibility with the inference base used to do the finite element analysis part of this work. Then delamination and crack development are discussed and analyzed.

5.4.3.1 Back-Calculation of Material Properties

The back-calculation program RPEDD1 (Ref 53), developed at The Center for Transportation Research, is used to back-calculate material properties. The back-calculation is done for various sections on the North Loop. Table 5.4 show the modulus of elasticity for the concrete layers, subbase, and roadbed for the March 1987 and March 1988 surveys. These properties were calculated from deflections obtained using the Dynaflect deflection measurement system.

From these results it can be seen that only minor differences exist between the modulus values of sections or between the modulus values for the first two observations. The modulus values for the March 1990 survey are also shown. Because a Falling Weight Deflectometer was used to obtain deflections in the 1990 survey and the Dynaflect machine was used to obtain March 1987 and 1988 deflections, deflection measurements cannot be directly compared and, as can be seen from the data in Table 5.4, modulus values differ significantly. However, the trend in the modulus of elasticity of the concrete between sections is the same for the Dynaflect and for Falling Weight Deflectometer data. The subbase and roadbed moduli do not follow the same trend, mainly due to the differences in the evaluation procedures.

The Falling Weight Deflectometer procedure calculates deflections using loads varying from 4000 pounds to 16,000 pounds with 7 sensors one foot apart. The Dynaflect loading is 1,000 pounds with 5 sensors. The results are, therefore, not directly comparable.

The back-calculated modulus values for March 1990 show that the concrete layers are still in good shape, with high modulus values. This is important because, according to slab theory, the concrete layer is the most important factor in stress calculations.

5.4.3.2 Delamination Development

Delamination of bonded concrete overlays was first noticed on the North Loop in the March 1987 condition survey on the inside two lanes in both directions. The time at which the delamination took place was uncertain, because it was detected a few years after construction, but no sounding tests were done between the time of construction and March 1987. On the 2-inch and 3-inch sections on the South Loop, delamination was detected on the two inside lanes. Only a very small percentage of delamination was reported and, again, it was the first time it was sounded. The questions, therefore, are whether delamination is a progressive failure of bonded concrete overlays which can ultimately lead to total failure or is an early-age problem which is not progressive but increases the maintenance eventually required on the overlay.

Voigt et al (Ref 54) reported that delamination was found on two bonded concrete overlay projects with jointed concrete pavements. It was concluded that in one case the delamination was caused by

Table 5.4 Moduli of elasticity, in psi, back-calculated from dynaflect data, for March 1987 and 1988 and falling weight deflectometer data for March 1990

		Modulus of Elasticity (psi)		
Date	Section	PCC Layer X 10E6	Subbase x 10E5	Roadbed X 10E3
Mar-87	102	3.6	1.9	23.0
	103	3.1	1.3	17.7
	104	3.0	1.3	18.8
	105	3.4	1.8	19.2
Mar-88	102	3.5	2.0	21.9
	103	3.1	1.8	15.1
	104	3.2	1.9	19.7
	105	2.3	0.8	19.2
Mar-90	102	5.9	4.0	29.8
	103	5.6	4.0	28.7
	104	6.0	0.9	31.2
	105	4.5	2.8	32.4

large temperature changes within the first days after construction. The other case experienced half of the delamination the first year, with the other half occurring over the next four years. Only 0.3 percent of the total was found to be delaminated. The delamination occurred mostly at the corners of the slab edges and the transverse joints (Ref 55). No significant delamination was found at transverse cracks. It was concluded that the cause was that inadequate bond was obtained during construction. On test sections in Houston under surveillance of The University of Texas at Austin, it was observed that delamination occurred within 24 hours after construction. It progressively increased until one month after construction, when it reached a plateau and there were no further significant increases.

The purpose of this analysis is, therefore, to compare three stages of the delamination surveys on the North Loop and establish whether the delamination was progressive or not. This will aid in establishing the significance of delamination in long-term performance of bonded concrete overlays. One important factor in the analysis of delamination is the variability because the surveys were conducted at different times, as well as the variability between operators. An experiment was conducted in Houston in December 1987 by the Center for Transportation Research to evaluate operator variability. Two sections, each 50 feet long and 12 feet wide, were sounded by four different operators. The percentage of delamination each operator found in each section was tabulated and analyzed and is shown in Table 5.5.

By obtaining a pooled variance a best estimate of the standard deviation, 0.35 percent, was found. It is, therefore, assumed that the data were normally distributed. The critical value for the operator error, with 95 percent confidence level, can be represented by the standard deviation multiplied by the value for $Z_{0.025}$, which is 1.96. Therefore, the critical operator error is equal to 0.69 percent, which means that only if the observed delamination increases by more than 0.69 percent can it be said with 95 percent certainty that the delamination increases.

Analysis of Each Year

Figure 5.2 shows the delamination for the three different survey times. It can be seen from the figure that the same trend for each survey exists. An analysis of variance was completed for each survey year.

The results showed significance only for aggregate type, except for the 1990 survey, in which direction and lane interaction were also significant. This means that a significant amount of the variability in the model is due to the aggregate type.

Silicious river gravel (SRG) pavement experienced much higher delamination than the limestone (LS) pavement. However, the largest portion of the

Table 5.5 Operator variance experiment data

	% Delamination Measured	
Operator Number	Section A	Section B
1	1.92	3.87
2	1.35	4.08
3	2.25	4.17
4	2.02	3.48
Mean	1.89	3.90
Std Dev	0.38	0.31

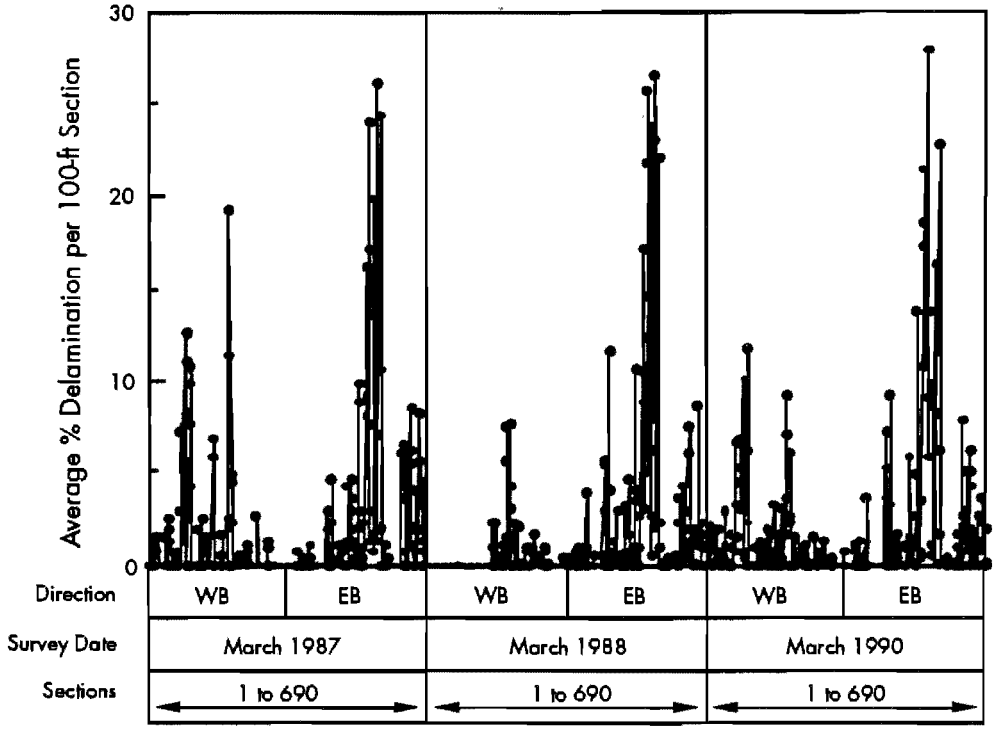

Figure 5.2 Delamination by survey year

test sections were constructed using SRG. The time of placement varied and, therefore, the environmental factors could have had a big influence on the fact that SRG showed much higher delamination. Therefore, we can conclude only that there was a difference in delamination between SRG and limestone pavements for the tests section surveyed.

Analysis of Full Factorial

An analysis of the full factorial was completed and provided two interactions which were significant: the interactions of direction with traffic and of direction with time. The conceptual model for this analysis is

% Delamination = f(Traffic x Direction, Time x Direction).

Figures 5.3 and 5.4 show the average percentage of delamination by direction and time and by direction and traffic, respectively. The time levels selected were 6 to 24 months as low, 25 to 42 as medium, and 43 to 54 as high. The traffic levels selected were 0 to 500,000 ESAL as low, 500,000 to 900,000 as medium, and 900,000 to 1,600,000 as high.

It is evident from these two figures that no real trend exists between delamination and traffic, but that the directional factor is very important. The data were obtained from test sections in the east and west directions, which were constructed at different times.

Table 5.6 shows an analysis of variance of only the main effects. It shows that the direction, reinforcing, aggregate, and temperature differences between temperature at placement and minimum temperature during the first night after placement are all significant. The conceptual model is

% Delamination = f(Direction, Reinforcing, Aggregate, Temperature Differential).

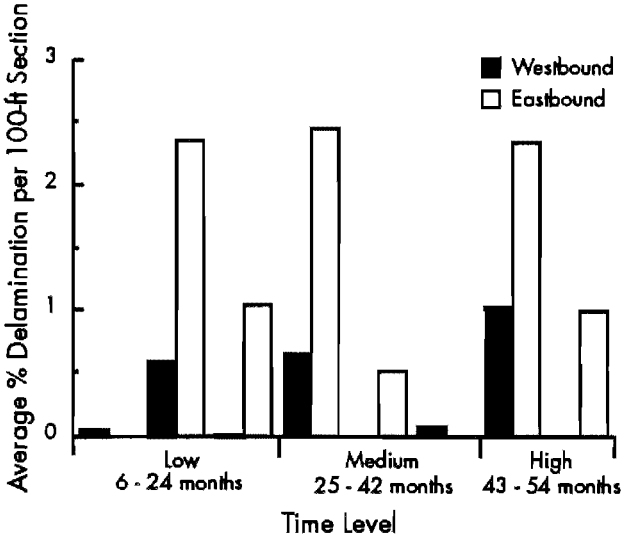

Figure 5.3 Direction and time interaction

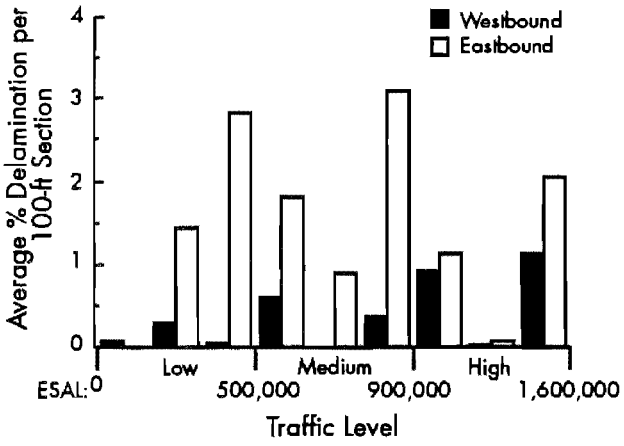

Figure 5.4 Direction and traffic interaction

However, to evaluate the progressiveness of delamination, direction and lane should not be part of the analysis because each direction and lane is modeled by traffic or time. It was also found that time and traffic are highly correlated, so only one of the two can be used as a variable.

T-Test and Analysis of Variance

T-tests between the delamination results of March 1988 versus March 1987, March 1990 versus March 1987, and March 1990 versus March 1988 were run and no significant differences were found between any of these. The results of the T-tests are shown in Table 5.7.

In order to explain the delamination phenomenon, several models were used to evaluate the variability. However, the highest R^2 value obtained was 16 percent. The conceptual model for this analysis is

% Delamination = f(Aggregate, Temperature Differential).

The delamination was transformed to the fourth root in the model. Due to the fact that the traffic and time variables are highly correlated, only the time variable was used in the analysis. The square root of the delamination was also used, but it formed a linear relation with the residuals. The fourth root also formed a linear relationship with the residuals, but the gradient was smaller and the R^2 increased slightly. The R^2 can be increased further by using higher roots of delamination, but the increase is marginal and the residuals do not decrease much. Aggregate, temperature differences between temperature at placement and minimum temperature during the first night after placement, and the interaction of this temperature difference with time and year are significant at the one percent level. The model does not explain the variability very well so it must be assumed that factors not evaluated in this model are important and are responsible for the linear effect of the residuals plot. Because the increases in delamination from 1987 to 1990 are not significant, the time variable

Table 5.6 Analysis of variance for delamination

Source	DF	Sum of Square	Mean Square	F-Value	PR > F
Model	8	1,580	197	25.4	0.0001
Error	1,911	14,856	8		
Corrected Total	1,919	16,436			

Source	DF	Sum of Square	F-Value	PR > F	Significant
Direction	1	822.196	105.76	0.0001	Yes
Lane	1	0.074	0.01	0.9220	No
Reinforcing	1	270.865	47.71	0.0001	Yes
Aggregate	1	240.696	30.96	0.0001	Yes
Grout	1	16.149	2.08	0.1497	No
Traffic	1	22.565	2.90	0.0886	No
Time	1	19.143	2.46	0.1168	No
Temp Difference	1	81.934	10.54	0.0012	Yes

Table 5.7 T-test comparison of differences = 0

Comparison	Mean	Std Error	T	Prob > |T|	Significant
Delamination 1988 – Delamination 1987	0.0071	0.0647	0.1096	0.9128	No
Delamination 1990 – Delamination 1987	0.0634	0.0841	0.7532	0.4516	No
Delamination 1990 – Delamination 1988	0.0687	0.0923	0.7444	0.4570	No

and year variable are not important. The only factors showing significance are the aggregate and temperature differences. However, the aggregate was significant for each year the data were collected, as previously mentioned. The only variable left to describe this variability is the temperature difference. An analysis of variance considering only reinforcement, aggregate, grout, and temperature difference explains only 7 percent of the variability, but the residuals show that the model fits the results better without time variables.

This implies that the early-age variables, of which temperature difference is typical, are very important. It is, therefore, concluded that delamination is an early age phenomenon. It was shown by van Metzinger et al (Ref 56) that factors creating high shear stresses, or high movements, in the overlay at early ages, as well as factors influencing the strength growth of the interface strength, cause delamination.

Early-Age Analysis

An analysis of variance was also performed evaluating the early-age effects measured on the development of delamination. The factors discussed in the previous paragraphs explained less than 17 percent of the variability in the measurements. In the early-age variables analysis, many factors and their interactions were found to be significant. Evaporation rate, humidity, and temperature difference were all significant. However, only 22 percent of the variability was explained. The analysis of variance also confirms that the early development of the concrete has the largest influence on the delamination phenomenon observed on bonded concrete overlays. Modeling of this phenomenon using early-age variables was done by Lundy (Ref 57).

Conclusions

It can, therefore, be concluded that delamination of bonded concrete overlays is an early-age problem which occurs during the first few weeks after construction. Delamination is not progressive, but its influence on the long-term performance of the pavement is uncertain, and delaminated areas may ultimately need maintenance before areas which are not delaminated.

5.4.3.3 Transverse Cracking Development

The evaluation of the transverse cracking is divided into an annual analysis, a combined analysis with all variables, and, finally, an analysis without direction and lane to evaluate the progression of the increase in the number of cracks per 100-foot section.

Analysis Per Year

In an analysis of variance study of each year, the most important parameter obtained from the analysis was the aggregate type, which was significant in all three years. This suggests that the initial crack development depends highly on the aggregate type used. This is very similar to newly constructed, continuously reinforced concrete pavements. In general, the concrete made with silicious river gravel showed more cracking than concrete made with limestone aggregate (Ref. 64).

Analysis of Full Factorial

An ANOVA for a full factorial was completed. Only 22.9 percent of the variability in the data is explained by the model. When only the main effects are analyzed similar variables shown significance, as when the interactions are included in the analysis. The ANOVA for only main effects is shown in Table 5.8. The conceptual model is

Number of Transverse Cracks = f{Direction, Lane, Reinforcing, Time, Temp. Differential}

However, ANOVA does show that there is a significance in the direction, between lanes, reinforcement type, traffic, time, the temperature difference between concrete temperature and lowest temperature during the first night after construction, and various other interactions. Lanes in the east direction showed a higher number of transverse cracks than the westbound lanes. The wire reinforced sections showed a higher number of transverse cracks per section than the fiber sections. Lane 2 showed more cracking than lane 1. The traffic and time variables did not show any particular trend. The temperature difference showed an increase in cracking as the temperature differential increased. This means that more cracks formed when the temperature difference was high during the early-age development of the concrete pavement. No specific conclusions can be made from the interactions.

T-Tests of Differences Between Years

Before proceeding with an evaluation of different models excluding the direction and lane parameters, t-tests comparing March 1987 to March 1988, March 1987 to March 1990, and March 1988 to March 1990 were done. The t-tests between the data of various years showed no significant difference between March 1987 and March 1988. As can be seen from Table 5.9 the comparisons of 1990 data showed a significant increase above that of 1987 and 1988.

It is necessary to model the development of progression of the cracks, but it is also important to evaluate the effect of delamination on the formation of cracking. An analysis must, therefore, be made looking at transverse cracks in areas delaminated versus those in areas not delaminated, and of cracks between the different years of analysis.

Table 5.8 ANOVA for full factorial for tranverse cracks

Source	DF	Sum of Square	Mean Square	F-Value	PR > F
Model	8	92,964	7,870	51.24	0.0001
Error	1,893	290,746	154		
Corrected Total	1,901	353,710			

Source	DF	Sum of Square	F-Value	PR > F	Significant
Direction	1	1,138.669	7.41	0.0065	Yes
Lane	1	449.113	2.92	0.0874	No
Reinforcing	1	25,583.154	166.57	0.0001	Yes
Aggregate	1	14,282.962	92.99	0.0001	Yes
Grout	1	3.547	0.02	0.8792	No
Traffic	1	97.049	0.63	0.4268	No
Time	1	852.480	5.55	0.0186	Yes
Temp Difference	1	3,761.784	24.49	0.0001	Yes

Table 5.9 T-test of differences = 0

Comparison	Mean	Std Error	T	Prob > I T I	Significant
TCracks 1988 – TCracks 1987	– 1.3084	0.6912	– 1.8930	0.0589	No
TCracks 1990 – TCracks 1987	5.5211	0.6016	9.1775	0.0001	Yes
TCracks 1990 – TCracks 1988	6.3913	0.6710	9.5244	0.0001	Yes

Analysis Without Direction and Lane

The next step in the analysis was modelling the transverse cracks and evaluating delaminated and non-delaminated areas. Table 5.10 show the analysis of variance of only the main effects of transverse cracks without direction and lane. Significance exists in the reinforcing, aggregate, time, and temperature differential. A conceptual model for this analysis is

Number of Transverse Cracks = f(Reinforcing, Aggregate, Time, Temperature Differential)

When the time is plotted versus the number of transverse cracks, no real trend exists. In an analysis with interactions the interaction of reinforcing with time was also significant. Twenty percent of the variability is explained. A plot of the residuals versus

Table 5.10 ANOVA for transverse cracking excluding direction and lane

Source	DF	Sum of Square	Mean Square	F-Value	PR > F
Model	6	61,219	10,203	66.1	0.0001
Error	1,895	292,491	154		
Corrected Total	1,901	353,710			

Source	DF	Sum of Square	F-Value	PR > F	Significant
Reinforcing	1	32,179.12	208.48	0.0001	Yes
Aggregate	1	16,337.77	105.85	0.0001	Yes
Grout	1	4.59	0.03	0.8631	No
Traffic	1	200.49	1.30	0.2545	No
Time	1	2,687.02	17.41	0.0001	Yes
Temp Difference	1	6,107.22	39.57	0.0001	Yes

predicted values of the model showed that the model explains the data sufficiently. It must then be assumed that factors not measured in this dataset are responsible for the rest of the variability in the development of the transverse cracks. The by-year analysis showed that the aggregate is significant. It must, therefore, be assumed that the development of cracking is dependent on the aggregate type and reinforcing used in the pavement, which is the same conclusion made from the 2-inch and 3-inch sections on the South Loop.

The time analysis is also significant; it gives an indication of the development of transverse cracks with time. Figure 5.5 shows a plot of the average number of transverse cracks per 100-foot section versus the year of analysis. A Student-Newman-Keuls test was performed on the averages and it showed that all three are significantly different from each other. It can, therefore, be concluded that no real trend exists between the transverse cracks and year of analysis and that the variability with measurements and operators is an important factor in the analysis. It can also be argued that other factors, such as misalignment of test sections between the three different condition surveys, can cause variability not explained by the model.

Analysis of Delaminated Areas

An ANOVA for the areas delaminated was completed. The conceptual model is

% Delamination = f(Aggregate, Temperature Difference)

The analysis showed that the aggregate type, temperature difference between the concrete temperature and lowest ambient temperature during the first night after placement, and an interaction between temperature difference and reinforcing are significant.

The analysis suggests that the cracking in delaminated areas depends on the early-age factors and the aggregate type. This is very much the same as the results of the analysis per year done previously. The model explains only 15 percent of the variability.

Figure 5.6 shows the average number of transverse cracks per section for delaminated sections. A Student-Newman-Keuls test was done to compare the means of each different year of survey.This test showed significant difference in transverse cracking between 1990 versus 1987 and 1988 survey results. No significant difference was found between 1987 and 1988 results.

It can be seen from Fig 5.6 that an increasing trend exists between the number of transverse cracks and time. The development of this cracking will be discussed later when a stress analysis of delaminated pavements is made. We can therefore conclude that transverse cracks increases significantly in delaminated areas.

Analysis of Non-Delaminated Areas

The analysis procedure used for delaminated areas was used for non-delaminated areas. The conceptual model can be illustrated by the following equation:

% Delamination = f(Aggregate, Analysis Year)

Only the aggregate and year of analysis were found to be significant. The aggregate was also significant for the by-year analysis, which again showed the difference in crack development for different aggregates. A Student-Newman-Keuls test was performed to compare the average number of transverse cracks per section for each year. It showed significant differences between all three years condition

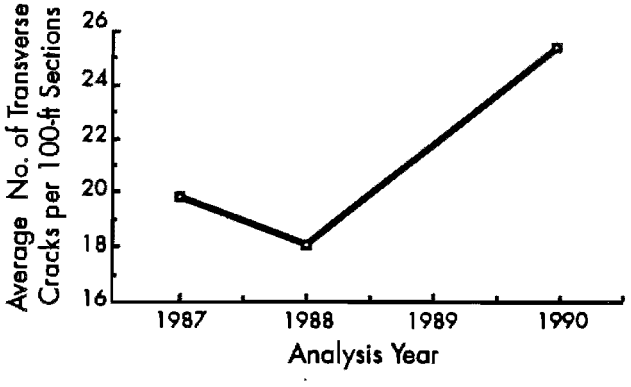

Figure 5.5 Average number of transverse cracks per 100-foot section for delaminated and non-delaminated aeas

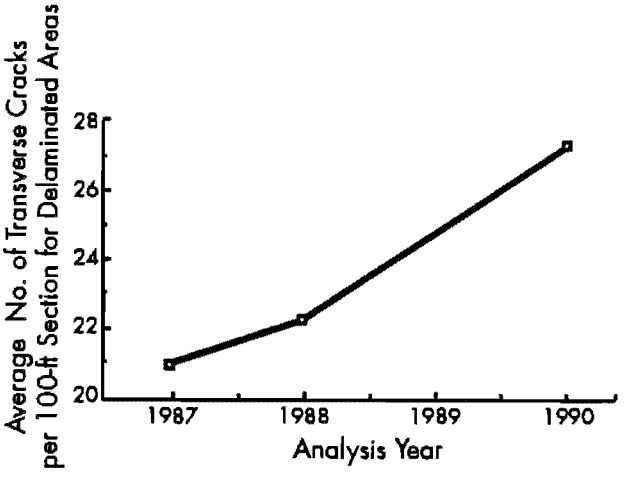

Figure 5.6 Average number of transverse cracks per 100-foot section for delaminated sections

surveys were performed. Figure 5.7 shows a plot of the average number of cracks versus time of survey. It is evident that nothing constructive can be concluded from these data. Further surveys will be needed to evaluate any trend which may exist in the development of transverse cracks. These surveys should be done after a few years to see if the effects of traffic and time are significantly important or if they are important only in delaminated areas.

The model describes 23 percent of the variability. Again it can be concluded that factors not measured in this dataset are responsible for the lack of explanation of the variability.

Conclusions

We can conclude that transverse cracks increase in delaminated areas, but no statistical evidence was found that transverse cracks increase in non-delaminated areas. It is also concluded that further surveys are needed to evaluate the development of transverse cracks in non-delaminated areas and to further evaluate the trend which exists in non-delaminated areas.

5.4.3.4 Analysis of Longitudinal Cracking

Longitudinal cracking data were obtained only during the March 1987 and March 1990 condition surveys. The procedure followed before was used.

Analysis by Year

Table 5.11 shows the factors significant for the analysis of variance for each year. The only main effect significant was the aggregate in 1987. The interactions significant are all connected to the temperature difference, which shows the importance of the early ages of the pavement development on longitudinal cracking.

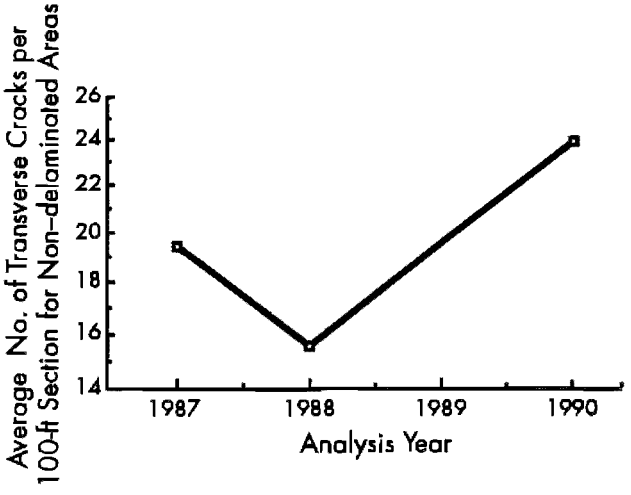

Figure 5.7 Average number of transverse cracks per 100-foot section for non-delaminated areas

Table 5.11 Significant factors from ANOVA of longitudinal cracking by year

March 1987	Aggregate
	Temperature Difference*Direction
	Temperature Difference*Lane
	Temperature Difference*Time
	Temperature Difference*Traffic
March 1990	Direction*Lane
	Temperature Difference*Direction
	Temperature Difference*Lane
	Temperature Difference*Time
	Temperature Difference*Traffic
	Temperature Difference*Direction*Lane

Because it is difficult to establish the time at which the sawcut between the lanes should be made, it is possible for longitudinal cracking to develop before the pavements are sawed. These premature cracks are included in the database, which explains the significance of interactions with temperature difference. Only 16 percent of the variability is explained in the 1987 analysis while 51 percent of the variability is explained in the 1990 analysis.

Full Analysis

No main effects were found to be significant in the analysis of variance and no relationship were found between the significant interactions. This analysis included the direction and lane variables. Forty percent of the variability is explained. The ANOVA results when only main effects are analyzed are shown in Table 5.12. An analysis of variance was also done to evaluate the influence of the year of analysis as well as of delaminated areas versus non-delaminated areas.

There is no significant difference in the length of longitudinal cracks in delaminated versus non-delaminated areas. There is, however, significantly more longitudinal cracking in 1990 versus 1987. An analysis of variance was run with direction and lane variables omitted and the year variable included in the data. Twenty-six percent of the variability is explained in the model, which uses the square root of the cracking with all the other variables linear except traffic, which is modeled using the log of the traffic. The ANOVA table for an analysis of only main effects is shown in Table 5.13. The main effects of traffic, temperature difference, and time are significant. The conceptual model is

Length of Longitudinal Cracks = f(Traffic, Temperature difference, Time)

Table 5.12 ANOVA for longitudinal cracking

Source	DF	Sum of Square	Mean Square	F-Value	PR > F
Model	8	91,846	11,481	16.58	0.0001
Error	1,346	932,260	693		
Corrected Total	1,354	1,024,106			

Source	DF	Sum of Square	F-Value	PR > F	Significant
Direction	1	7,447	10.75	0.0011	Yes
Lane	1	1,652	2.39	0.1227	No
Reinforcing	1	8,823	12.74	0.0004	Yes
Aggregate	1	1,130	1.63	0.2017	No
Grout	1	1,758	2.54	0.1114	No
Traffic	1	262	0.38	0.5385	No
Time	1	2,324	3.36	0.0672	No
Temp Difference	1	31,495	45.47	0.0001	Yes

Table 5.13 ANOVA for longitudinal cracking without direction and lane

Source	DF	Sum of Square	Mean Square	F-Value	PR > F
Model	6	81,974.31	13,662.38	19.55	0.0001
Error	1,348	942,131.28	698.91		
Corrected Total	1,354	1,024,105.58			

Source	DF	Sum of Square	F-Value	PR > F	Significant
Reinforcing	1	15,700.08	22.46	0.0001	Yes
Aggregate	1	2,415.77	3.46	0.0632	No
Grout	1	1,973.06	2.82	0.0932	No
Traffic	1	7,435.11	10.64	0.0011	Yes
Time	1	15,834.18	22.66	0.0001	Yes
Temp Difference	1	48,220.44	68.99	0.0001	Yes

The interactions of traffic and time, time and year, and traffic and year are also significant. It has been noted before that there is much more longitudinal cracking in 1990 than in 1987. In plots of longitudinal cracks versus traffic level and temperature difference no conclusions could be made concerning any trend that may exist.

Figure 5.8 shows a plot of traffic versus average length of longitudinal cracking. The levels discussed before are used. It is evident from this figure that no real trend exists between traffic and longitudinal cracking. Plotting residuals against length of longitudinal cracking shows an increasing linear relationship. Several models were used but the residuals were never random and they gave a linear trend, suggesting that variables other than those measured have an influence on the development of longitudinal cracking.

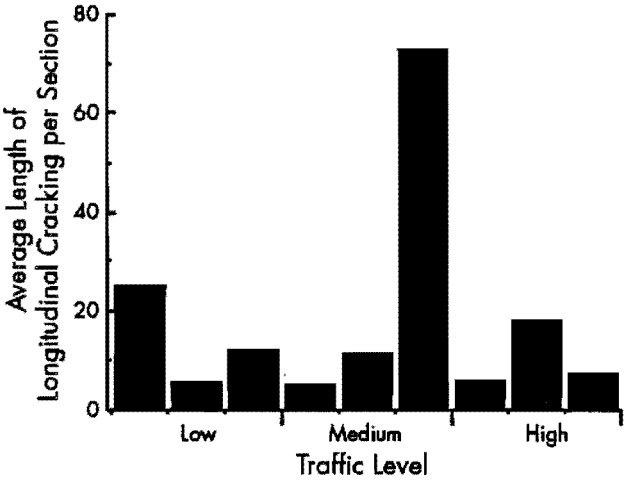

Figure 5.8 Average length of longitudinal cracking versus traffic

Further compounding the problem of modeling longitudinal cracking is the lack of data concerning the sawcuts made at early ages. Some areas may have been sawcut before cracking while others were not. A longitudinal crack that developed is part of this dataset although some areas were sawed and then cracked after sawing and parallel to the crack which are not reflected in the data. It is, therefore, difficult to evaluate longitudinal cracking from the data available.

Conclusions

It can be concluded that, although the length of longitudinal cracking increased from 1987 to 1990, no evidence was found that it is related to traffic or time. Although the traffic and time parameters were found to be significant, no relationship exists. The temperature difference was also found to be significant but no conclusion can be made because data were not available indicating whether the pavement cracked before or after sawcutting.

5.5 CONCLUSIONS

This chapter evaluates the field performance of test sections under surveillance of The University of Texas at Austin. The results from the statistical analysis must be used with the computer analysis results to develop the conceptual evaluation of a design system for bonded concrete overlays.

It can be concluded that delamination of bonded concrete overlays is an early-age problem which occurs the first few weeks after construction. Delamination is not progressive over the period investigated, but the influence on the long-term performance of the pavement is uncertain. It should ultimately need maintenance in delaminated areas before areas which are not delaminated, which will have an economical impact.

It can further be concluded that reinforcing type, thickness, and aggregate are important in transverse crack development in bonded concrete overlays. Another factor from these results, which is important in the analysis of bonded concrete overlays, is that different reinforcing procedures produces different crack spacings. Wire-reinforced sections show smaller crack spacings than fiber-reinforced sections.

We can also conclude that transverse cracks increased in delaminated areas but statistical evidence was not found that transverse cracks increased in non-delaminated areas. It is also concluded that further surveys are needed to evaluate the development of transverse cracks in non-delaminated areas and to further evaluate the trends which exist in these areas.

It can be concluded that, although the length of longitudinal cracking increased from 1987 to 1990, no evidence was found that it is related to traffic or time. Although these parameters were found to be significant no relationship exists. The temperature difference was also found to be significant, but a conclusion can not be made because of the fact that no data were available telling whether the pavement cracked before or after sawcutting. The sections on the South Loop showed that reinforcing significantly influences the formation of longitudinal cracking, which also depends on environmental factors, specifically during construction.

Although traffic did not show any significant effect on longitudinal or transverse cracking development, it should be noted that the BCO analyzed are only up to seven years old. The cracks formed due to volume changes during early ages have not shown a correlation with traffic, but, as the pavement ages, fatigue cracking will become more apparent in the analysis.

The information obtained from the evaluation of the field performance of BCO can be conceptually illustrated using the following equations:

Number of Transverse Cracks = f{Reinforcing, Aggregate, Thickness, Time, Temperature Differential}

Length of Longitudinal Cracks = f{Reinforcing, Temperature Differential}

% Delamination = f{Aggregate, Temperature Differential}

With these conclusions in mind, the conceptual philosophy can be developed, together with a computer analysis of the pavement for a design system for bonded concrete overlays, which is discussed in the next chapter.

CHAPTER 6. ANALYSIS OF WHEEL AND ENVIRONMENTAL STRESSES IN BONDED CONCRETE OVERLAY SYSTEMS

6.1 INTRODUCTION

In the previous chapters a design system was discussed, factors influencing long-term performance of bonded concrete overlays were evaluated, and a sensitivity analysis was completed from which the most important factors affecting the long-term performance were obtained. Furthermore, an analysis tool, namely, a finite element method analysis program, was evaluated and it was concluded that the FEM program can be used for stress calculation of concrete pavements. Data from two test section projects in Houston were also evaluated and all of the data were incorporated in the analysis of bonded concrete overlays.

The purpose of this chapter is to evaluate the stresses in BCO and to model some of the field observations discussed previously. As mentioned earlier, because most BCO are not very old, long-term performance failure criteria are difficult to evaluate and the discussion in this chapter will have to be refined as the performance of BCO is further observed.

It was found in the previous chapter that some variables influence stresses due to wheel loading more than stresses caused by environmental conditions and visa versa. By using the appropriate variables, those which influence long-term performance for each of the wheel loading and environmental conditions, a stress calculation for different conditions can be made, to evaluate pavement response.

A related purpose of this chapter is to analyze the imposed loadings and environmental conditions of an overlaid system, to evaluate the pavement response to these loadings, and to use the results to produce a failure mechanism for the system. The mechanism of failure depends not only on the more sensitive variables but on the system as it exists when first opened to traffic. The early-age-strength development, as well as crack formation due to shrinkage and temperature differentials, creates a certain crack spacing. These cracks can be either reflective cracks or cracks developed only in the overlay. The influence of the possible early-age-developed systems, which can exist as the pavement is opened to traffic, on long-term performance is also discussed. Finally the traffic loading and environmental conditions are combined to evaluate the combined effect of the wheel loading and environmental conditions.

6.2 WHEEL LOADING

Many factors other than the pavement system and material properties are important when wheel loads are considered. The loads, their distribution on the pavement, the stress development, and the existing pavement condition are also important. The existing pavement condition is not only that of the pavement which is overlaid but also that of the bonded overlay section at the time the traffic is opened to traffic. These factors are discussed in the following paragraphs

6.2.1 Wheel Loads

The distribution of wheel loads on pavements is extremely complex. The AASHTO Design Guide (Ref 1) standardized on an 18-kip equivalent single axle load to compute fatigue performance and reliability for concrete pavements, and all loads are changed to 18-kip equivalent single axle loads using equivalency factors. The equivalencies are calculated on either a stress or a deflection basis. The AASHTO Design Guide shows equivalency factors for various structural numbers, present serviceability indexes, and loads which vary from 2 to 50-kip axle loads. In practice, the wheel loads change considerably in magnitude and distribution.

6.2.1.1 Magnitude

The magnitude of the wheel loads on a certain highway is difficult to evaluate since the vehicles vary from different size cars to unloaded trucks to heavily loaded trucks, which can be loaded to maximum capacity or to only half or three-quarters of their capacity. Truck-tractors, semi-trailers, and trailer combinations are the vehicles which normally cause the most damage to pavement systems. These vehicles are limited to certain legal loads by law. Overloading is allowed only with specifically issued permits. However, the revenues obtained from these

overload permits do not pay for the damage caused to the pavement by the loads (Ref 59). Furthermore, the fines paid by trucks for overloading do not cover the damage done by the trucks. These factors, apart from whether they involve legal problems, do influence the performance of the pavement. Overloading can cause an exponential growth in distress development, which is not designed for in normal design procedures.

For design purposes, the AASHTO 18-kip ESAL is used. The legal loads can be converted to 18-kip equivalencies. The legal loads in Texas are a maximum of 20,000 pounds on any single axle and 34,000 pounds on any tandem axle, and the overall gross weight should not exceed 80,000 pounds. Consecutive tandem axles can carry 34,000-pounds loads if they are more than 36 feet apart (Ref 60). Figure 6.1 shows a layout of three truck types, their type number, and the specific allowable load distribution (Ref 61).

The legal magnitude of an actual axle load can, therefore, be anywhere between the axle load of a car, which is approximately 1500 pounds, and a 34,000 pound tandem load.

6.2.1.2 Typical Distribution of Wheel Loads on Highways

The load distribution on highways depends on several different independent distributions. There are a load distribution variation between different trucks of the same truck or vehicle type, a distribution of trucks or cars between different lanes on highways , a distribution between different types of vehicles on highways, and a seasonal and daily distribution of trucks and cars.

Load Variation Within Vehicle Type

The loads shown in Figure 6.1 are the legal loads but not necessarily the operating loads. For example, in East Texas, US Highway 59 is used by the forest industry. Trucks are used to transport logs to

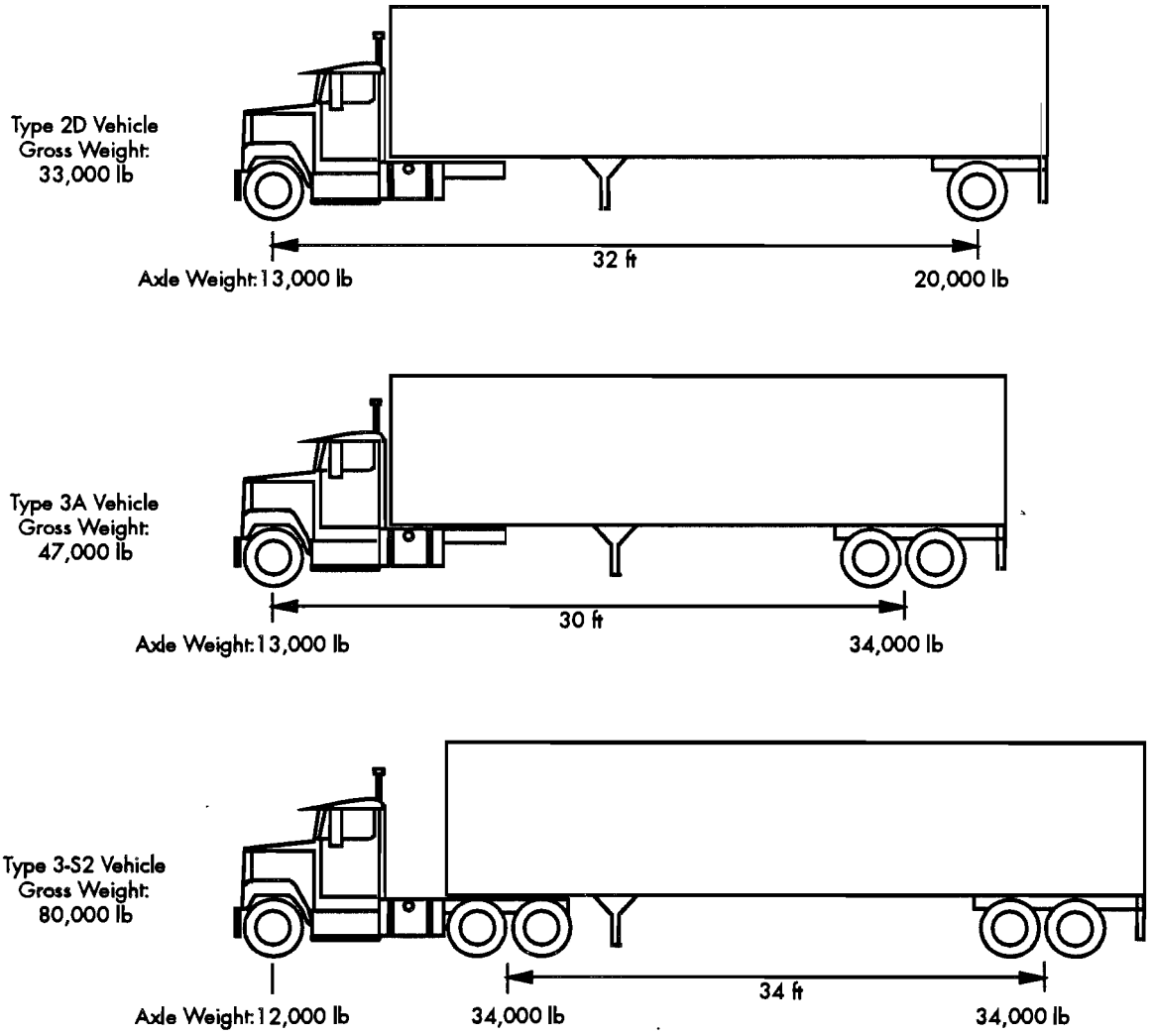

Figure 6.1 Configurations for type 2D, 3A, and 3-S2 trucks

the Port of Houston. When they go to Houston they are loaded, and when they return they are normally empty. The southbound side of the highway is, therefore, exposed to much higher loads than the northbound side. However, to design a road for specific industries and/or industry growth is difficult due to the amount of uncertainty fixed to the economy and growth potential of certain areas.

This illustrates the problems concerned with estimating the magnitude of loads which use a certain facility. It is also difficult to project future traffic growth due to fluctuations in economic stability and development pattern due to technological advancement.

Figure 6.2 illustrates the variance in average daily axle applications for the steering and tandem axle loads for Type 3-S2 trucks on a four-lane highway. The values shown for a four-lane highway will change for a two or eight-lane highway. The distribution may also change, depending on the area in which the highway is situated. The figure does show the variability which exists between truck loads on highways. This variability also exists between other vehicles, such as passenger cars, although the load is much lower.

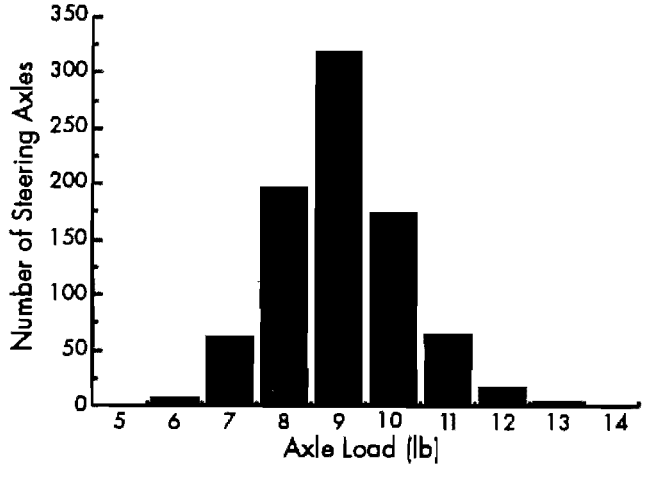

(a) Steering axle

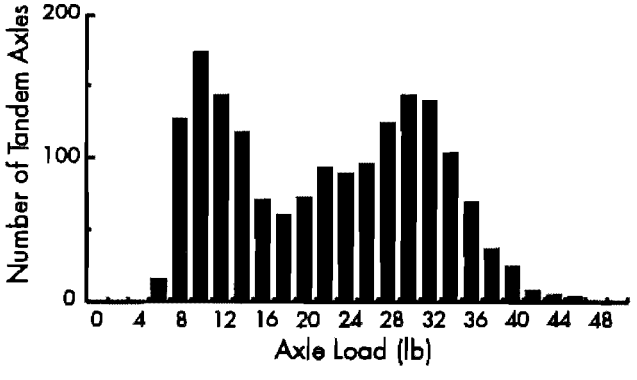

(b) Tandem axle

Figure 6.2 Average daily applications by Type 3-S2 trucks on the right lane of a four-lane highway (Ref 62)

Vehicle Distribution on Highways

The distribution of trucks and cars on the different lanes is important for pavement design as well as verification of a design model. Trucks causes the highest damage to the pavement, which makes them the most important load factor.

Therefore, it is necessary to know the distribution of trucks, as well as of heavy versus light trucks. Heavy trucks are defined as trucks with more than three axles while light trucks are those with three axles or less. The distributions for the 1983 data are shown for a three-lane highway, North Freeway in Houston, and for a four-lane highway, East Loop 610 in Houston, in Table 6.1.

In Table 6.1, Lane 1 is always the inside lane. It is apparent from this table that the middle lanes carry not only the highest percentage of vehicles but also the highest percentage of trucks. These values are important because they influence the amount of loading on a lane, and there is a big difference between an outside lane and an inside lane. An outside lane may react like an edge loading condition, which gives higher stresses than the interior loading condition of the inside lanes.This is discussed in a later section.

Vehicle Type Distribution on Highways

The types of vehicles on highway systems are also important. Normal traffic counts give vehicle numbers, with no distinction between different types of vehicles. Different trucks have different numbers of axles. It is, therefore, necessary to know how many trucks with how many axles use the highway. The distribution of trucks is especially important because they cause the most distress in a pavement system. On two major highways in Texas, IH-35 at Austin and US-59 north of Houston, the number of each type of trucks was counted and converted into percentages, which are shown in Table 6.2.

From the table, it is apparent that the most widely used trucks are the 3-S2 semi-trailers. The second most used truck is the two-axle truck, which carries a lighter load than semi-trailers but causes more damage than passenger cars.

Seasonal and Daily Vehicle Distribution on Highways

Another important distribution is the seasonal and daily traffic distribution. This is important because of the combined influence of environmental conditions and wheel loading on the pavement.

Table 6.1 Vehicle distribution between lanes on a three- and a four-lane highway in Houston (Ref 63)

North Freeway, Houston					
	% Vehicles of Total Counted in 24 hours				
Vehicle Type	Lane 1	Lane 2	Lane 3	Lane 4	All Lanes
Passenger	33.7	36.3	23.4		93.4
Light Trucks	0.2	0.4	0.5		1.0
Heavy Trucks	1.4	3.1	1.2		5.7
Total per Lane	35.2	39.7	25.1		100.0

East Loop IH610, Houston					
	% Vehicles of Total Counted in 24 hours				
Vehicle Type	Lane 1	Lane 2	Lane 3	Lane 4	All Lanes
Passenger	20.4	27.5	24.1	14.4	86.5
Light Trucks	0.7	1.6	2.2	1.4	5.9
Heavy Trucks	1.3	2.2	3.0	1.2	7.7
Total per Lane	22.5	31.3	29.2	17.0	100.0

Table 6.2 Proportion of different trucks combined for two locations in Texas: IH-35 at Austin and US 59 north of Houston (Ref 62)

Truck Type	Proportion on Road (%)
3-S2	71
3-Axle	4
2-S1	4
2-Axle	20

In order to evaluate the combined stresses due to the environment and the wheel loading, a traffic distribution for the season and day can be obtained. Seasonal variations can be due to holidays and to industries which are seasonally dependent, such as agriculture. This is difficult to establish but can have a big influence on the pavement performance. The daily distribution and daily environmental conditions cause an induced stress in the pavement. The environmental stress within a pavement can be calculated from temperature differentials and moisture movement within the concrete and combined with the acting wheel loads on the pavement. Figure 6.3 shows a typical vehicle distribution during the day for IH-45 south in Houston.

It is apparent from the figure that the peak morning hour for non-truck vehicles does not coincide with the peak for truck vehicles. Truck traffic picks up just after rush hour in the morning and stays constant until about six o'clock at night, when it starts to decrease. This is typical for that area but may be totally different for another area.

6.2.2 Loading Distribution on Pavement

The load distribution on the pavement structure itself also varies. The structure can either be in an interior or edge loading condition. If we evaluate an interior condition, the load distribution is not as critical as it is for an edge distribution.

6.2.2.1 Edge Condition

The edge condition is very important because the stresses at the edge condition are higher than the stresses in the interior of the pavement, due to the boundary conditions. The loading distribution at the edge depends on the roadway geometry and large trucks or passenger cars. Large trucks tend to cause passenger car drivers to drive closer to the edge. Furthermore, curves in the road tend to cause passenger

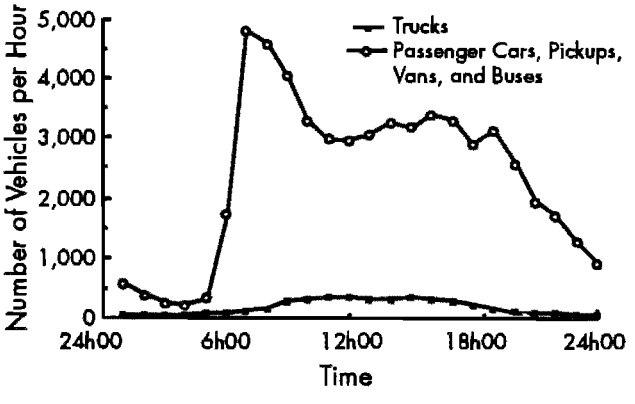

Figure 6.3 Daily traffic distribution of trucks and non-trucks on north bound IH-45 south in Houston (Ref 63)

cars to get closer to the edge around the inside corner. Lee et al (Ref 62) found that truck lane distribution patterns did not vary between Austin and Houston under similar conditions. It was also found that smaller vehicles drive closer to the pavement edge than larger vehicles. Figure 6.4 shows a typical frequency distribution of lateral placement tractor-semi-trailer trucks on tangent sections.

The distribution is important because the farther inward from the edge the wheel load is, the smaller the controlling stress. If the Westergaard edge condition equation is used for 100 percent of exterior lane axles the total damage will be over-estimated, due to the higher stress. The Westergaard edge condition equation is based on the full tire load on a half circle area at the edge of the pavement (Ref 33).

6.2.2.2. Interior Condition

The same distribution can be used for an interior condition as well as for an edge condition for truck loading. The interior condition stress is lower than the edge condition unless the load transfer efficiency is very low. The reinforcing, dowel, or tie bars providing the load transfer can be broken due to fatigue or rusting, which will change the interior condition to an edge condition. This is discussed later. The factors discussed in this section were used to calculate the number of ESAL used in the statistical analysis of field data discussed in the previous chapter.

6.2.3 Analysis Procedure for Stresses Developed by Wheel Loads Using FEM

Wheel load stresses in overlaid systems are calculated using the finite element method discussed previously (Section 4.2.5). Using this method involves certain assumptions, a certain analysis method, and certain limitations.

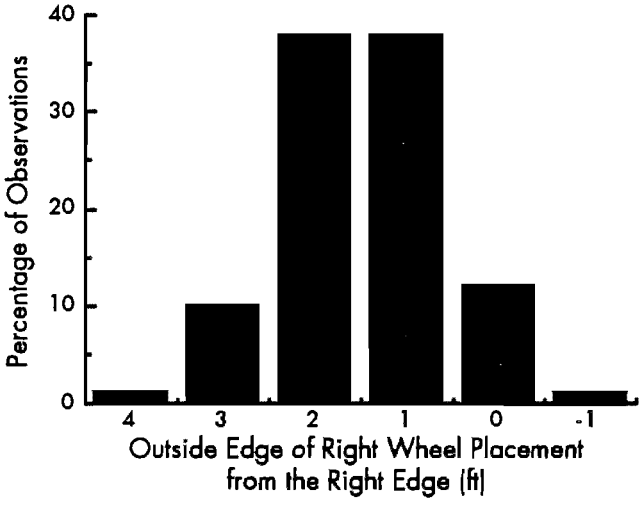

Figure 6.4 Frequency distribution of lateral placement of tractor-semi-trailer trucks on straight section (Ref 62)

6.2.3.1 Assumptions

Certain assumptions must be made to be able to use the program. First, as discussed before, the program was developed to evaluate plane strain problems. The actual wheel load stresses in a concrete pavement system are an axi-symmetric problem. Therefore, the assumption is made that, by increasing the section analysis width or reducing the load used in the analysis, a stress similar to that obtained by Westergaard's equation is obtained. Inherent in this is the assumption that the Westergaard equations are true, compared to elastic layered theory.

It is also assumed that the subbase and lower layers do not significantly influence the stress values within the pavement very much, which also comes from the assumptions inherent in the Westergaard equations.

A further assumption is that the pavement will actually respond to cracking as the pavement observed in the two-dimensional program did, while the actual system is three-dimensional. It is, therefore, assumed that, although boundary conditions change due to cracking within the pavement system, the stresses obtained from such an analysis are still true.

6.2.3.2 Analysis Method

The analysis method followed uses a section width, which provides equivalent Westergaard stresses, and computes stresses for different loads and system variables. The finite element method program is used to evaluate an analysis factorial, which is used to establish stress equations that include the variables influencing the long-term performance of the overlaid system, as evaluated in previous chapters. Furthermore, the effect of the existing system at the time the overlaid system is opened to traffic, as well as the remaining life of the existing pavement, is analyzed.

6.2.3.3 Limitations

From the above paragraphs, it can be concluded that this analysis method does have certain limitations and uncertainties. The biggest limitation is that the program is a plane strain program used to calculate axi-symmetric stresses. Combining the wheel load stresses and environmental stresses will be done only with difficulty and some uncertainty.

The extreme amount of computer time necessary to complete a full factorial necessitates the use of fractional factorials as well as the use of only the most sensitive variables influencing long-term performance of the overlaid system.

Another limitation is that the crack development within the pavement system is analyzed as a wide strip acting the same throughout the width. Cracking may occur in a meandering way and the percentage

delamination may be higher at the edge of the pavement than at the interior. These facts cannot be modeled using the finite element program.

However, although these limitations exist and several assumptions had to be made in order to analyze the pavement in a cost-effective manner, the stress development obtained from the analysis can be used to evaluate long-term performance by applying it to the system using good engineering judgement and field observations.

6.2.4 Calculation of Wheel Load Stresses

In a Chapter 4 it was concluded that the crack spacing, existing pavement modulus, existing pavement thickness, and overlay thickness influence the stress development in BCO. From the statistical analysis of field data, it was found that cracking can either be reflective or non-reflective. Before developing an analysis factorial from which stress equations for wheel load stresses can be developed for BCO, the effect of reflective and non-reflective must be discussed.

6.2.4.1 Analysis Factorial

In addition to the sensitive variables in the overlay stress development, the cracking pattern inherited from the construction period and early-age cracking are also important. These cracks can be either reflective or non-reflective cracks.

Reflective Cracking

Figure 6.5 shows reflective cracks and the related stress distribution for a 3 and a 5-foot crack spacing. Figure 6.5 (a) shows a load centered between the cracks while Figure 6.6 (a) shows the loading on the cracks. This is typical of the silicious river gravel overlays discussed in the previous chapter.

The stress distribution underneath each of these loads was calculated using an 8-inch existing pavement on a 6-inch cement-treated base with a 4-inch overlay. The stress at the crack can be evaluated and its importance is discussed later. The stress distribution between a 3 and a 5-foot crack spacing can be evaluated from these graphs and the effect of non-reflective cracking can be compared to these graphs to establish an analysis factorial for evaluating wheel load stresses.

Figure 6.6 also shows the stress distribution for the 3 and 5-foot crack spacings with the load at the crack.

A slight increase in stress is found for the higher crack spacing versus the smaller crack spacing, which was concluded earlier. The stress at the crack is also higher for the larger crack spacing. These stresses are compressive stresses, which will eventually reduce the load transfer ability at the crack due to compression fatigue. Only the top 4 inches are in compression. The compression force is kept in equilibrium by the friction between layers and, slightly, by the reinforcing in the existing pavement. Lower in the slab, due to the crack, the tensile stress should be zero. Small stresses shown in the graphs are due to the stress calculation procedure in the FEM program.

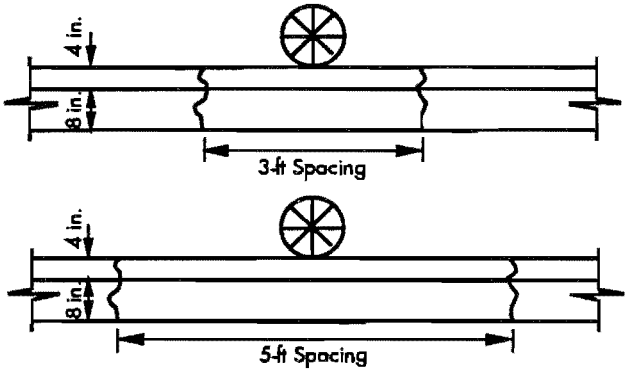

(a) Wheel load position between cracks for typical crack spacings in BCO

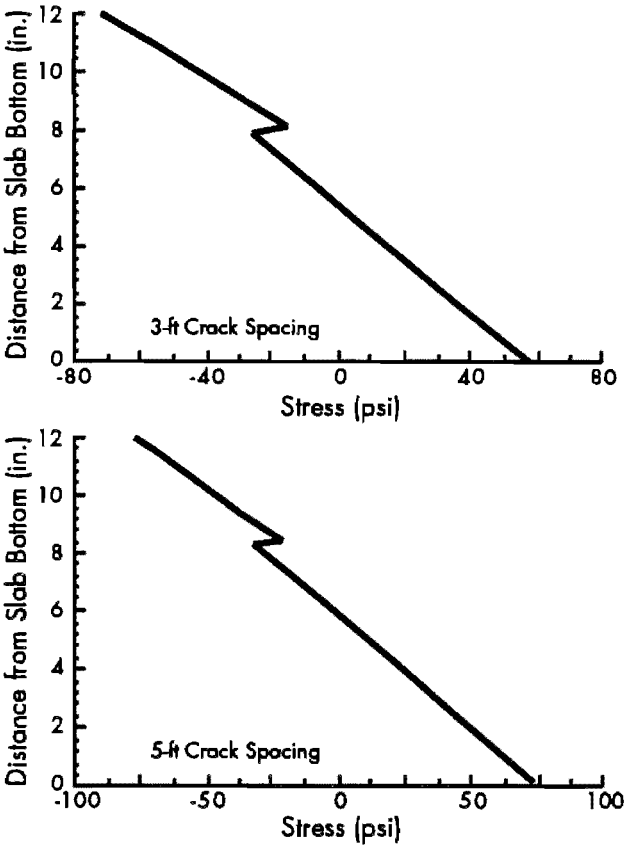

(b) Stress distribution directly underneath load, load in center between cracks

Figure 6.5 Wheel load position and stress distribution for typical crack spacings in BCO with load between cracks

Non-Reflective Cracking

Figure 6.7 shows a typical layout of non-reflective cracks. For the purpose of this analysis a 5-foot crack spacing is assumed. Two scenarios exist. As shown in Figure 6.7, the existing pavement can be cracked with no cracking in the overlay or the overlay can be cracked with no cracking in the existing pavement.

The stress distribution for the analysis of the two cases is shown in Figure 6.8. Figure 6.8(a) coincides with Figure 6.7(a) and Figure 6.8(b) coincides with Figure 6.7 (b).

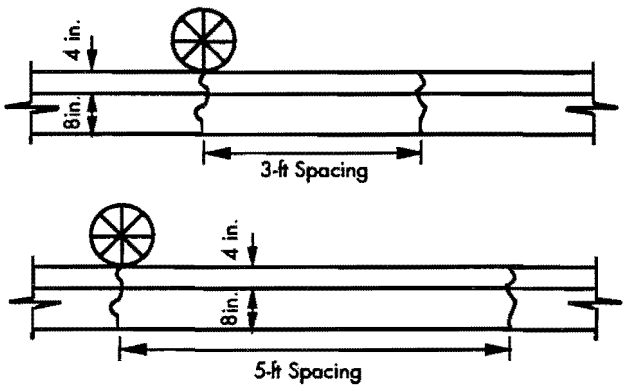

(a) Wheel load position above crack for typical crack spacings in BCO

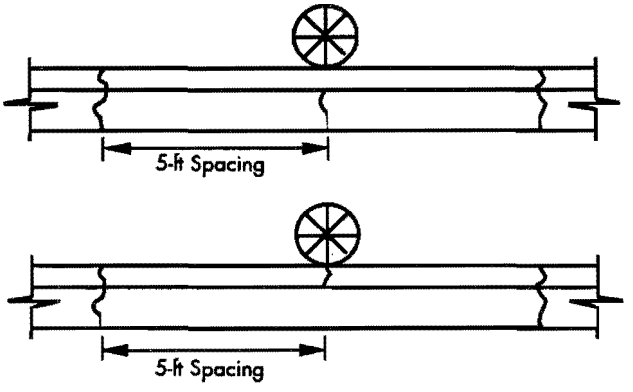

Figure 6.7 Scenarios for reflective cracking

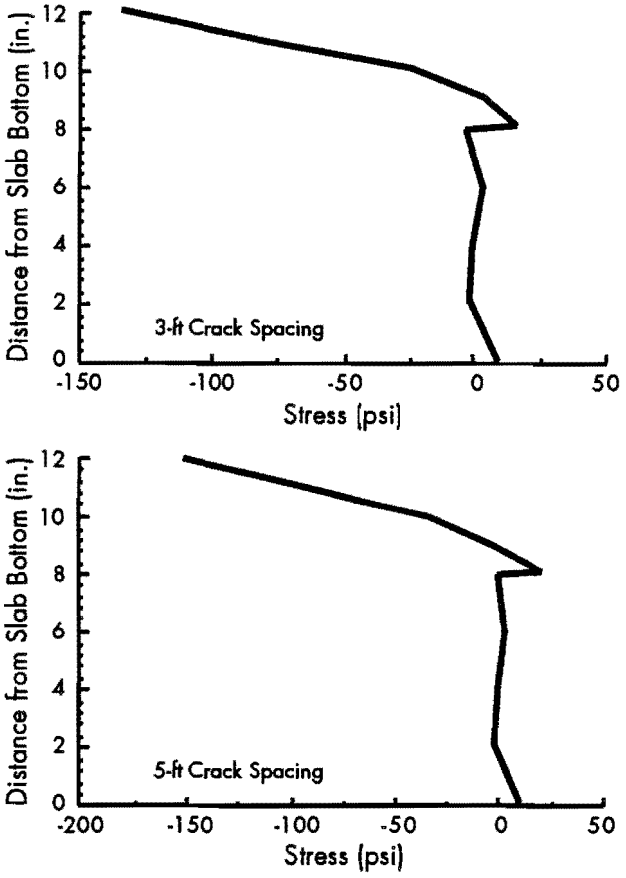

(b) Stress distribution directly underneath load, load at crack

Figure 6.6 Wheel load postion and stress distribution for typical crack spacings in BCO with load at cracks

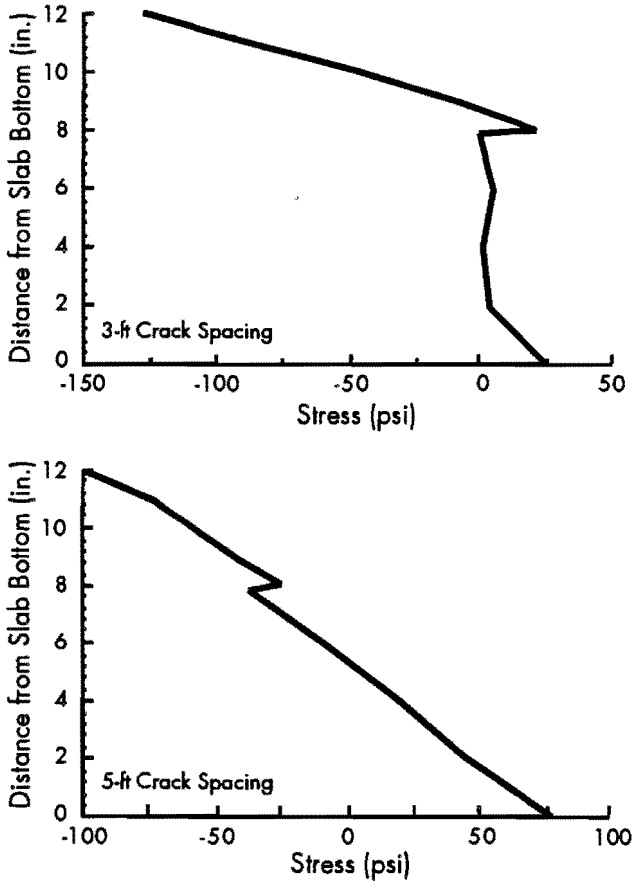

Figure 6.8 Non-reflective cracking scenarios
(a) Above. Overlay uncracked, existing pavement cracked
(b) Below. Overlay cracked, existing pavement uncracked

If these two figures are compared to the figure for 5-foot crack spacing stress distributions (Figure 6.5 and Figure 6.6), it can be seen that only a minor difference exists and approximately the same stress distribution exists. When a crack in the overlay is not a reflective crack, a wheel load will put most of the crack in compression and all of the tension in the existing pavement, which explains why similar stresses are obtained. From this, it can be concluded that the maximum tensile stress is not influenced by cracking in the overlay and the evaluation can be made at the center between cracks.

Analysis Factorial

From Table 4.9 it was seen that at a crack spacing of 5 feet the stress is about the same as for higher crack spacings. An analysis using a crack spacing of 10 feet showed no significant increase in stress above that of a 6-foot crack spacing, and it is concluded that at 6 feet the stress is the same when the crack spacing is increased. Only crack spacings of 5 feet and below are, therefore, considered. Table 6.3 shows a layout of the factorial. The factorial is analyzed at three load levels. Legal truck loads were discussed before and from Figure 6.2 it can be concluded that two peaks exist, at tandem axle loads of 12,000 pounds and 32,000 pounds. These two levels are changed to a single axle load. The three load levels selected are 9,000 pounds, 12,000 pounds, and 18,000 pounds, so that a wide inference base is covered.

A k-value was also included in the analysis and it was calculated using the method described previously. An equation was developed from the stress analysis for the maximum tensile stress at the bottom of the pavement.

Table 6.3 Analysis factorial for wheel loading

Crack Spacing / Elastic Modulus: Exist Pvt / Overlay Thickness / Exist Pvt Thickness		Load Case 1					
		CS1			CS2		
		E1	E2	E3	E1	E2	E3
De1	Do1		X			X	
	Do2		X			X	
	Do3		X			X	
De2	Do1	X	X	X	X	X	X
	Do2	X	X	X	X	X	X
	Do3	X	X	X	X	X	X
De3	Do1		X			X	
	Do2		X			X	
	Do3		X			X	

6.2.4.2 Discussion of Results

Equation 6.1 was developed from the stress factorial analysis. It is very similar to the Westergaard equation. If it is compared to the Westergaard equation, stress values will compare favorably, although some variation will exist. The variation is attributed to the fact that the FEM program uses a plane strain evaluation, which is converted to an axi-symmetric problem. The residuals plotted favorably.

$$\sigma = 0.288*\{P/(D_o+D_e)^2\}*\{\ln(CS)\}*\{\ln[((E*(D_o+D_e)^2)/12*k)^{0.25}]\} \quad (6.1)$$

where

- σ = maximum tensile stress at bottom of slab, in psi,
- P = wheel load, in pounds,
- D_o = overlay thickness, in inches,
- D_e = existing pavement thickness, in inches,
- CS = crack spacing in existing pavement, in feet,
- E = modulus of elasticity of existing pavement, in psi,
- k = modulus of subgrade reaction, in pci.

As the crack spacing is reduced, the tensile stress perpendicular to the cracks is reduced. At 6 feet the stress is still the same as the Westergaard stress, but below a crack spacing of 6 feet the stress is reduced. The spacing of longitudinal joints (cracks) formed by sawcuts on highways is 12 feet. This means that the stress in the transverse direction will be higher than in the longitudinal direction. The fatigue in the transverse direction will, because of the higher stress, increase faster than in the longitudinal direction. The failure mechanism for overlays will, therefore, be the same as for normal concrete pavements, and a punchout will eventually form. However, as discussed in Chapter 3, the fatigue factor at the interface is unknown. As the working crack loses its ability to provide load transfer, an uncracked overlay may become cracked or delaminated and small overlay punch-outs may be formed. This is discussed later in this chapter. We can, therefore, conclude that Equation 6.1 is an equation which can be used to evaluate stresses at small crack spacings; this conforms to current conceptual theory, but it quantifies the theory since previous work by Won (Ref 64) ignored aggregate interlock and load transfer to compute the equation developed in that work.

6.2.5 Effect of Delaminated Areas on Stress Calculations

In the previous chapter it was concluded that a significant increase in transverse cracking occurs in delaminated areas. The effects on a delaminated area are modeled by using the FEM program. Figure 6.9 shows a typical delaminated area with a wheel load passing over it.

A typical section from the test sections in Houston was analyzed. A 10 degree Fahrenheit differential was used on the overlay and a 9,000-lb ESAL was placed on the crack. Figure 6.10 show the stress at the top of the overlay, from the crack and up to 18 inches away from the crack. The pavement was modeled as delaminated for 18 inches on each side of the crack. When the temperature at the top of the overlay is lower than that at the bottom of the overlay, it will cause upward curling. When it curls, a cantilever is created, with the edge of the cantilever at the crack, as shown in Figure 6.9.

It is evident from Figure 6.10 that a very high tensile stress exists at the top of the overlay due to the cantilever action, because the temperature differential is causing a small separation between the existing pavement and the overlay. As the wheel load passes over it, a high tensile stress is developed at the top. The stress shown in Figure 6.10 is about one-third of the tensile flexural strength of the concrete. When this stress level is used in a pavement fatigue equation, the pavement will crack long before a crack is formed in the center of the 5-foot crack spacing section analyzed before. This explains the increase in transverse cracking in delaminated areas on the North Loop test sections in Houston discussed before.

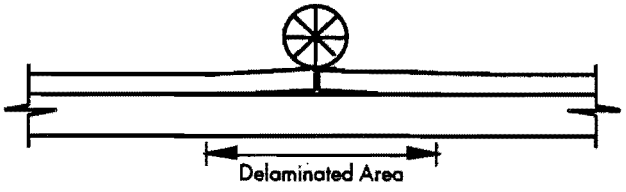

Figure 6.9 Delaminated area with wheel load passing over

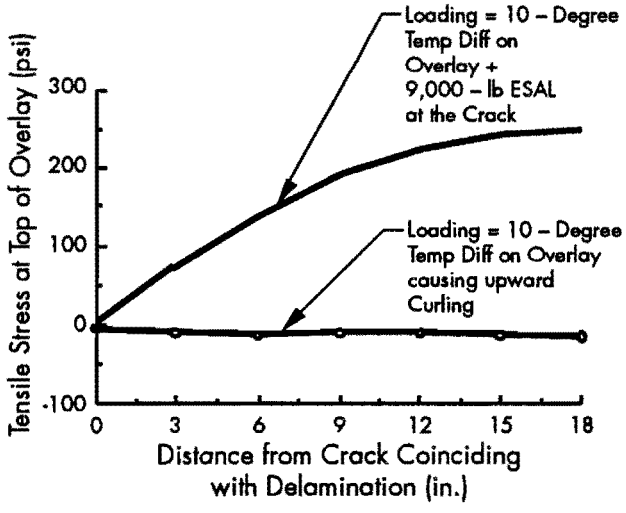

Figure 6.10 Tensile stress at top of overlay due to wheel loading

6.2.6 Effect of Existing Pavement Condition on BCO Wheel Load Stresses

The work discussed in the two previous sections shows that the same stress performance exists in the overlaid pavement as in normal PCC pavements. It also shows the increase in development of cracks in delaminated areas as found in the evaluation of the field performance in Chapter 5. The final step in analyzing wheel loads is considering the effect of an extremely poor existing pavement or, in other words, the effect of a pavement with a very short remaining life. On test sections in Houston, it was concluded that the working cracks are extremely tight and that the load transfer in most of the pavements was still extremely high. The effect of the remaining life is evaluated at cracks, because the stress depends only on the existing pavement between cracks, as discussed before.

6.2.6.1 Evaluation of Remaining Life of Existing Pavement on BCO Stresses

The FEM program is used to evaluate the stress distribution in an overlay when the crack is badly eroded, by modeling the pavement with a low modulus of elasticity and evaluating the stress directly above the crack. The stresses obtained from this analysis are shown in Table 6.4. It can also be assumed that, for cracks which are opened wide and have a low load transfer efficiency, the modulus at the crack will be lower than the modulus between cracks. Bagate et al (Ref 65) proposed a method for obtaining modulus values at cracks from Falling Weight Deflectometer measurements. These values can be used to evaluate the modulus at cracks or as input into Equation 6.2, which was developed from the results in Table 6.3. Three levels of modulus values were used for the existing pavement. The system shown in Figure 6.7(a) is analyzed. The results are discussed in the following section.

6.2.6.2 Discussion of Results

The tensile stress for a thinner overlay at a low modulus of elasticity is lower than that for the thicker overlays. The reason is that the stiffness (modulus multiplied by the moment of inertia) of the 2-inch overlay is much less than that of the 8-inch

Table 6.4 Analysis of stress in overlay above an existing pavement crack for various modulus of elasticity values for the existing pavement and overlay

Exist Pvt Thick	Overlay Pvt Thick	E Overlay	4,500			6,000		
		E Existing	500	2,000	4,500	500	2,000	4,500
		Stress						
8	2	Comp	-257	-223	-174	-298	-256	-200
		Tens	55	17	-6	93	41	11
		Shear	40	44	-34	45	56	43
	4	Comp	-206	-181	-1	-2	-209	-163
		Tens	116	82	48	150	110	69
		Shear	18	22	17	21	22	19
	6	Comp	-159	-138	-108	-180	-157	-122
		Tens	109	84	55	132	105	73
		Shear	11	13	12	13	13	12
10	2	Comp						
		Tens						
		Shear						
	4	Comp	-188	-153	-110	-2	-177	-127
		Tens	102	59	28	133	84	44
		Shear	16	17	136	19	19	15
	6	Comp						
		Tens						
		Shear						
12	2	Comp						
		Tens						
		Shear						
	4	Comp	-173	-121	-80	-201	-140	-93
		Tens	90	40	13	119	58	24
		Shear	15	12	9	17	14	10
	6	Comp						
		Tens						
		Shear						

existing pavement with a 500 ksi modulus. In effect, the pavement changes from a layered system to a plate theory system. This is shown in Figure 6.11, which is a plot for a modulus of 500 ksi for the existing pavement and 4500 and 6000 ksi for the overlays. As soon as the ratio of overlay stiffness and existing pavement stiffness reaches approximate unity, the system reacts as a plate system. Before unity, it acts as a layered system. An evaluation of different thicknesses was made using the layered theory program ELSYM5 and the same trend was followed: the 2-inch pavement showed the smallest stress values, the 4-inch showed the highest, and the 6-inch stress values were a little lower than the 4-inch.

It must be noted that this is not a reason for using very thin bonded overlays on heavily cracked pavements, because there are problems not related to tensile or flexural stress. From Figure 6.12, it can be seen than the shear stress in the 2-inch BCO is

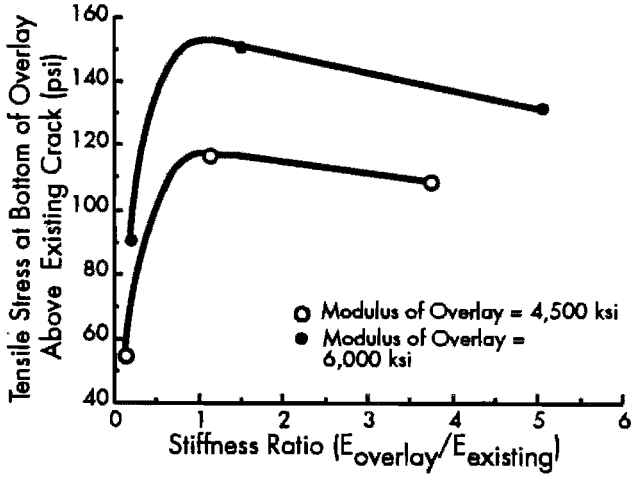

Figure 6.11 Stress at bottom of overlay above a crack versus the stiffness ratio of overlay versus existing pavement

much higher than that in the other two thicknesses analyzed. This means that the 2-inch pavement will have a higher probability of shear fatigue failure than the thicker overlays. Furthermore, the deflections will also be higher, which may not be functionally acceptable.

The stress equation developed from the data in Table 6.4 is

$$\sigma_{over} = 209.773 + (9000/P)\{-0.017931E_e - (424232/E_o) + 205.74(D_o/D_e - (D_o/D_e)^2) - 22.942(D_e/D_o)\} \quad (6.2)$$

where

σ_{over} = stress at the bottom of the overlay above the crack in an existing pavement, in psi,
P = wheel Load, in lb,
E_e = existing pavement modulus of elasticity, in ksi,
E_o = overlay modulus of elasticity, in ksi,
D_e = existing pavement thickness, in inches, and
D_o = overlay thickness, in inches.

By using this equation and the previous equivalent stress equation, stresses can be calculated for examining the stress level at which the pavement will operate. It was mentioned before that reflective cracking cannot be assumed as the norm. Therefore, as discussed before, at the time the pavement is opened to traffic, a cracking pattern already exists. If the pavement has a low remaining life, which can cause high tension stress in thicker pavements and shear stress in thin pavements, cracks in the existing pavement will reflect through and a system such as that shown in Figure 6.13 may occur. Such cracking will cause large areas to have very short crack spacings and can lead to punch-outs in the system if it coincides with longitudinal cracking that may exist or develop. Therefore, if the remaining life, measured as modulus of elasticity, produces stress values in the BCO above the crack higher than those at the bottom of the slab, then an overlay will deteriorate faster than the existing pavement. Block cracking will form, which can lead to punch-outs. Therefore, the fatigue stress above the crack, when the number of ESAL is calculated for the stress above the crack, should be the same as that for the between-crack fatigue life. This will ensure good performance and minimize premature failures.

The stress development at the interface depends on the amount of movement available when a wheel load passes over the crack. The total compressive force at the reflected crack, which in most cases will all be in the overlay section, compressed the concrete between the cracks, as shown in Figure 6.14.

This force is restrained only by the shear and tension at the interface. If we use a rough calculation of the compressive force for an 8-inch existing pavement with a modulus of 4500 ksi, an overlay modulus of 6000 ksi, and a crack spacing in the overlay of 6 inches, a shear stress of approximately 40 psi is obtained. This is at least four times more than what is normally expected. Although, as discussed before, fatigue testing of the bond interface is non-existent,

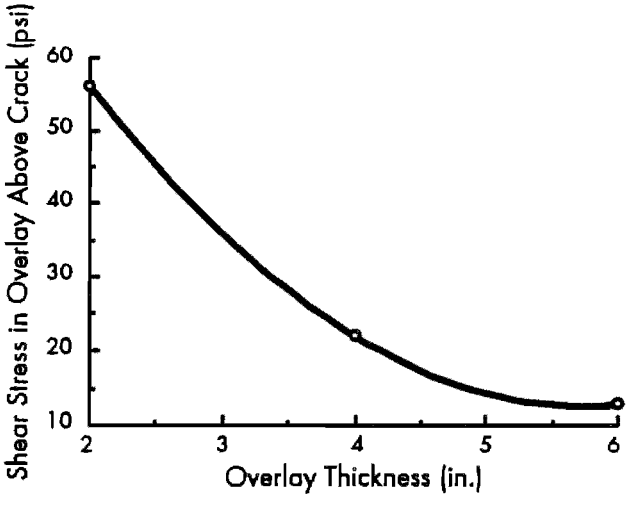

Figure 6.12 Shear stress versus thickness in overlay above a crack

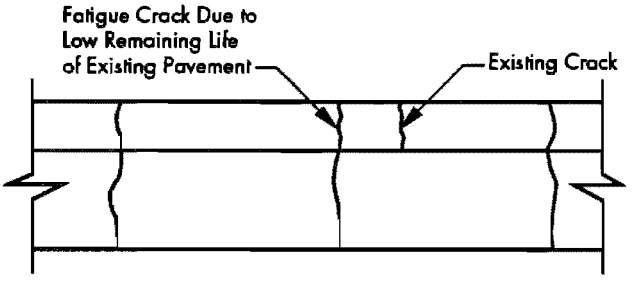

Figure 6.13 Reflective cracking due to fatigue

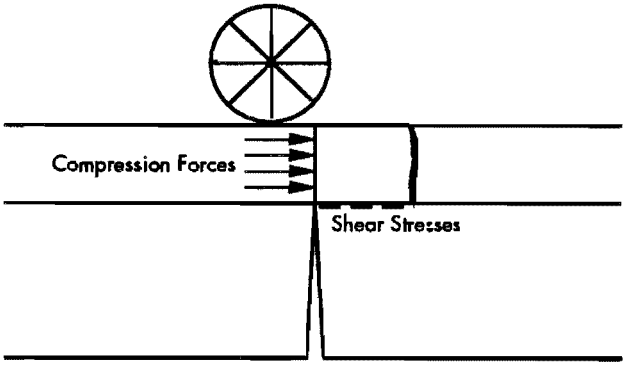

Figure 6.14 Effect of reflective cracking near existing cracks

such an increase will decrease the fatigue life and eventually cause punch-outs.

6.3 ENVIRONMENTAL STRESSES IN BCO

The influence of environmental conditions on the performance of concrete pavements is well known. Concrete pavements are reinforced to control cracking caused by changing environmental conditions, such as temperature, shrinkage, and moisture movements. The influence of some of these environmental conditions is discussed in the following sections.

6.3.1 Temperature Distribution in Concrete Pavements

To be able to calculate temperature stresses within a concrete pavement system, the temperature distribution within the concrete is needed. The concrete temperature depends on the daily air temperature, which varies with the seasonal temperature distribution.

6.3.1.1 Daily Temperature Distribution.

The daily temperature distribution was assumed to be a sinusoidal function (Ref 66), with the daily high and low as the maximum and minimum values on the curve and the period being twice the time difference between the times at which the high and low temperatures occur. The same function can be used for seasonal temperatures, using the highest and lowest average seasonal temperature, as well as the time between the occurrences of these temperatures. The temperature can be given as

$$T(t) = T_{avg} + ((T_{max}-T_{min})/2)*Sin((2*pi*t/t_o) \quad (6.3)$$

where

- $T(t)$ = temperature at time t, in degrees Fahrenheit,
- T_{avg} = average between high and low temperature,
- T_{max} = maximum day temperature,
- T_{min} = minimum day temperature,
- t = time in hours, and
- t_o = period which is twice the difference between times of occurrences of maximum and minimum temperatures.

The concrete pavement temperature depends on the air temperature but is out of phase with it. The air temperature influences the surface temperature of the concrete, from which heat is lost to the pavement system or to the environment, depending on the temperatures of the various systems.

6.3.1.2 Temperature Distribution in Concrete Pavement

Temperature within a concrete slab follows the atmospheric temperature but is out of phase with it by a certain amount. The distribution through the concrete slab can be assumed to be exponential (Ref 66). Therefore, the equation describing the temperature within the concrete is assumed to be

$$T(z,t) = T_o*e^{-kz}*Sin((2*pi*t)/t_o)-kz) + T_{avg.surface} \quad (6.4)$$

where

- $T(z,t)$ = temperature at a point inside the concrete, in degrees Fahrenheit,
- z = positive downward measurement from the concrete surface, in feet,
- T_o = amplitude of the surface temperature function,
- k = square root of (pi/t_o*h^2),
- h = thermal diffusitivity (ft^2/hr), and
- $T_{avg.surface}$ = average of the maximum and minimum surface temperatures.

The amplitude of the surface temperature function was obtained by using the maximum and minimum surface temperatures for each day. The surface temperatures used were obtained from results of experiments done at The University of Texas evaluating concrete temperature due to an induced temperature on a concrete pavement specimen. The function obtained from these results is

$$T_{surface}=-1.1613+1.1357*T_{ambient} \quad (6.5)$$

Using these functions, the temperature distribution can be obtained within the concrete pavement at any depth, as well as at any time during the day. A typical temperature distribution in the concrete for Houston conditions is shown in Figures 6.15 and 6.16. Figure 6.15 shows summer distributions at 6 am and 3 pm. Figure 6.16 shows winter distribution at 6 am and 3 pm. The ambient temperatures used were the high and low temperatures for that area during 1986.

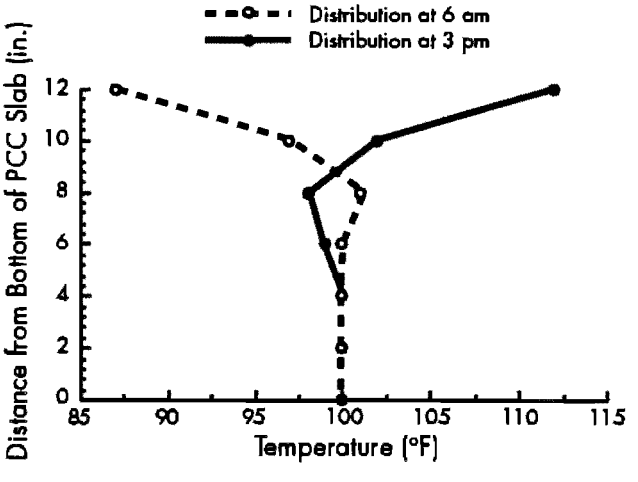

Figure 6.15 Temperature distribution through concrete section during the summer in Houston

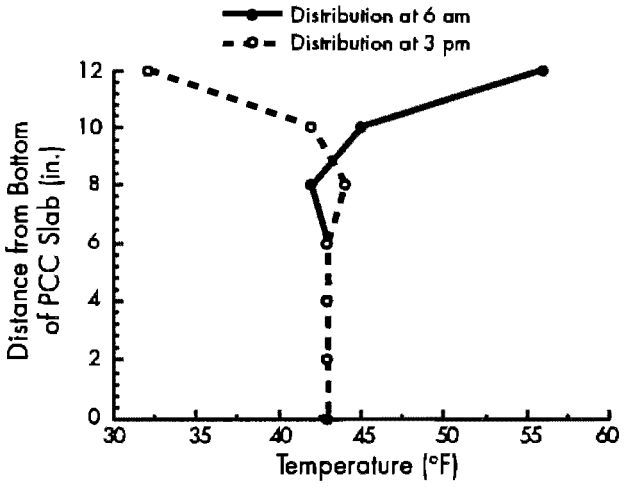

Figure 6.16 Temperature distribution through concrete section during the winter in Houston

These temperature distributions are used in the following section, where the environmental stresses are evaluated using the finite element method. The same format is used as is used with wheel loading, where reflective and non-reflective cracking are first analyzed.

6.3.2 Calculation of Environmental Stresses Using FEM

The environmental stresses when the existing pavement is cracked and the overlay uncracked and visa versa were analyzed. The results are shown in Figure 6.17. It is apparent from Figure 6.17 that the stress at the crack is close to zero. The fact that some stress values are shown is due to the FEM program operation. The highest stress between the two cases is about the same. These stresses are not very

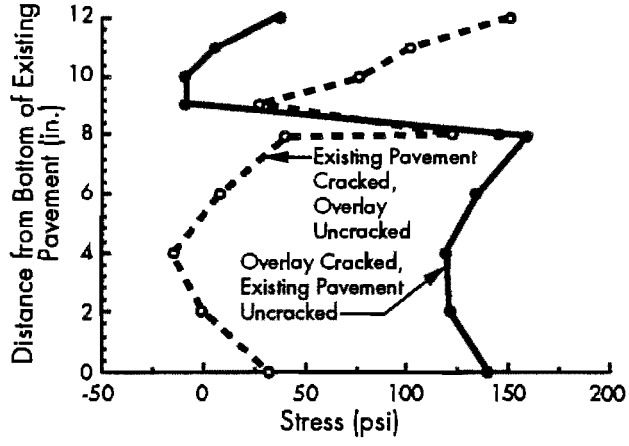

Figure 6.17 Normal stress through concrete section for exisitng pavement cracked, overlay uncracked; existing pavement uncracked, overlay cracked

high for the extreme case in Houston, shown previously. It is much lower than the tensile strength of the concrete. The important factor is, however, the shear stress at the interface, which is shown in Figure 6.18.

The shear stresses and tension stresses are much lower than the strength for shear and tension at the interface shown in an earlier chapter. The shear and tension due to wheel loading are also small, so we can conclude that these stresses will not influence the failure mechanism of the overlay. However, the fatigue mechanism of fatigue failure in shear or tension, at the interface, is unknown, as discussed previously.

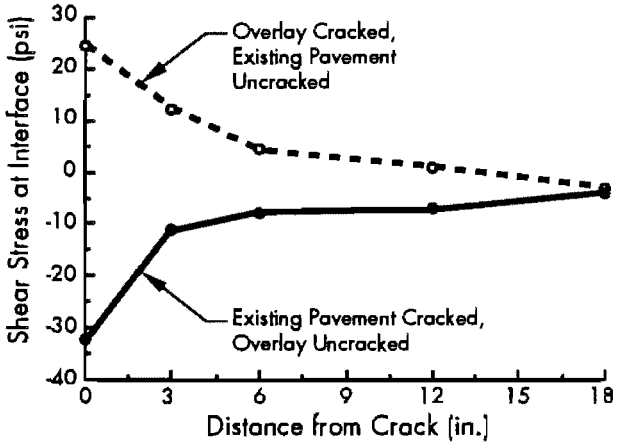

Figure 6.18 Shear stress at interface at cracks

Because BCO's are still in a very early stage of monitoring and no real failure data are available, the equations previously developed for fatigue are used in this analysis, which is discussed later. It is concluded from this section that the temperature stresses do not exceed the strength and, even with wheel loading added to it, will still be smaller than the strength. A method for incorporating temperature stresses in the fatigue equation is discussed later, but, because fatigue equations for the anticipated failure mechanism do not include temperature stresses, temperature stresses were not used in the development of the design system proposed in this work.

6.3.3 Moisture Stresses in Concrete Pavements

In Chapter 3 shrinkage and moisture are discussed. Stress due to shrinkage of concrete is reduced by cracking as well as by plastic cracking at an early age. The moisture distribution in Figure 3.11 provides very high tensile stresses in the top one inch of the pavement. This will ultimately crack, especially during the early-age development of the concrete. These cracks will proceed down to about

one inch below the surface of the overlay, reducing the tensile stress. Shrinkage stress is reduced due to cracking as well as creep. Creep can reduce the shrinkage strain up to 20 % (Ref 67). It can therefore be concluded that the shrinkage stress existing within the pavement system will be small, not only due to the above factors but because the interface between the existing pavement and the subbase has deteriorated and therefore allows more slippage, compared to slippage during the earlier stages of the existing pavement.

6.4 INFLUENCE OF THE COMBINATION OF ENVIRONMENTAL STRESS AND WHEEL LOADING ON BCO

Saxena and Dounias (Ref 68) concluded that an easy way to evaluate the combined effect of temperature and wheel loading is to add the two together. The only time this will cause problems is when separation occurs. This separation may increase the stress in the pavement significantly, as is also shown in Figure 6.10, where the system is delaminated. Saxena and Dounias found such separation at only the edges of a pavement. Due to the fact that the CRCP pavements are continuous and the edges are normally placed against a shoulder, the probability of separation is small, which increases the validity of adding the stress values. When fatigue calculations are made, the wheel loading may either increase or decrease stress in the pavement. However, the fatigue life is dependent on the wheel loading only when fatigue equations such as those discussed earlier are used. Only when minimum to maximum stress ratio fatigue equations are used is the temperature loading important (For example Figure 3.8).

In this work it is assumed that the concrete base layers are still in good condition and that the concrete slab and subbase slab are not separated vertically.

6.5 CONCLUSIONS

It is concluded from this chapter that it is difficult to evaluate traffic distribution and weight due to the variability of truck weights and distributions on highways. The methodology explained in the beginning of this chapter was used to calculate the amount of traffic experienced on the test sections analyzed in the previous chapter. Although a lot of variability exists, it can be concluded that this method is the best possible way to obtain realistic prediction of ESAL. Traffic counters close to the experimental sections were used.

The wheel load stresses were analyzed and equations were developed for stress calculations in BCO (Equations 6.1 and 6.2). It was found that an existing pavement with a fully bonded concrete overlay is similar to a full-depth pavement in terms of the tensile stress at the bottom of the concrete pavement, and that the remaining life of the existing pavement does influence the stress development of the pavement.

Finally, it is concluded that the shear and tension stresses are generally low at the interface and that no debonding will occur, due to stresses being higher than strengths. It is also important to note that the stresses are much lower than 50 percent of the strength, which was a limit set by some researchers and was discussed previously. The fatigue due to temperature loading occurs so slowly that the wheel load fatigue is much more important.

CHAPTER 7. DEVELOPMENT OF AN EMPIRICAL-MECHANISTIC DESIGN METHOD FOR BCO

7.1 INTRODUCTION

In the previous chapters, the factors influencing the long-term performance of bonded concrete overlays were discussed and analyzed. From each chapter, specific conclusions were made that will influence the design and performance of overlays. These factors also include data collected from test sections, which proved to be of utmost importance, because the data showed that BCO do not react exactly as previously thought. For example, as discussed in Chapter 2, it has been generally accepted that BCO cracking is reflective from the existing pavement, but this was proved to be not valid, since test sections showed that reflective cracking does not always exist.

The factors discussed and analyzed in the previous chapters are used in this chapter to form a design philosophy for BCO, to show the mechanisms of failure that can exist in BCO. This design philosophy is obtained from combining the results in the previous chapters. A design system is selected and a long-term performance prediction model is then selected for use with BCO. The long-term performance model must be modified as the BCO deteriorate and failure data become more available. This is part of the recommendations for future research.

7.2 MODEL PHILOSOPHY

The philosophy used in developing the model is based on the punchout mechanism of concrete pavements, which is discussed later. The philosophy for loading and thickness design is discussed in the following paragraphs. The conceptual mechanisms developed using the specific loading and overlay type and thickness are discussed later.

7.2.1 Wheel and Environmental Stress Distribution

In the previous chapter, the system for evaluating the wheel loads on highway pavement was discussed. These loads can be changed to 18-kip ESAL loads and then used in the long-term performance evaluation. The environmental stresses are neglected because their influence on fatigue modeling is to create a stress state and in-field verified models that are used later; the environmental stresses are not considered. The design philosophy is therefore based on wheel load stresses. These stresses are calculated for an 18-kip ESAL which is related to the number of 18-kip ESAL applications inherent in a long-term performance model. Equations were developed for stresses in bonded concrete overlay systems. These equations are used to calculate stresses and then to calculate the allowable number of applications. Miner's hypothesis can then be used to assure that the number of applications before failure is higher for the selected system than the applications needed to cause failure. However, different failure criteria exist, and the one which best suits the design system should be selected.

7.2.2 Thickness and Reinforcing Design Equations

It was found that the influence of the reinforcing used on wheel load stress calculations is small and that the primary effect of the reinforcing on the overlay is to obtain load transfer restoration; if delamination occurs it will keep the concrete intact for a longer period than if it were unreinforced. Furthermore, if the same percentage of reinforcing is used in the overlay as in the existing pavement, the probability of reflective cracking is higher. The reinforcing design does, therefore, not influence stress values but does influence formation of cracks.

The thickness design philosophy is based on the remaining life of the existing pavement and the expected future traffic. The stress equations developed in this work (Equations 6.1 and 6.2) are combined with equations developed elsewhere to assure that the different criteria are met and that the performance of the overlaid pavement is as intended.

7.3 CONCEPT OF FAILURE

One of the biggest problems associated with pavements is determining what failure is and how it is defined. The AASHTO Guide (Ref 1) uses the Present Serviceability Index (PSI) as a tool to decide when the pavement has failed. For PCC pavements,

the PSI is a rating of the road depending on the slope variance of the road, which is equivalent to the roughness. The PSI ranges from 0 to 5 with 5 being the value of a new, well constructed pavement. It is suggested in the Guide that resurfacing or reconstruction be done when the PSI value is 2.5 or 3. For highways in general, two types of failure exists: structural failure, which depends on the definition of failure used, and functional failure, in which the pavement becomes hazardous to the user. This is conceptually shown in Figure 7.1.

7.3.1 Functional Failure

Functional failure is related to the user. The ability to serve the user in a way which he or she feels is safe and without irritation is part of the functional purpose of the pavement. If the pavement deteriorates in such a way that it becomes unsafe or uncomfortable, the pavement has failed functionally. Figure 7.1 shows two levels of functional failure.

If no maintenance is done, the road will deteriorate and the curve will eventually flatten out near the time of failure. As can be seen from the figure the deterioration rate starts to stabilize at the end of the pavements useful life. Livneh (Ref 69) explains that the pavement is in poor condition, but is able to support some minor level of traffic. Functional failure is very important because it establishes the usefulness of the pavement, but, for design purposes, structural failure is used and is discussed below.

7.3.2 Structural Failure

Structural failure occurs when the pavement shows some type of distress which can be observed and which reduces the PSI value. Structural failure, as shown in Figure 7.1, occurs before functional failure. Structural failure as modeled by different fatigue equations, and mentioned before, can occur at first cracking; Class 3 and 4 cracking, as defined at the AASHTO Road Test; or 50 feet of cracking per 1,000 square feet of pavement, just to name some. These conditions of failure should be correlated with the mechanism of failure in a long-term performance equation. A failure mechanism for concrete pavements is punchouts. Won (Ref 64) modeled punchouts, and the same methodology is used for BCO. However, from the data and the analysis done in this work, it became evident that BCO could have more than one mechanism of punchout failure.

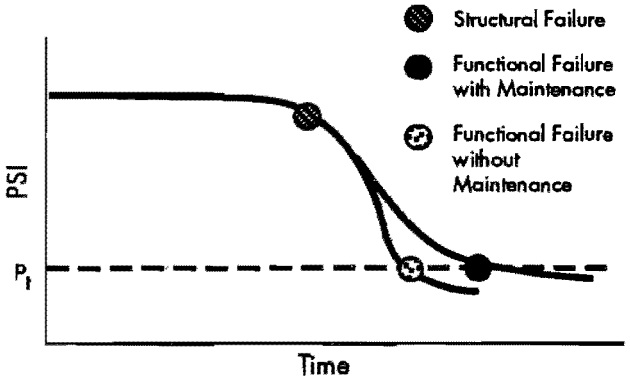

Figure 7.1 Present serviceability index versus time showing functional and structural failure

7.3.2.1 Concrete Failure

From the field data analysis, we can identify three different structural failure mechanisms. The first is a premature failure caused by delaminated areas. The mechanism of failure cannot be used for design purposes because delamination is an early-age problem and with good construction control it can be eliminated. Thus, with good bonding the slab acts as a unit and fatigue can be considered in the normal procedure. A model for delamination could be used to estimate the time before major repairs are needed, which would help in the distribution of funding at a project management level, but the percentage delamination, for example, found on the North Loop in Houston is very small and does not justify using such a model. The second failure mechanism is punchouts in areas of non-reflective cracking and the third is in areas with reflection cracking.

Punchouts in Delaminated Areas

Figures 7.2 to 7.5 shows conceptually how the failure occurs. The y-y stress is the transverse stress and the x-x stress is longitudinal stress. These sketches provide further insight into the failure mechanism of delaminated areas found on concrete pavements. Figure 7.2 shows an overlay with a delaminated area. It was shown in previous chapters that the cracking in delaminated areas increases significantly more than in non-delaminated areas.The mechanism of failure was shown in Chapter 6. The first step in the mechanism is therefore the formation of transverse cracks at the edge of the delaminated areas, as shown in Figure 7.3. As the transverse cracking develops, the delaminated area forms an unbonded beam as wide as the delaminated area, which is kept intact only by the reinforcing steel. However, because it is an unbonded system, tensile stresses will develop at the bottom of the overlay, as shown in Figure 7.4. This will cause longitudinal cracks and, eventually, a punchout in the overlay, as shown in Fig 7.5. These punchouts will then have to be repaired.

The areas in Houston surveyed in 1990, still have not produced a significant increase in overlay punchouts, although the delaminated areas are nearing the end of the fifth year under traffic. The 18-kip ESAL varied from 500,000 to 1,600,000 applications.

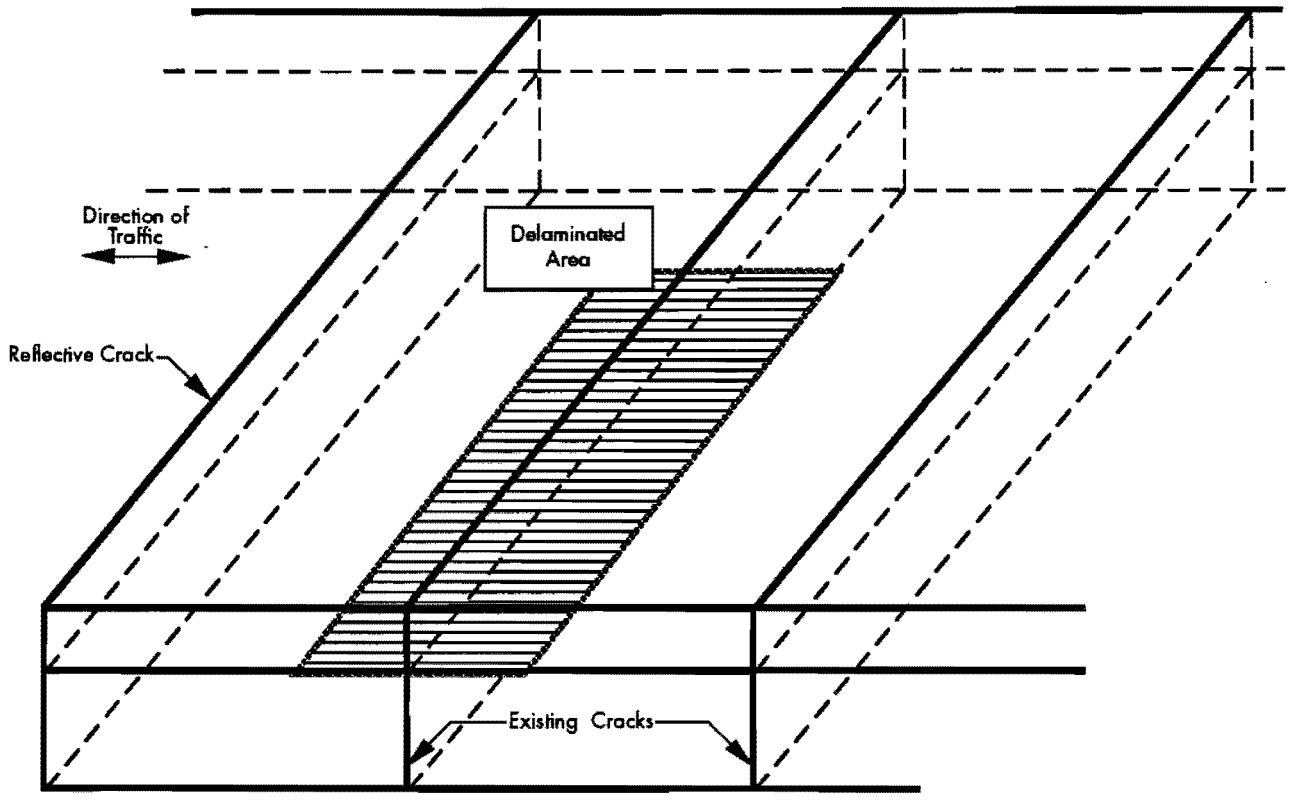

Figure 7.2 Delaminated area in BCO pavement

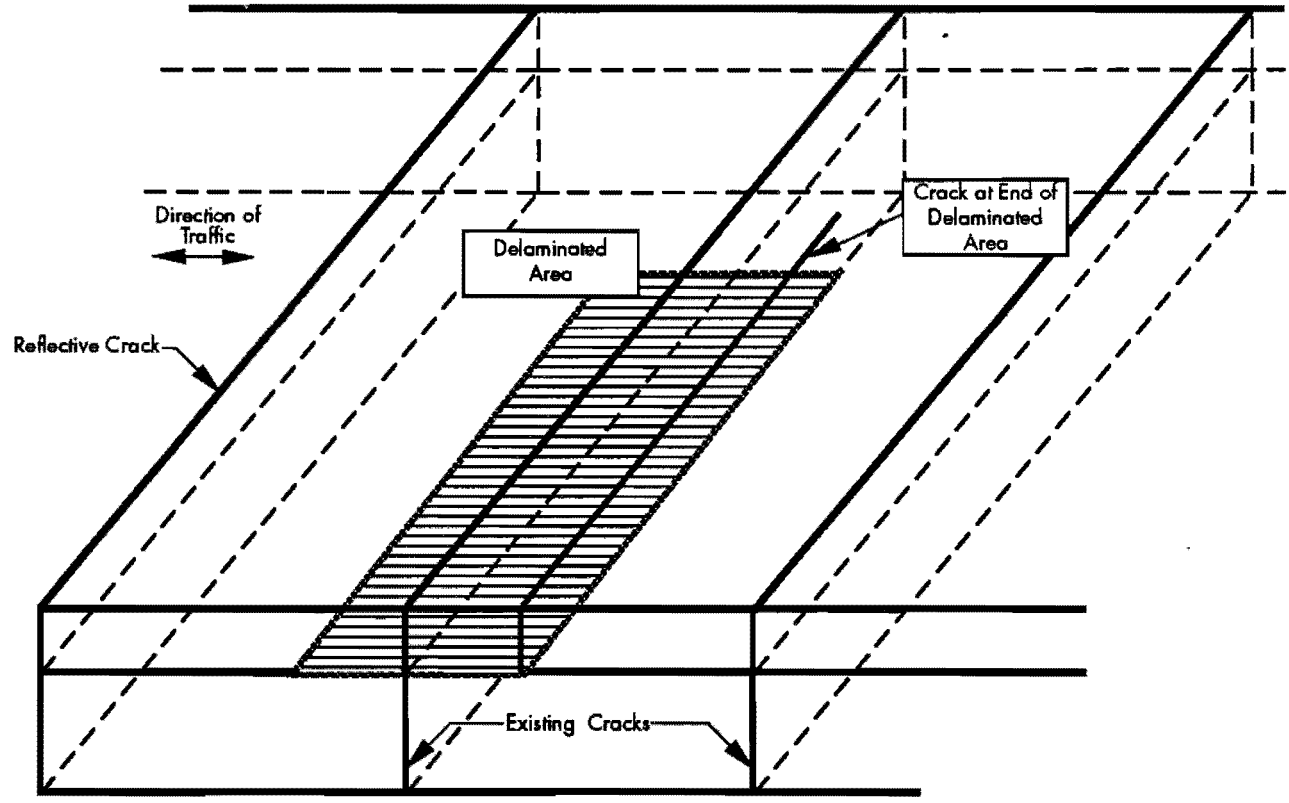

Figure 7.3 Transverse cracking in delaminated areas

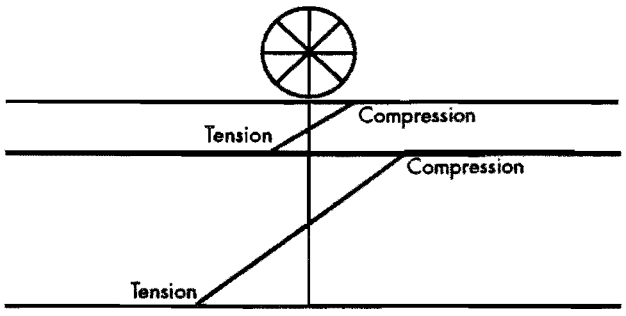

Figure 7.4 Conceptual layout of stresses in unbonded overlays

The rate of failure is therefore not severe. However, for concrete pavements, the rate of failure increases very quickly near the end of their lives. The same is true for delaminated areas. Full-depth repair should, however, restore the system fully.

Non-Reflective Cracking Areas

The mechanism of structural failure in areas with non-reflective cracking is uncertain due to the lack of data showing failures. Depending on the state of the existing pavement, the existing crack may reflect through and closely spaced cracks may be obtained in the overlay. This is shown in Figure 7.6. The block of concrete between the transverse and longitudinal cracks is cracked on all four sides of the overlay, but on only three sides of the existing pavement. The mechanism of failure can then either be that another crack forms in the existing pavement and a full punchout occurs or that the piece of BCO is debonded. The only way it can debond is if high shear or tension forces are exhibited at the interface. This can happen only if the existing cracks are wide enough for dirt to collect in the cracks while it is wide, for example, in the morning, and, as it closes during the afternoon, high shear forces are exerted on the concrete at the interface. The mechanism is shown in Figure 7.7. This is very similar to the mechanism of failure for spalling of concrete pavements at cracks. The longitudinal cracks can be either reflective cracks from the existing pavement structure or cracks due to shrinkage during the initial hardening period.

Reflective Cracking Areas

The mechanism proposed for areas where reflective cracking occurs is the same as that for newly constructed pavements. As the crack spacing is reduced, and the load transfer is reduced at the crack, the transverse stress becomes much higher than the longitudinal stress, which increases the probability of longitudinal cracking. This is

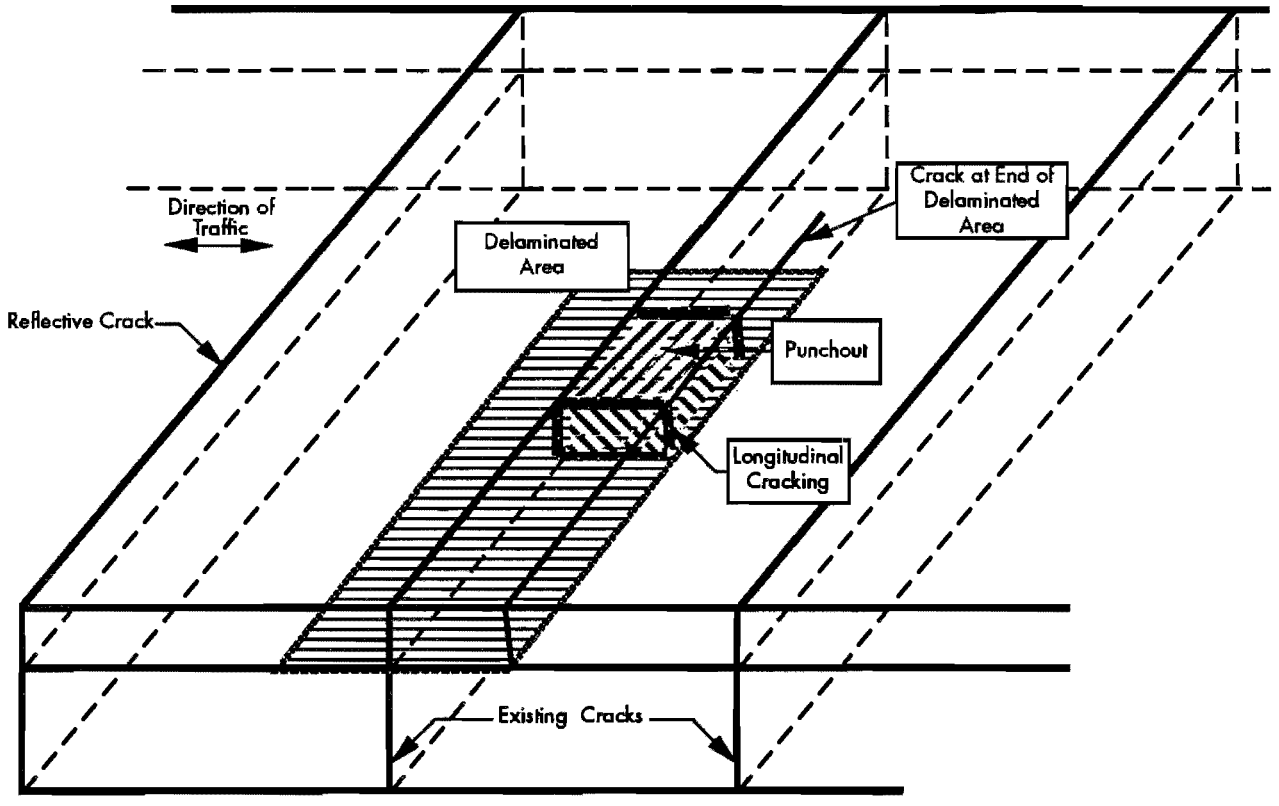

Figure 7.5 Longitudinal cracking development and punchout failure in delaminated areas

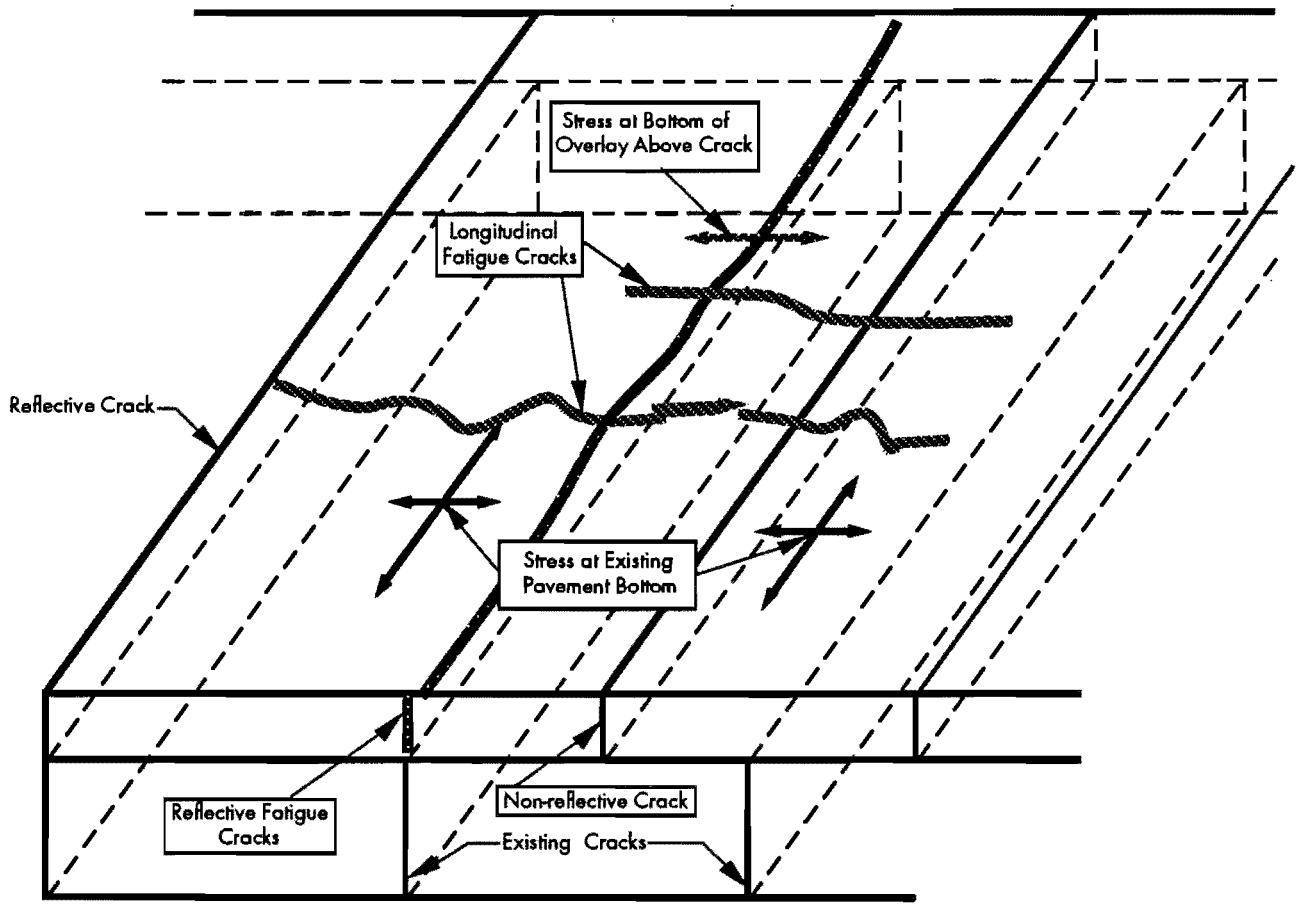

Figure 7.6 Cracking in initial non-reflective cracking areas

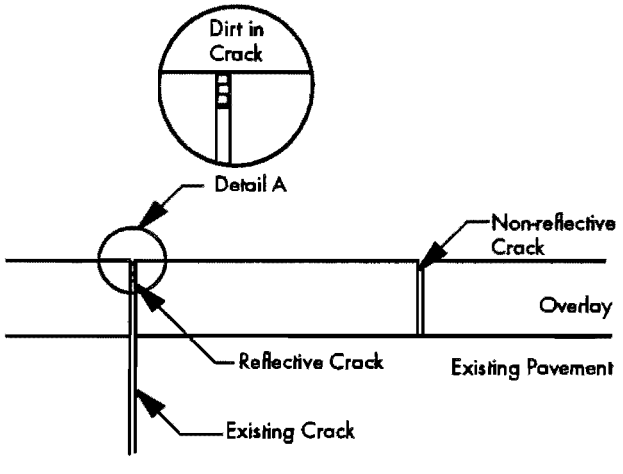

Figure 7.7 Mechanism for overlay punchout

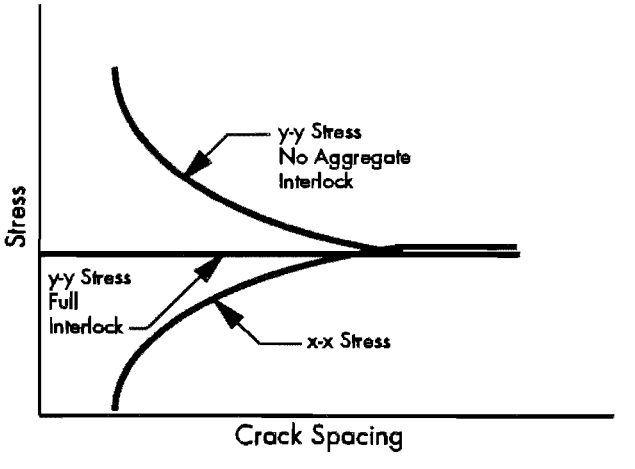

Figure 7.8 Conceptual layout of transverse and longitudinal stresses in PCC pavements

conceptually shown in Figure 7.8. Punch-outs occur when longitudinal cracks are connected to transverse cracks. As Won (Ref 64) stated, the prediction of punchouts, therefore, amounts to the prediction of the formation of longitudinal cracking. By modeling the longitudinal cracking, punchouts can, therefore, be predicted, which is an indication of the structural long-term performance of the concrete pavement.

Figure 7.9 shows a typical punchout in a concrete pavement.

The three structural failure types discussed can all occur. However, by good construction control, delamination can be greatly reduced, and, due to the small percentage of delamination of in-service pavements, delamination does not appear to be a long-term performance factor because it can be prevented. For the non-reflective areas, the failure mechanism is difficult to model due to the fact that dirt or other material infiltrates the pavement, especially where working cracks are extremely wide, which allows intrusion of dirt, which produces high shear stresses when the pavement expands during the warm part of the day. That leaves only the conventional punchout as a failure mechanism and this is discused further.

7.3.2.2 Failure of Dowel Bars, Tie Bars, or Reinforcing

It was stated before that, the lower the load transfer at a crack, the higher the stresses in the overlay itself. One way of obtaining good load transfer is by using dowel or tie bars along longitudinal joints or reinforcing across longitudinal and transverse joints. If the bars are across a joint, the load transfer will normally be good and an interior condition will prevail as the most important mechanism. However, as time goes by and water infiltrates the crack, the reinforcing will rust and eventually break, which will reduce the load transfer significantly. An interior pavement condition will, therefore, slowly change, as the crack becomes larger, to an edge condition. Very little data are available on the number of repetitions a reinforcing bar in a pavement will take before failure. Snyder et al (Ref 70) show data where bars lasted for 5.45 million ESAL's over a 9-year period. Special load transfer devices showed good performance and dowel bars showed a significant number of failures.

7.4 PROPOSED DESIGN SYSTEM

A design system for BCO must be looked at in two ways. The first is to determine whether or not the system is feasible for designing a BCO, and the second is to determine the thickness that should be used to support the ESAL expected. Figure 2.2 shows a flowchart of a typical overlay design procedure. The design system proposed in this work is diagrammatically shown in Figure 6.10 with the figures and equations which should be used in the calculation.

7.4.1 BCO Construction Criteria

In the first part of this chapter structural failure and functional failure are discussed. If we use a PSI graph, as shown in Figure 7.11, we see that at some stage it will be more economical to construct an unbonded overlay or to perform new construction, while at other times bonded concrete overlay construction will be more feasible. The point at which it is no longer feasible to construct a BCO should be determined before the design process to ensure cost-effective performance of the overlay. Field data on

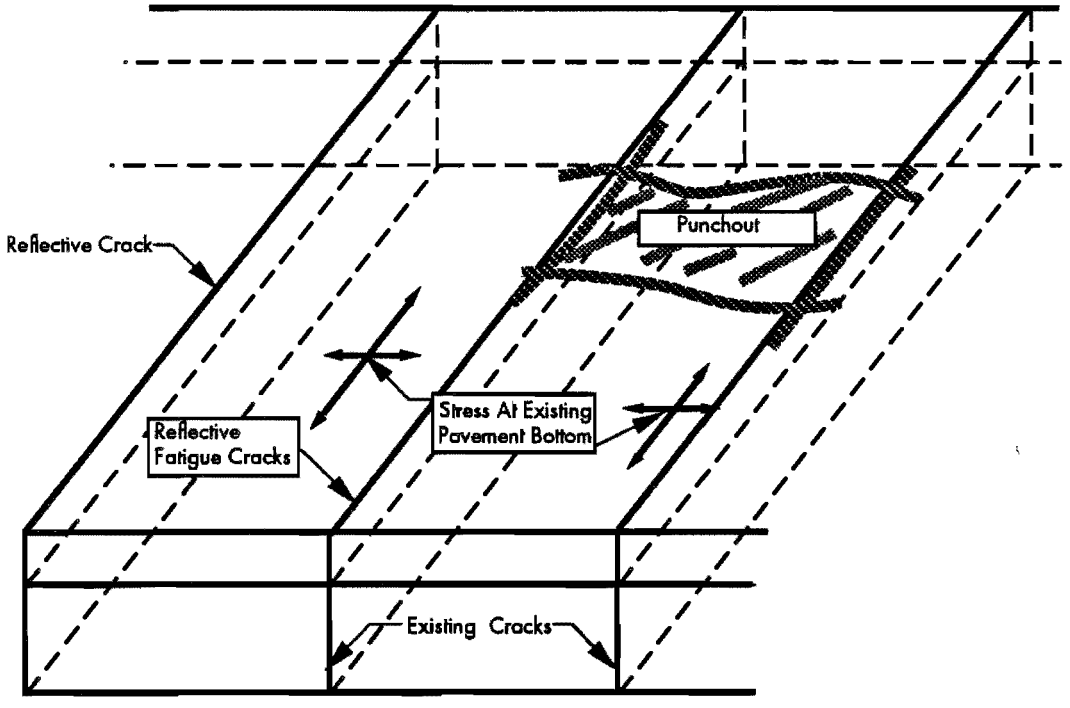

Figure 7.9 Typical punchout in PCC pavements

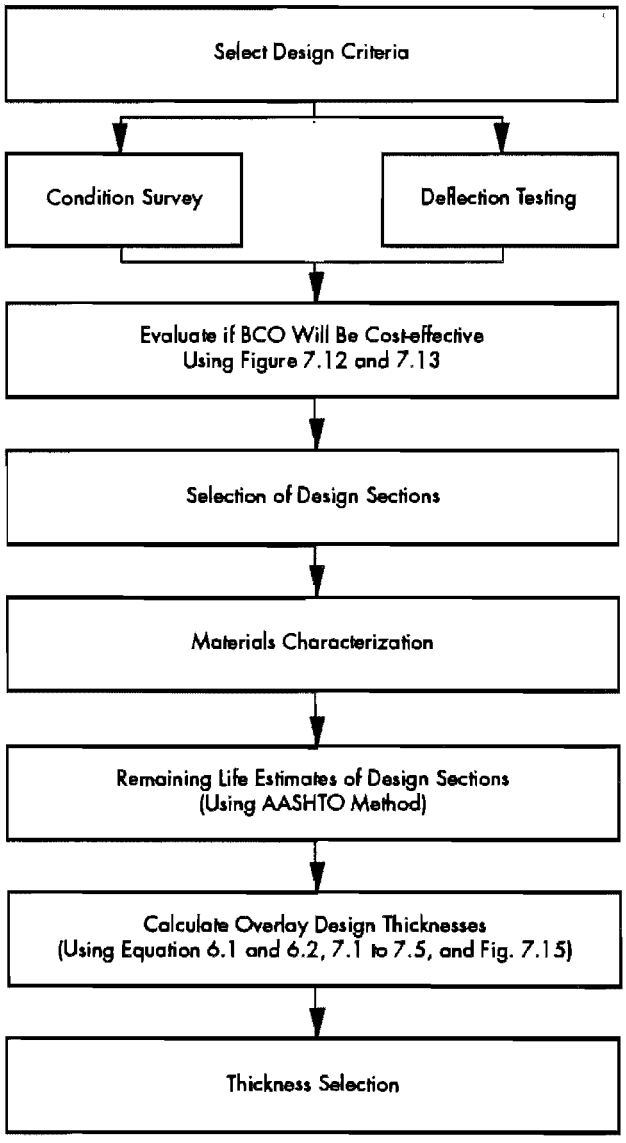

Figure 7.10 Diagrammatic layout of proposed design procedure

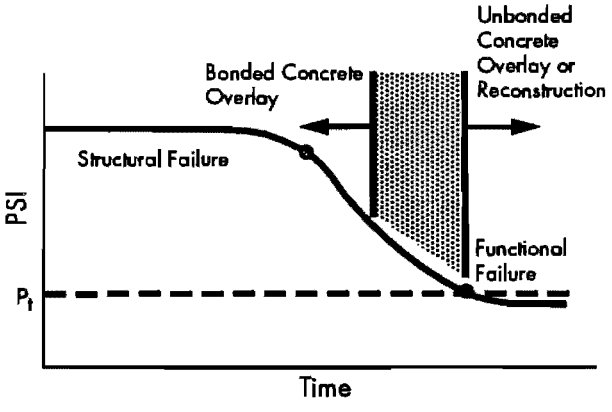

Figure 7.11 Time of type of overlay construction

this subject do not exist and a cut-off point for BCO can be based on various criteria. The philosophy followed in this work follows. As the existing pavement deteriorates the effective modulus at a crack will decrease. If an overlay is placed over an existing pavement, the stresses at the crack, at the bottom of the overlay, will depend on the stiffness of the existing pavement, as shown in Table 6.4. However, it was also noted previously in this chapter that, as the load transfer is reduced at cracks, the transverse stress becomes the critical stress. One effect of overlay placement is restoration of load transfer.

However, if the stress at the bottom of the overlay is high, a crack will form quickly and deteriorate to the state the existing crack was in before overlaying. Furthermore, reflective cracks will also deteriorate to the state the existing crack was in before overlaying, as noted by Voigt (Ref 54). For the overlay method to be cost-effective, the stress at the bottom of the overlay must, therefore, be not greater than the governing transverse stress at the bottom of the existing pavement, with full aggregate interlock, because it then provides the highest level of ESAL.

This is because the overlay will not fail before a longitudinal crack is formed. If it is higher than the transverse stress it will crack first, or a reflective crack will deteriorate quickly so that the transverse stress will increase and increase the probability of longitudinal cracking which governs failure of the concrete pavement.

By using the data in Table 5.4 and equating different deflections at the crack and at midspan for an existing pavement stiffness of 4500 ksi at midspan, the ratio of deflection at the crack versus that at midspan was obtained and plotted against the ratio between maximum tensile stress in the overlay and full interlock transverse stress in the existing pavement. This is shown in Figures 7.12 and 7.13. In Figure 7.12 a BCO with a 4500-ksi modulus of elasticity was evaluated and a modulus of 6000 ksi was evaluated in Figure 7.13.

From these two figures it can be concluded that, when a low modulus overlay such as a 4500-ksi concrete is used, a BCO can be used as the overlay if the maximum crack deflection divided by the maximum between-crack deflection is less than 1.7. If a higher modulus concrete is used a deflection ratio of 1.25 should be the limit.

This is the first step in the design process. If a BCO is advisable, the next step is to design an appropriate thickness for the anticipated design life traffic.

7.4.2 Thickness Design

The thickness design depends on the remaining life of the existing pavement. By using a method such as the one described in the AASHTO Guide, a

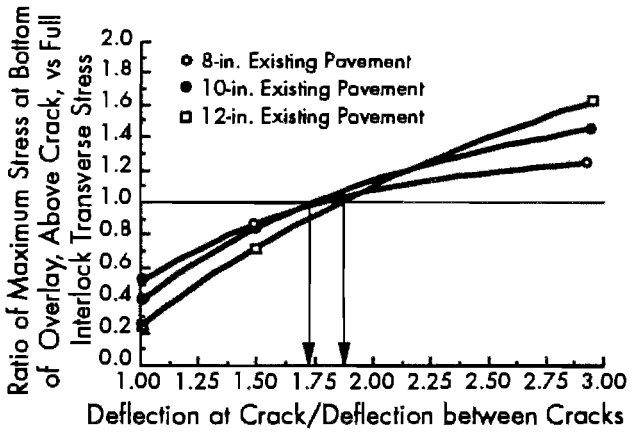

Figure 7.12 Stress ratio versus deflection ratio for overlay modulus of elasticity of 4500 ksi

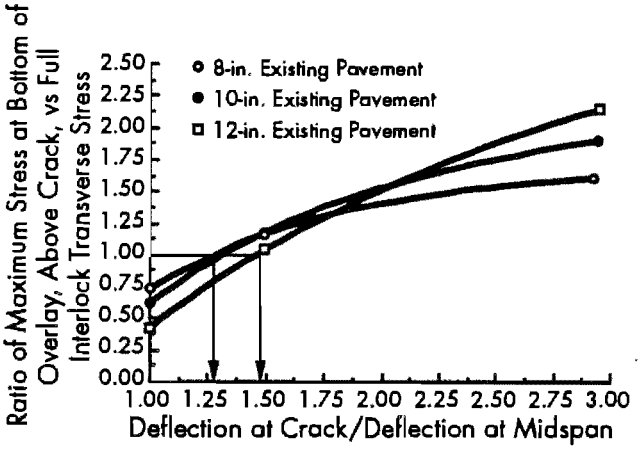

Figure 7.13 Stress ratio versus deflection ratio for overlay modulus of elasticity of 6000 ksi

remaining life for the existing pavement can be calculated. Therefore, by selecting a thickness for overlay, calculating the stress decrease due to the overlay, and evaluating the pavement with some type of long-term performance model, an overlay thickness can be selected which produces adequate structural support until the expected level of traffic is reached. The next section discusses a long-term performance model which can be used.

From the data analysis and computer analysis in this work, it was found that as the crack spacing is decreased the longitudinal stress between cracks is reduced, which was also found by Won (Ref 64). With crack spacing of less than 6 feet, as is the case for most of the BCO constructed in Houston, the transverse stress is the controlling stress. When an overlay is placed on top of the existing pavement, it increases the thickness of the pavement but it also restores load transfer at cracks. This is conceptually shown in Figures 7.14 to 7.16.

In Figure 7.14 it can be seen that, depending on the crack spacing, the transverse stress state can be calculated.The x-x stress can be calculated using Equation 6.1, developed in this work. The y-y stress depends on the quality of aggregate interlock. The lower the effectiveness of aggregate interlock, the lower the load transfer efficiency. As the load transfer efficiency (aggregate interlock) is reduced the transverse stress is increased for a specific crack spacing. Because the stress at 6 feet is approximately the same for the y-y stress versus the x-x stress, as shown before, Eq 6.1, with a crack spacing of 6 feet, can be used to calculate the y-y stress for full aggregate interlock. The y-y stress for no aggregate

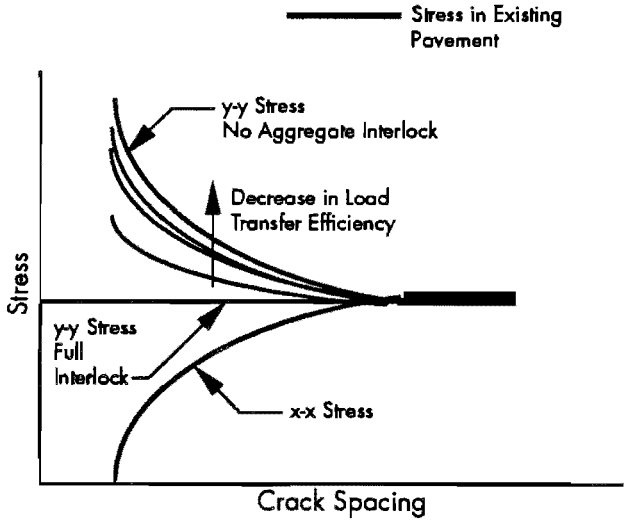

Figure 7.14 Stress in existing pavement before overlay

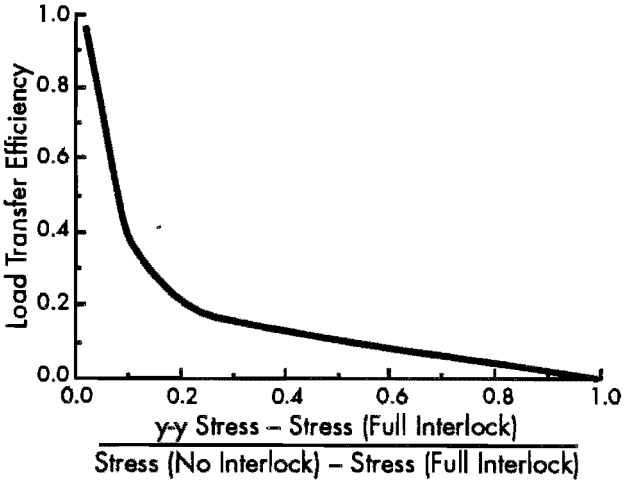

Figure 7.15 Load transfer versus increase in stress due to loss of load transfer

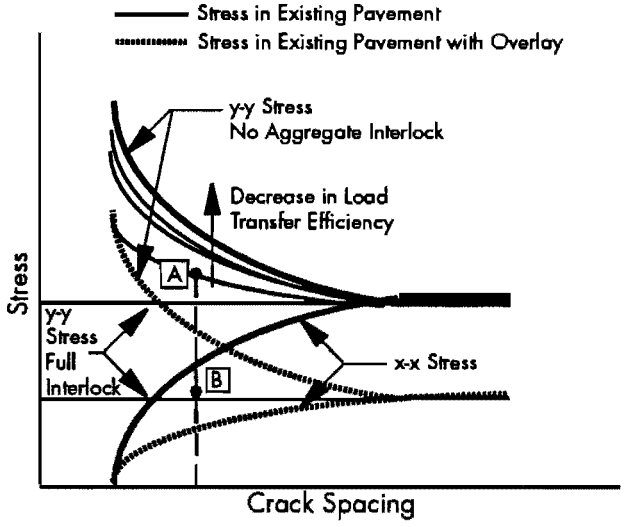

Figure 7.16 Stress distribution with overlay placed on existing pavement

interlock can be explained using the equation developed by Won:

$$\sigma = e^{9.8474D-1.8143X-0.4477} \quad (7.1)$$

where

- σ = Transverse wheel load stress for 9000-lb load, in psi,
- e = base of the natural log,
- D = pavement thickness, in inches, and
- X = crack spacing, in feet.

The stress changes, therefore, from full aggregate interlock during construction to a certain percentage thereof, depending on the load transfer. Figure 7.15 shows a conceptual increase in transverse (y-y) stress due to a reduction in load transfer.

This curve depends on the type of load transfer installed. It will vary between aggregate interlock versus a combination of aggregate interlock and reinforcing bars. However, a three-dimensional program which can model the effect is not available at this time. The form of the relationship in the reduction in load transfer is, however, close to what is seen in the field. Load transfer will stay intact for a long period, but when it starts to fail the failure rate will increase significantly.

When an overlay is placed on the existing slab, the stress state changes from point A (Figure 7.16) to point B, which is a big reduction in stress and is due to the added thickness. Point B will initially be at the full aggregate interlock level and will deteriorate from there, as conceptually shown in Figure 7.13. In order to quantify stresses better, a relationship between reduction in load transfer and ESAL is needed, but that type of information is not available at this time. It has been concluded that, for a PCC concrete overlay with a 4500-ksi modulus of elasticity, a BCO should not be constructed if the deflection at the crack divided by the deflection between cracks is more than 1.25. This is a load transfer efficiency of approximately 80 percent. We can then assume that, during the life of the pavement, it will have, on the average, 80 % load transfer efficiency.

It is therefore proposed that, until more data relating load transfer to time and longitudinal stress are obtained, the design stress for the overlay be calculated as

$$\sigma = 0.08(\text{Stress}_{\text{no interlock}} - \text{Stress}_{\text{full interlock}}) + \text{Stress}_{\text{full interlock}} \quad (7.2)$$

The value of 0.08 is defined in this work as the load transfer factor. The load transfer factor is, therefore, dependent on the load transfer efficiency. The governing stress can therefore be calculated for each selected thickness of the overlay to be placed on an existing pavement. The selection of a specific overlay thickness will depend on the thickness needed to satisfy the ESAL requirements obtained from a long-term performance model.

7.5 LONG-TERM PERFORMANCE PREDICTION MODEL

The design system proposed in the previous paragraphs depends greatly on the long-term performance model selected or developed. The method discussed above is based on a mechanistic approach derived from observations observed in the field and then modeled. The long-term prediction model selected must incorporate the mechanistically developed part of the analysis and tie it to the field performance. Due to the fact that no long-term performance data are available for BCO's, it is necessary to select existing equations which will best describe the model developed. Many fatigue curves are available. A model which describes the development of longitudinal cracking is that of Taute (Ref 3), who based his analysis on a cracking index of 50 feet per 1000 square feet of pavement. He found that this failure condition corresponds approximately to a rate of defect of three defects (punchouts and patches) per mile per year. The model is

$$N = 46000\ (f/\sigma)^3 \quad (7.3)$$

where

- N = Number of 18-kip ESAL,
- f = flexural strength of the concrete in psi, and
- σ = governing stress in the concrete in psi.

For each thickness selected, a method for predicting the governing stress was proposed in the previous section. The remaining life of the existing pavement is also known, by using the AASHTO

guide method. If traffic is used as the basis for calculating remaining life, then the remaining life of the existing pavement, if we assume Miner's hypotheses is valid, is

$$\text{Remaining Life} = 1 - (n_{actual}/N_{predicted}) \quad (7.4)$$

where

n_{actual} = actual number of ESAL during its life and

$N_{predicted}$ = number of ESAL predicted (calculated) for the pavement.

The stress obtained from a specific thickness selected and used with Eq 7.2 should satisfy the following equation:

$$n_{future} = N_{future\ predict}(1 - (n_{actual}/N_{predicted})) \quad (7.5)$$

where

n_{future} = number of estimated ESAL for the design life of the overlay, and

$N_{future\ predict}$ = predicted (calculated) ESAL for a specific thickness.

The thickness which satisfies this equation will, therefore, be the selected design overlay thickness. Figure 7.17 shows the proposed design procedure diagrammatically, with the specific equations to be used for each section. Figure 7.17 is an expansion of the section "Calculate Overlay Design Thickness" in Figure 7.10.

Won (Ref 64) has shown a method of punchout prediction which can also be used for overlays and which could be used for budgeting for maintenance purposes.

7.6 EXAMPLE PROBLEM

Data used to design a BCO for the South Loop of IH610 in Houston are used to illustrate an example problem (Ref 71). The remaining life was calculated based on a distress index obtained from condition surveys. The estimated number of 18-kip ESAL for a 20-year design life was established at 15,577,000. The existing pavement modulus was back-calculated as approximately 5,000,000 psi, while the overlay modulus is also assumed to be 5,000,000 psi. The average crack spacing is assumed to be 3 feet, while the remaining life was estimated at 80 percent. The existing pavement is 8 inches thick. The modulus of subgrade reaction was assumed to be 250 pci, and the flexural tensile strength to be 700 psi.

Table 7.1 shows the stresses calculated for 2-inch, 4-inch, and 6-inch overlays using Equations 6.1, 6.2 and 7.1. The governing stress is then selected and used in calculating the number of ESAL the facility can carry before failure. The thickness is then

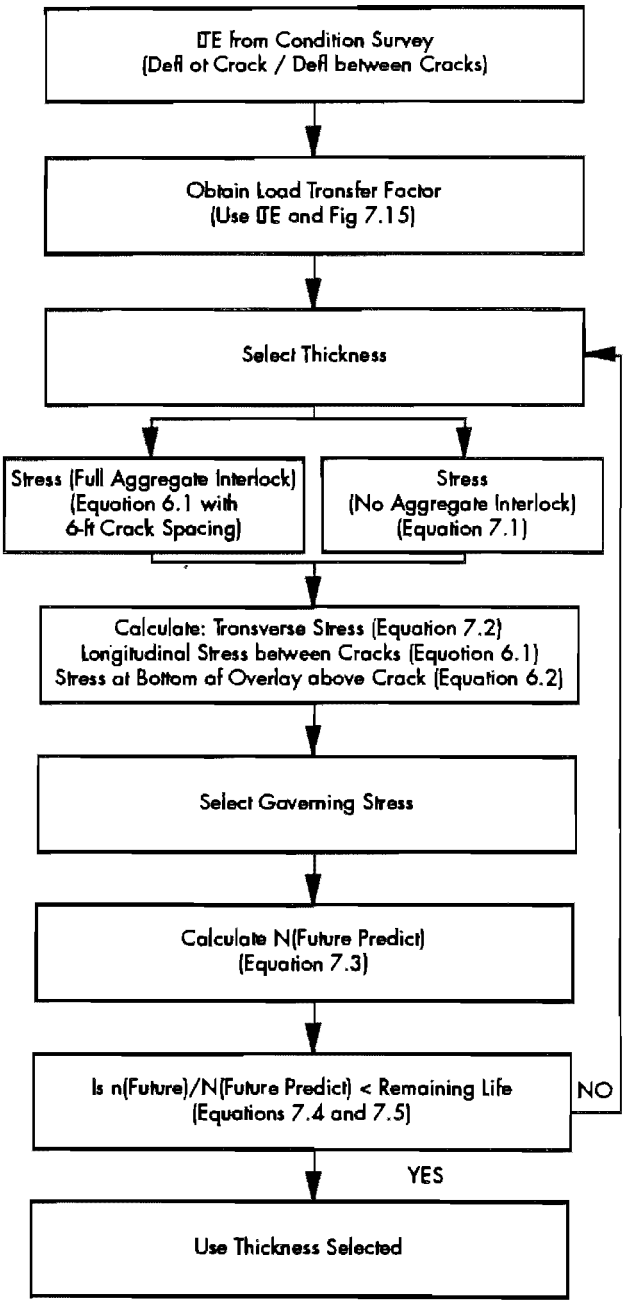

Figure 7.17 Layout of proposed design procedure

plotted against the number of 18-kip ESAL, as shown in Figure 7.18. From this figure the thickness necessary to last 20 years, or, as evaluated in Figure 7.18, the thickness necessary to last 15,577,000 repetitions of ESAL can be obtained.

From Figure 7.18 it can be concluded that an overlay thickness of approximately 4.5 inches will be adequate to extend the life of the pavement for another 20 years, at which time punchouts will start developing at a rate of approximately 3 per mile per year.

Table 7.1 Stresses and 18-kip ESAL for example problem

		Overlay Thickness (in.)		
		2	4	6
Stress (psi)	Transverse Stress (Eq 7.2)	154	103	78
	Longitudinal Stress (Eq 6.1)	86	62	47
	Stress in Overlay (Eq 6.2)	–297	–9	29
Traffic (ESAL)	N (Future Predict) (Eq 7.3)	4,355,514	14,439,105	33,385,405
	n (Future) (Eq 7.5)	3,484,411	11,551,284	26,708,324

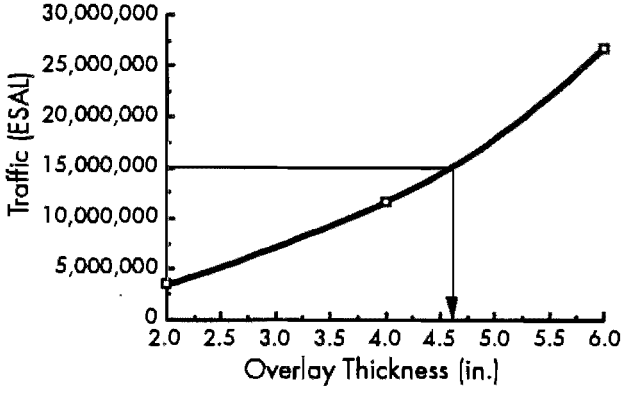

Figure 7.18 Overlay thickness versus 18-kip ESAL

7.7 CONCLUSIONS

A design method for BCO is proposed; it is based on fatigue cracking of BCO. The knowledge gained from the statistical analysis of field data and analysis using the FEM program was used to develop the design system.

However, the findings in this study should be verified using field data. It can also be concluded that BCO should not be placed if the deflections at the cracks are more than 1.25 to 1.7 times the between-crack deflections. In addition to the deflection criteria, previous research has established that when the rate of punchouts/lane/mile/year reaches a value of three, the rate compounds rapidly. Thus, this value represents the outside limit for the feasibility of a BCO.

CHAPTER 8. SUMMARY, CONCLUSIONS, AND RECOMMENDATIONS FOR FUTURE WORK

8.1 SUMMARY

The specific objectives of this work were to model phenomena observed on overlays in Houston, to analyze the behavior of bonded concrete overlays incorporating wheel and temperature stresses, to develop a method for establishing at which point a BCO should not be placed, to develop an easy useable design method, and to accurately describe the long-term performance of BCO. All of these purposes except the last one have been accomplished.

In Chapter 2, a design system is examined and its important aspects and current methods are evaluated. The design of BCO was then discussed further, in particular, the limitations of the current methods and the specific design procedures. By using an FEM program which modeled cracks and the interface between the overlay and existing pavement, the factors influencing the performance of BCO were ascertained using a sensitivity analysis. These factors were used to evaluate the stress in BCO due to wheel loading as well as to the influence of environmental stress. Field data were used to develop the methodology for failure mechanisms and the design method. However, the long-term performance evaluation depends on existing methods, because existing BCO are not yet old enough to provide information on their long-term performance.

A better understanding of BCO was achieved through a study of their fatigue cracking. The mechanical behavior of BCO was analyzed using fatigue cracking as well as field data from test sections in Houston.

8.2 CONCLUSIONS

The most widely used design equations for BCO are the Corps of Engineers overlay design equations. These equations are based on accelerated testing of overlays on airport pavements. Two problems exist in using these equations. First, they must be applicable to highway pavements. Second, the fatigue or long-term performance criterion of failure is inherent in the COE equations as well as in the rigid pavement design equation used. The different design equations have different failure criteria. The COE equation is based on first structural crack, while the AASHTO Guide rigid equation is based on Class 3 and Class 4 cracking. From this it may be concluded that the use of long-term performance prediction within the design equations to model concrete overlays is not valid. Since most of the currently used equations are based on empirical testing, factors such as interface bond strength, crack spacing, and other structural features are not fully addressed by these equations.

It is concluded that the factors listed in Table 3.2 are all important in the long-term performance of bonded concrete overlays. These factors are used in the determination of the performance of BCO. An important area in which a lack of information exists, specifically about fatigue, includes the compression, shear, and tensile fatigue at the interface between existing pavements and bonded concrete overlays. It was concluded that, although Miner's hypothesis is not representative of concrete behavior in some instances, it is the best method available.

From Chapter 4 it can be concluded that the modulus values of the existing pavement and overlay, thermal coefficients of existing pavement and overlay, and the crack spacing all significantly influence stresses due to environmental conditions. Stresses due to wheel loads are significantly influenced by modulus value of the existing pavement, crack spacing, overlay thickness, and existing pavement thickness.

In section 5.4.3.2 it is concluded that delamination of bonded concrete overlays constitutes an early-age problem, which occurs in the first few weeks after construction. Delamination is not progressive, but the influence on the long-term performance of the pavement is uncertain. It should ultimately need maintenance before areas which are not delaminated, and this will have an economical impact.

From Chapter 5 it can further be concluded that reinforcing type, thickness, and aggregate are important in transverse crack development in bonded concrete overlays. Another factor from these results, which is important in the analysis of bonded concrete overlays, is the fact that different reinforcing

procedures produce different crack spacings. Wire reinforced sections are not significantly different in between-, after-, and before-overlay crack spacing, while fibers significantly increase crack spacing.

The wheel load stresses were analyzed and an equation was developed for stress calculations in BCO in section 6.2.4.2. It was further concluded that a BCO will act the same way as a newly constructed pavement, but that the remaining life of the existing pavement does influence the stress development of the pavement.

In section 7.4 a design method for BCO is proposed which is based on fatigue cracking of BCO. The knowledge gained from the statistical analysis of field data, and an analysis using the FEM program, were used to develop the design system. It can also be concluded that BCO should not be placed if the deflections at the crack are more than 1.25 to 1.7 times the deflections between cracks, as shown in section 7.4.1. Also, when the rate of punchouts/lane/mile/year reaches a value of three, the feasibility of a BCO is limited.

It is finally concluded that the findings in this study should be verified using long-term performance field data.

8.3 LIMITATIONS

The development of this work is based on certain assumptions. These assumptions need to be made where a lack of information exists or in order to simplify a problem.

First, the stresses in the pavement were evaluated with a plain strain FEM program and then converted to equivalent Westergaard stresses. Variability exists within this transposition of stresses.

The FEM program does not model reinforcing within the concrete extremely well because no slippage is allowed between the reinforcing bar and the concrete. This is extremely important for temperature loading.

The lack of data in the area of fatigue at the interface between the overlay and the existing pavement, in shear, compression, and tension, may have an influence on defining the failure mechanism of the BCO.

The very limited information on the development of a reduction in load transfer with time (which influences transverse stress) is also an important factor which reduces the accuracy of the design method.

The development of the equations in this work is based on the Westergaard equation, and only one modulus of subgrade reaction is used. This is based on the assumption that the modulus of subgrade reaction does not influence the stresses within the concrete very much. For very low or very high modulus of subgrade reactions this may not be true.

The long-term performance model used is based on concrete pavements rather than overlaid pavements. The lack of long-term performance data for BCO necessitates the use of existing models.

8.4 RECOMMENDATIONS FOR FUTURE WORK

The most important factor not explored, due to the lack of data, is the long-term performance prediction model used. Two paths can be followed in future research. Either the existing test sections in Houston can be monitored, and results in 10 to 15 years can be used to evaluate the long-term performance of BCO, or an accelerated test method can be used. With the advent of the mobile load simulator (MLS), which is currently under development in Texas, a machine is available which can be used to evaluate quickly the long-term performance of BCO and to verify the model developed in this work.

The effect of time and traffic on the reduction of load transfer at cracks in CRCP is also important, and the MLS can be used in this area as well. This is research needed not only for BCO but also for CRCP.

The influence of temperature on the fatigue life of overlays should be incorporated in a long-term performance model developed for overlays. The temperature stress gives the state of stress the pavement is experiencing as the wheel load passes. The fatigue of concrete depends on the ratio of maximum to minimum stress. An easy method for evaluating this should be developed.

REFERENCES

1. "AASHTO Guide for Design of Pavement Structures," American Association of State Highway and Transportation Officials, Washington, D.C., 1986.
2. Bruce, A. G., and Clarkeson, J., "Highway Design and Construction," The Haddon Craftsman, Pennsylvania, 1950.
3. Taute, A., McCullough, B. F., and Hudson, W. R., "Improvements to the Materials Characterization and Fatigue Life Prediction Methods of the Texas Rigid Pavement Overlay Design Procedure," Research Report 249-1, Center for Transportation Research, The University of Texas at Austin, November 1981.
4. Tayabji, S. D., and Okamoto, P. A., "Thickness Design of Concrete Resurfacing," Third International Conference on Concrete Pavement Design and Rehabilitation, Purdue University, West Lafayette, Indiana, 1985.
5. Department of the Army and the Air Force, "Rigid Pavements for Airfields," Technical Manual 5-825-3, Washington, D.C., August 1988.
6. Ray, G. K., "Design of Concrete Overlays for Pavements," Title No. 64-40, *American Concrete Institute Journal*, August 1967.
7. Tayabji, S. D., Okamoto, P. A., "Thickness Design of Concrete Resurfacing," Third International Conference on Concrete Pavement Design and Rehabilitation, Purdue University, West Lafayette, Indiana, April 1985.
8. Treybig, H. J., McCullough, B. F., Smith, P., and von Quintus, H., "Overlay Design and Reflection Cracking Analysis for Rigid Pavements," Volume 2-Design Procedures, Research Report No. FHWA-RD-77-67, Federal Highway Administration, Washington, D.C., August 1977.
9. Schnitter, O., Hudson, W. R., and McCullough, B. F., "A Rigid Pavement Overlay Design Procedure for Texas SDHPT," Research Report 177-13, Center for Highway Research, The University of Texas at Austin, May 1978.
10. Bagate, M., McCullough, B. F., and Fowler, D. W. F., "A Mechanistic Design for Thin-Bonded Concrete Overlay Pavements," Research Report 457-3, Center for Transportation Research, University of Texas, September 1987.
11. Highway Research Board, "The AASHO Road Test," Report 7, Summary Report, Highway Research Board Special Report 616, Washington, D.C., 1962.
12. Kesler, C. E., "Fatigue and Fracture of Concrete," National Ready Mixed Concrete Association, Stanton Walker Lecture Series on the Material Sciences, Presented at the University of Maryland, College Park, Maryland, November 18, 1970.
13. Mindess, S., and Young, F., *Concrete*, Prentice-Hall, pp 77-78, Englewood Cliffs, New Jersey.
14. Norby, G. M., "Fatigue of Concrete - A Review of Research," *Journal of the American Concrete Institute*, Vol. 30, No. 2, August 1958, Proceedings Vol. 55.
15. Murdock, J. W., "A Critical Review of Research on Fatigue," Engineering Experiment Station Bulletin 475, University of Illinois, College of Engineering, 1965.
16. Doyle, J. N., Kung, S. H. L., Murdock, J. W., and Kesler, C. E., "Second Progress Report - Mechanism of Fatigue Failure in Concrete," T & A.M. Report No. 601, University of Illinois, September 1961.
17. Antrim, J. D., "The Mechanism of Fatigue in Cement Paste and Plain Concrete," *Highway Research Record 210*, Highway Research Board, 1967, pp 95-107.
18. Neal, J. A., Kung, S. H. L, Murdock, J. W., and Kesler, C. E., "Third Progress Report-Mechanism of Fatigue Failure in Concrete," T &

A.M. Report No. 623, University of Illinois, August 1962.

19. Kaplan, M. F., "Crack Propagation and Fracture of Concrete," *Journal of the American Concrete Institute*, November 1961.

20. Glucklich, J., "The Flexural Static and Fatigue Failure of Portland Cement Mortar," T. & A.M., Report No. 622, Univ. of Illinois, Aug 1962.

21. Award, M. E., and Hilsdorf, H. K., "Strength and Deformation Characteristics of Plain Concrete Subjected to High Repeated and Sustained Loads," Abeles Symposium: Fatigue of Concrete, Papers Presented at 1973 ACI convention in Atlantic City N.J., ACI publication SP41-1, Detroit, 1974.

22. Hilsdorf, H. K., and Kesler, C. E., "Fatigue Strength of Concrete under Varying Flexural Stresses," *Proceedings*, Am. Concrete Inst., Vol. 63, 1966, pp 1059-1076.

23. Holmen, J. O., "Fatigue of Concrete by Constant and Variable Amplitude Loading," Fatigue of Concrete Structures, Edited by S.P. Shah, ACI Publication SP75-4, Detroit, 1982.

24. Van Ornum, J. L., "Fatigue of Concrete," Transactions, ASCE, Vol. 58, 1907, pp 294-320.

25. Vesic, A. S., and Saxena, S. K., "Analysis of Structural Behavior of Road Test Rigid Pavements," *Highway Research Record No. 291*, Highway Research Board, National Academy of Sciences—National Research Council, Washington, D.C., pp 156-158, 1969.

26. Raithby, K. D., and Galloway, J. W., "Effects of Moisture Condition, Age, and Rate of Loading on Fatigue of Plain Concrete," Abeles Symposium: Fatigue of Concrete, Papers Presented at 1973 ACI Convention in Atlantic City N.J., ACI publication SP41-2, Detroit, 1974.

27. Klaiber, F. W., and Lee, D., "The Effect of Air Content, Water-Cement Ratio, and Aggregate Type on the Flexural Fatigue Strength of Plain Concrete," Fatigue of Concrete Structures, Edited by S.P. Shah, ACI Publication SP75-5, Detroit, 1982.

28. Murdock, J. W., and Kesler, C. E., "Effect of Range of Stress on Fatigue Strength of Plain Concrete Beams," *Journal of the American Concrete Institute*, Vol. 30, No. 2, August 1958, pp 221-233.

29. Ballinger, C. A., "The Cumulative Fatigue Damage Characteristics of Plain Concrete," *Highway Research Record 370*, Highway Research Board, 1971, pp 48-60.

30. Flint, A. L., and Childs, S. W., "Field Procedure for Estimating Soil Thermal Environments," Soil Sci. Soc. AMER. Proc., Vol. 51, 1987.

31. Miner, M. A., "Cumulative Damage in Fatigue," *Journal of Applied Mechanics*, September 1945.

32. Chung, Y. S., Meyer, C., and Shinozuka, M., "Modeling of Concrete Damage," *ACI Structural Journal*, Title No. 86-S28, Vol 86, No. 3, May-June 1989.

33. Westergaard, H. M., "Computation of Stresses in Concrete Roads," Proceedings of Fifth Annual Meeting, Highway Research Board, Proceedings of 5th Annual Meeting, Washington D.C., December 1925, pp 90-112.

34. Huang, Y. H., and Wang, S. T., "Finite-Element Analysis of Concrete Slabs and its Implication for Rigid Pavement Design," Highway Research Report, No. 466, 1973, pp 55-69.

35. Ioannides, A. M., Thompson, M. R., and Barenberg, E J., "The Westergaard Solutions Reconsidered," Workshop on Theoretical Design of Concrete Pavements, Netherlands Center for Research and Contract Standardization in Civil and Traffic Engineering, Epen, The Netherlands, 5-6 June 1986.

36. Eisenmann, J., "Westergaard's Theory for Calculation of Traffic Stresses," Workshop on Theoretical Design of Concrete Pavements, Netherlands Center for Research and Contract Standardization in Civil and Traffic Engineering, Epen, The Netherlands, 5-6 June 1986.

37. Yoder, E. J., and Witczak, M. W., *Principles of Pavement Design*, John Wiley & Sons, Inc., New York.

38. Aslam, M. F., Saraf, C. L., Carrasquillo, R. L., and McCullough, B. F., "Design Recommendations for Steel Reinforcement CRCP," Research Report 422-2, Center for Transportation Research, The University of Texas at Austin, November 1987.

39. Crawford, C. B., "Soil Temperature and Thermal Properties of Soils," Highway Research Board, Special Reports, No. 2, 1952.

40. de Gijt, J. G., Leidschendam, F. B. V., "The Measurement of the Soil Temperature with a Temperature Cone," Commissie voor Hydrologish Onderzoek, TNO, Verslagen en Mededelingen nr. 31., Publ. by TNO, The Hagens, Netherlands, 1983, pp 574-584.

41. Campanella, R. G., and Mitchell, J. K., "Influence of Temperature Variations on Soil Behavior," Jour. Soil Mech. and Found, Div., ACE, Vol. 94, No. SM 3, Proc. Paper 5958, pp 709-734, May 1968.

42. Chandra, D., Lytton, R. L., Yang, W., "Effect of Temperature and Moisture on Low Volume Roads," Research Report 473-2, Texas Transportation Institute, Texas A&M University, College Station, December 1988.

43. Goetz, R., and Muller, S., "Relationship Between the Daily Temperature Wave And the Development of the Natural Soil Profile," National Academy Sciences-National Research Council-Highway Research Board-Special Report 103, 1969, pp 51-65.

44. Mitchell, J. K., "Temperature Effects on the Engineering Properties and Behavior of Soils," National Research Council-Highway Research Board-Special Report 103, 1969, pp 9-28.

45. Turner, K. A., and Jumikis, A. R., "Subsurface Temperatures and Moisture Contents in Six New Jersey Soils, 1954-1955," Highway Research Board Bulletin 1956, nr. 135, pp 11-108.

46. Fang, H. Y., "Influence of Temperature and Other Climatic Factors on the Performance of Soil-Pavement Systems," National Research Council-Highway Research Board-Special Report 103, 1969, pp 173-185.

47. Sodha, M. S., Bansal, N. K., and Seth, A. K., *Variance of the Ground Temperature Distribution*, Applied Energy, Applied Science Publishers Ltd, England, 1981.

48. Luthra, S. P., Saluja, S. N., and Amar, R. C., "Investigation on Soil Temperature Variations," Indian Institute of Technology, Institute of Engineers, New Delhi (India), Jan. 1969, pp 169-175.

49. Richards, B. G., "Pavement Temperatures and Their Engineering Significance in Australia," National Research Council-Highway Research Board-Special Report 103, 1969, pp 254-266.

50. Chiang, C., McCullough, B. F., and Hudson, W. R., "A Sensitivity Analysis of Continuously Reinforced Concrete Pavement Model CRCP-1 for Highways," Research Report 177-2, Center for Highway Research, The University of Texas at Austin, Austin, Texas, August 1975.

51. Koesno, K., and McCullough, B. F., "Evaluation of the Performance of Thin Bonded Concrete Overlay on Interstate Highway 610 North, Houston, Texas," Research Report 920-2, Center for Transportation Research, The University of Texas at Austin, December 1987.

52. Bagate, M., McCullough, B. F., Fowler, D. W., and Muthu, M., "An Experimental Thin-Bonded Concrete Overlay Pavement," Research Report 357-2F, Center for Transportation Research, The University of Texas at Austin, November 1985.

53. Uddin, W., Meyer, A. H., Hudson, W. R., "A User's Guide for Pavement Evaluation Programs RPEDD1 and FPEDD1," Research Report 387-2, Center for Transportation Research, The University of Texas at Austin, July 1985.

54. Voigt, G. F., Carpenter, S. H., and Darter, M. I., "Rehabilitation of Concrete Pavements Volume II: Overlay Rehabilitation Techniques," Report No. FHWA-RD-88-072, Federal Highway Administration, 6300 Georgetown Pike, Mclean, Virginia 22101-2296.

55. Temple, W. H., and Cumbaa, S. L., "Thin Bonded PCC Resurfacing," Louisiana Department of Transportation and Development, FHWA/LA-85/181, 1985.

56. van Metzinger, W. A., Lundy, J. L., Suh, Y. C., and McCullough, B. F., "The Influence of Curing Temperature on the Design and Performance of Concrete Pavements," Annual Transportation Conference 1990, CSIR, Pretoria, Republic of South Africa, August 1990.

57. Lundy, J. L., "Delamination of Bonded Concrete Overlays at Early Ages," Dissertation completed for publication in August 1990, The University of Texas at Austin.

58. Seeds, S., McCullough, B. F., and Hudson, W. R., "A Design System for Rigid Pavement Rehabilitation," Research Report 249-2, Center for Transportation Research, The University of Texas at Austin, January 1982.

59. Report to the 69th Legislature Required by House Bill 89, "Oversize and Overweight Permit Program," State Department of Highway and Public Transportation, 25 January 1985.

60. Adams, J. B, and Gossett, L. E., "Texas Regulations Governing the Size and Weight of Commercial Vehicles," Texas Department of Public Safety, 1984.

61. DeBerry, B. L., "Effects of Heavy Trucks on Texas Highways," Supplement to the Report to The 65th Legislature Required by

Resolution 589, State Department of Highway and Public Transportation, 1 September 1978.

62. Lee, C. E., Shankar, P. R., and Izadmehr, B., "Lateral Placement of Trucks in Highway Lanes," Research Report 310-1F, Center for Transportation Research, The University of Texas at Austin, Austin, November 1983.

63. McCasland, W. R., and Stokes, R. W., "Truck Operations and Regulations on Urban Freeways," Research Report 338-1F, Texas Transportation Institute, Texas A & M University System, College Station, August 1984.

64. Won, M., "A Mechanistic Model of Continuously Reinforced Concrete Pavement," Doctorate Dissertation, The University of Texas at Austin, 1986.

65. Bagate, M., McCullough, B. F., Fowler, D. W., and Muthu, M., "An Experimental Thin-Bonded Concrete Overlay Pavement," Research Report 357-2F, Center for Transportation Research, The University of Texas at Austin, November 1985.

66. Fintel, M., and Khan, F. R., "Effects of Column Exposure in Tall Structures," PCA, EB018.01D, 1986.

67. Neville, A. M., *Properties of Concrete,* Third Edition, John Wiley & Sons Inc., New York, 1981.

68. Saxena, S. K., Dounias, G. T., "Mechanical and Environmental Stresses in Continuously Reinforced Concrete Pavements," *Transportation Research Record 1099,* 1986.

69. Livneh, M., "Comments on Modified Models for Maintenance and Rehabilitation Planning," *Transportation Research Record 1200,* 1988.

70. Snyder, M., Reiter, M. J., Hall, K. T., and Darter, M. I., "Rehabilitation of Concrete Pavements, Volume I - Repair Rehabilitation Techniques," Publication No. FHWA-RD-88-071, Federal Highway Administration, 6300 Georgetown Pike, Mclean, Virginia 22101-2296, July 1989.

71. "Design Analysis for Rehabilitation of the CRCP on Southeast Quadrant of Houston Loop 610," Unpublished report conducted for the Texas State Department of Highways and Public Transportation, Research Report 920-1, Center for Transportation Research, The University of Texas at Austin, October 1986.